STUDY OF

SUSPENDED STRIPLINE EXCITED

DIELECTRIC ROD RADIATOR

A Thesis Submitted

in Partial Fulfillment of the Requirements

for the Degree of

Master of Technology

by

Capt Rakesh Kaul

to the

DEPARTMENT OF ELECTRICAL ENGINEERING

INDIAN INSTITUTE OF TECHNOLOGY, KANPUR

March 1994

Certificate

15.3.94

It is certified that the work contained in the thesis entitled **STUDY OF SUSPENDED STRIPLINE EXCITED DIELECTRIC ROD RADIATOR**, by Capt Rakesh Kaul, has been carried out under my supervision and that this work has not been submitted elsewhere for a degree.

15, March 1994

Dr M Sachidananda

Professor

Department of Electrical Engineering

I.I.T. Kanpur

EE-1994-M-KAU-STU

Abstract

The characteristics of a Dielectric Rod Antenna, excited by a Suspended StripLine (SSL) are studied experimentally. Different parameters are considered, such as the length of the dielectric rod, the effect of shaping the dielectric rod and finally the effect of shorting out the side radiations. An approximate analysis using Green's function has been presented. The study aimed at characterizing the antenna, in terms of its physical dimensions, for array applications. The SSL, due to its planar structure was used for the feeding arrangement.

To

MY PARENTS

Acknowledgements

With deep sense of gratitude I acknowledge my gratefulness to Dr M Sachidananda for suggesting this topic, valuable guidance and immaculate supervision. Dr M. Sachidananda who is synonym for decency remains as a vital link in the chain of my memory.

I express my gratitude to Harish, Apu and Srikanth for their interest and help in my thesis, and for their wonderful company.

Facilites extended by the Department of Electrical Engineering and the Advanced Centre for Electronic Systems at I.I.T., Kanpur are acknowledged.

I am also grateful to all my defence and civilian friends at I.I.T., Kanpur for making my stay a memorable one.

Finally, I would like to thank my wife *Mitu* and son *Eashan* for their patience and understanding throughout the various stages of evolution of this manuscript.

Capt Rakesh Kaul.

Contents

List of Figures

Chapter 1

Introduction

1.1 General

Dielectric antennas are primary radiators which employ a system of dielectric elements, as distinct from a system of conductors, to radiate EM energy or to collect radiated EM energy. This definition does not include dielectric lenses, and which may be regarded as phase correction devices. Lenses are essentially secondary radiators which are excited by primary radiators.

There exists a family of such dielectric antennas, the principal members being :

1. The solid dielectric rod, figure 1.1.

2. The hollow dielectric tube, figure 1.2.

3. The dielectric horn, figure 1.3.

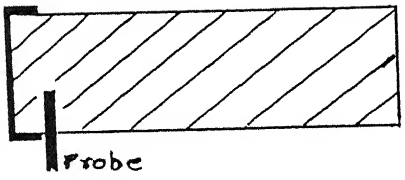

Figure 1.1: Solid dielectric rod

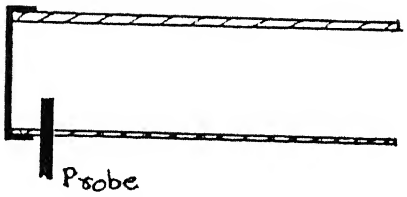

Figure 1.2: Hollow dielectric tube

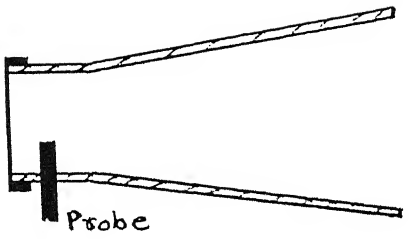

Figure 1.3: Dielectric horn

EM waves may be guided along the axis of a cylinder, of arbitrary cross section, at the surface of which exists a discontinuity in the dielectric properties of the media inside and outside the cylinder. A rod of dielectric material is an example of such a system.

1.2 Literature survey

Dielectric rod radiators have been studied and analyzed using various modes and means of analysis. However, no literature or reference is available on a dielectric rod radiator excited by a planar strip arrangement, either as a single element or in an array form.

When correctly dimensioned, [1] this radiator gives a single lobe radiation pattern with its maximum in the direction of the axis of the rod and its directivity proportional to the length of the rod.

Kishk and Shafai in their study, [1] have given a numerical solution to the dielectric

rod, radiation characteristics. They assumed the rod as a dielectric waveguide excited by a microwave metal waveguide. The far-field patterns were calculated, which were subsequently used to calculate the beamwidth, gain and its application as a feed for paraboloid reflector antennas. Different rod lengths, dielectric constant, rod diameter and different shapes were studied. They observed that by increasing the rod length the beamwidths could be decreased, i.e. the gain increases. Peak cross-polarization could be decreased by increasing the rod diameter, though it could be affected by the dielectric constant. It was found that the gain of the antenna could be increased by increasing the dielectric rod extension, the dielectric constant or the rod diameter.

A modal analysis of the dielectric rod antenna was presented by,[2]. They determined the gain, power radiated and beamwidth by enclosing the dielectric rod in a conducting pipe and assuming the pipe radius as very large. The radiation patterns and far-field amplitudes were determined for a wavelength of 10 GHz. Three rods of different diameters and dielectric constant were studied. As per their analysis, a reduction in the rod diameter, at a given frequency, widens the near-field beamwidth. ? [3], have presented a radiation characteristic of piece- wise homogeneous dielectric rod antennas. A scattering method was applied to the study of the radiation characteristics, using the volume equivalence principle. To improve the matching of the hybrid HE_{11} mode to the free space, they tapered the dielectric rod. The piecewise homogeneous dielectric antenna was composed of two rods of same cross-sectional dimensions, but with different permittivities. Thus, the matching was realized by continuously decreasing the rod permittivity.

Analysis of the dielectric rod available, [4], [5] ,etc have treated the dielectric rod as a waveguide excited by means of a probe, dipole, or as an extension of a waveguide.

Kiely's now classical monograph, [5] did much to stimulate the considerable inter-

est that was to follow, as did the availability of improved types of dielectric material. Kiely, in his monograph, has provided a critical review of the work existing upto 1953, previously scattered throughout the literature and to collect the design data. He approached the problem by three different methods. Each of these methods involved their own assumptions and did much to shed light on the behaviour of the EM field in such circumstances and to provide design data. Very little material has been provided upon antenna impedance and its variations with frequencies and antenna dimensions.

Professor Chatterjee, [6] in her book has provided the only, recent text on the topic since Kiely's monograph. the book performs as a reference work and as a guide for practical microwave antenna design.

In the interval between [5] and [6], a considerable ampount of work, both theory and experiment, has been done by [7], [8], [9] and others, on cylindrical surface waveguides and antennas including dielectric rod antennas. The recent renewed interest and the extensive work on dielectric waveguides by [10], [11] and work on optical fibres by [12] and [13] for use at optical frequencies have created scopes for applications in the mm-wave region.

1.3 Dielectric rod as an array element

1.3.1 Planar feeding structure

For the dielectric rod radiator feeding structure, keeping in view the array applications and the structure compactness, the *Planar transmission line* was choosen. The choices available for the planar feeding structure were the stripline, microstrip, suspended stripline,etc.

1.3.2 Advantages/disadvantages

The strip transmission line consists of a flat strip conductor situated symmetrically between two ground planes. The dominant mode of propagation is TEM, with the electric and magnetic field components lying entirely in the transverse plane.

In a microstrip, figure 1.4, a strip conductor on a dielectric substrate – the reverse side of which is metallized, a pure TEM mode cannot exist. However as the frequency increases above the microwave region, the dielectric substrate thickness reduces, thereby posing fabricational problems.

Microstrip antennas have extremely narrow bandwidth because of high Q-factor.. This can be overcome using parasitic elements or increased thickness. However, there would be more power loss due to surface wave. Efficiency of such antennas is very low because of considerable loss in the feeder network.

The SSL uses a thin dielectric substrate, containing the strip conductor, suspended midway between the top and the bottom ground planes.

1.4 SSL selection criteria

A better bandwidth, efficiency [14] and potential can be made available using a SSL excited antenna. The SSL feeding network is a low loss structure. It is more cost effective, since a thin, low price can be used without substantially increasing the losses.

1.4.1 Conductor loss mininimised

The presence of air gap in these structures reduces the concentration of EM energy near the ground planes. Hence, the conductor loss, which is the major contributing factor to the total loss is far less than in a microstrip.

1.4.2 Effective dielectric constant

Another effect of the air gap is to reduce the *effective dielectric constant* of the medium which results in an increased width of the strip conductor, and, thus, fabricational ease at even millimetre frequencies.

1.4.3 Structure robustness and Fixation

The dielectric substrate, with the planar feeding structure, sandwiched between the top and the bottom ground planes is provided with an inherent mechanical robustness and support. Also, the fixation and stability of the dielectric rods is resolved as these can be held perfectly stationary and with correct alignment, onto the SSL, through holes drilled in the top ground plane.

1.4.4 Planar feeding

The disadvantage for an array system is that the feed network must lie in a separate layer behind the radiating surface, so the complete antenna cannot be etched on a single substrate. There is a consequent increase in complexity. An additional disadvantage is that extra mechanical complexity and increased manufacturing costs result due to the need for inserting secured probes.

The planar feeding structure for an array could consist of a feed at one end, and the stripline branching off to the array dielectric rods positions.

1.5 Configuration studied

For this thesis the configuration studied, considering the above, is the *SSL excited dielectric rod radiator*. A single element, using circular-cylindrical Teflon rods, and one tapered rod, for varying stripline lengths was studied.

1.6 Array design characteristics

For an array, linear or planar, the characteristics desired would be:

- Highly directive elements, thus employing fewer elements.
- An uniform and easy to fabricate feeding structure (Planar transmission line).
- Preferably in the horizontal plane and with maximum radiation in the plane normal to it.
- A single main lobe with small side lobes.
- Steerability of the main beam.

1.7 Scope of study

An array consists of discrete elements, which are ordinarily identical and are similarly oriented for analytical and operational convenience. A linear-array of discrete elements is an antenna consisting of several individual and distinguishable elements whose centres are finitely separated and fall on a straight line.

In order to analyze an array, it is necessary to characterize a discrete element in all its entirety and properties.

The scope of this study is an experimental collection of data in order to characterize a single SSI excited dielectric rod radiator, for array applications.

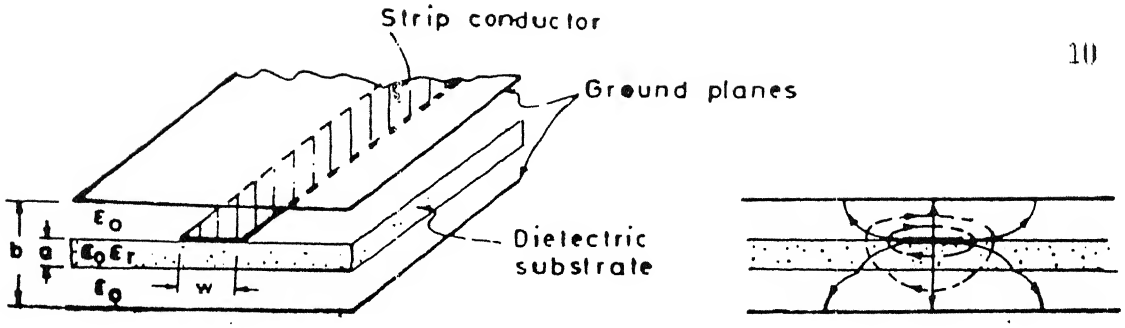

(a) Suspended stripline

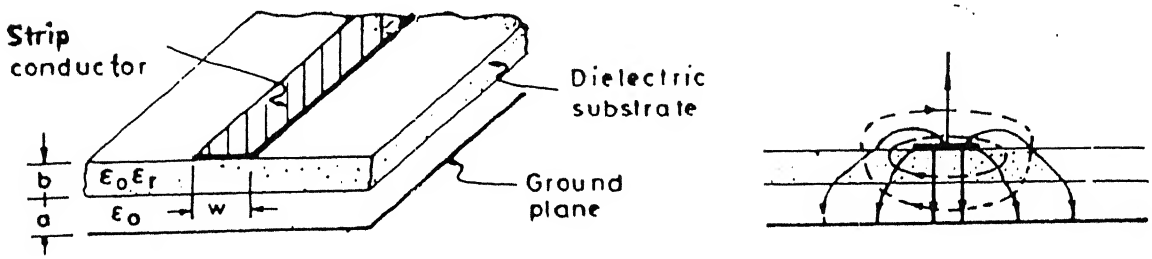

(b) Suspended microstrip

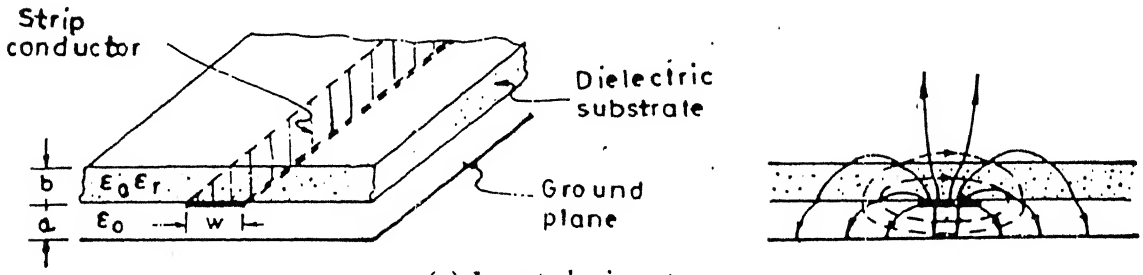

(c) Inverted microstrip

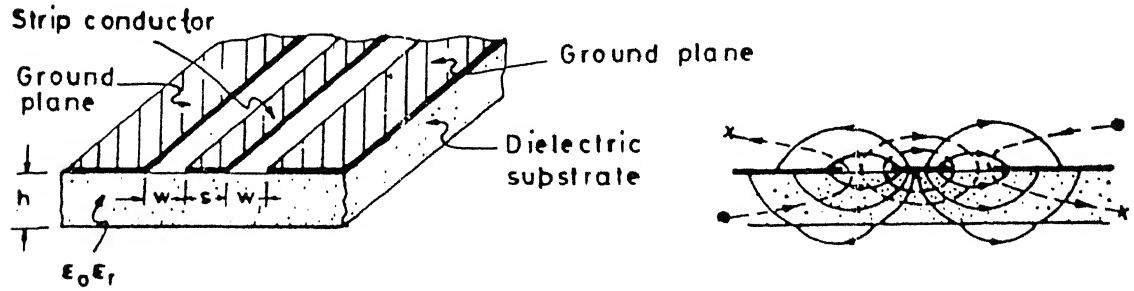

(d) Coplanar waveguide

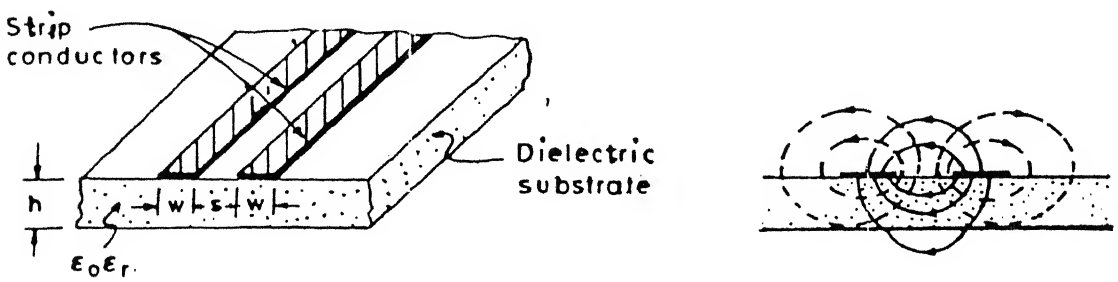

(e) Coplanar strips

Some variants of stripline, microstrip line, and slotline. (——— *E* field lines, – – – *H* field lines.)

Figure 1.4: Planar transmission lines

Chapter 2

Applications of Dielectric Rod Antennas

2.1 General

Dielectric rods have found several applications in practice where their special features make them particularly suitable and where their principal limitations are not of major importance. Where one requires a non-metallic antenna or one with its largest extent in a longitudinal direction, the dielectric rod is a suitable choice. its radiation pattern characteristics change very little with frequency which is advantageous from a communication point of view where frequently wide ranges of frequency are used. The rod also seals the aperture of its excitatioin system and the antenna is mechanically strong and robust. The effect of rain and moisture, [5], on the surface of the rod is detrimental to antenna gain and becomes increasingly so the higher the frequency employed. This effect limits the use of dielectric rod antennas to the longer centimetre wavelengths when the antenna is to be used out of doors on a non-weather -proof mounting.

2.2 Feeds

Short dielectric rod have been used to feed lenses as their radiation patterns are somewhat more flat-topped and provide relatively uniform illumination for a lens with smaller spill- over than is generally obtained from horn-feed systems.

2.3 Arrays

Arrays of two and four dielectric rods were extensively used in Germany during the last war as radar antennas and as search antennas for detecting allied radar transmissions. Their advantages in these applications are that they are non-metallic and can be designed to have very small windage, citeKi05, thus facilitating high rotational speeds which was particularly useful in the case of search radars.

A large rectangular array of forty-two dielectric rods was designed in America at the *Bell Telephone laboratories* and was used by the American Navy for gunnery fire control purposes.

It consisted of fourteen identical elements in a horizontal array; each element was a vertical array of three dielectric rods. The phase of each element was controlled and varied to produce beam-scanning in the horizontal plane, which required thirteen rotary phase changers geared and driven together in mechanism. This antenna represents the most extensive use of dielectric rods in practice to date.

2.4 Direction Finding

Dielectric rods excited in the E_{01} mode, [15], have a sharp null in the forward direction with a major lobe on each side. They could be used with advantage in certain types

of *direction-finding equipment* in which position finding on a sharp null is more accurate than on a broad maximum. They could also be used as *beacon antennas* if mounted vertically as the radiation pattern in the plane normal to the axis of the rod is a circle and there is no radiation in the vertical direction.

Chapter 3

Input Impedance: Approximate Analysis

3.1 Introduction

The SSL, because of its low loss, provides an attractive planar feeding structure at microwave and millimetre wave frequencies. No reference or paper is available on the analysis of this structure. In this chapter a brief introductory procedure is given, this can be elaborated upon in the future studies for better characterization of the SSL excited dielectric rod antenna.

3.2 Approximations

For the purpose of analysis, the structure may be visualised as a transition of a SSL to a circular dielectric waveguide. The bottom ground-plane may be viewed as a shorting plate, at one end of the rod, so that the structure radiates only from the other end. The effect of difference between the SSL substrate dielectric constant (2.22) and that of the Teflon rod (2.1) is neglected. The conductor strip is assumed to be of negligible thickness, and width w. Any presence of air-pockets between the rod-end and the SSL substrate is neglected.

3.3 Analysis

Figure 3.1 illustrates the type of SSL probe dielectric rod antenna to be analysed:

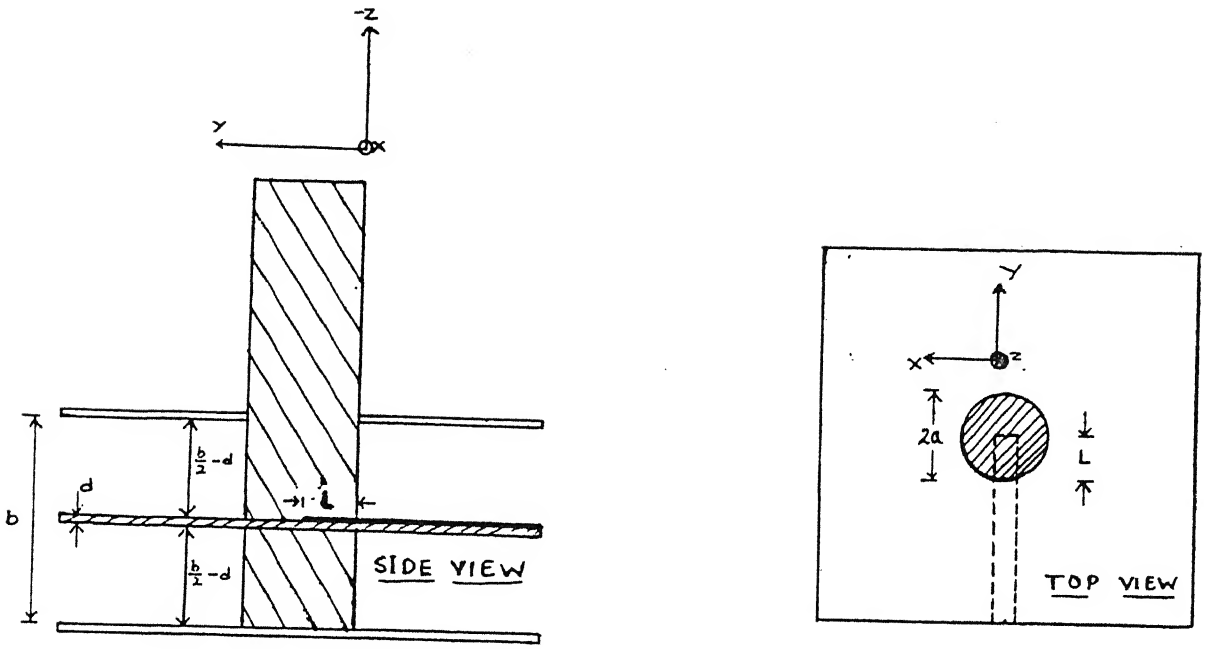

Figure 3.1: SSL Probe Dielectric Rod Antenna

It consists of a small SSL probe terminated, radially, in the centre of the guide. The probe extends to a distance L within the guide. The bottom ground-plane, at a distance $b/2 - d$, is assumed as a short-circuit.

The electric field in the guide may be determined from the electric currents flowing on the SSL probe and in the aperture surface. Let G be the Green's function corresponding to the electric field radiated by a unit source. The radiated electric field by the SSL probe and aperture surface currents will be given by:

$\vec{E}_t = \int_s \bar{\bar{G}} \cdot \vec{J} dz.$

J is the assumed current distribution on the probe. S is the total surface ($S_0 + S_a$, where S_a is the SSL probe aperture surface and S_0 is the SSL surface). The field

satisfies the following boundary conditions:

$$\hat{n} \times \vec{E} = \hat{n} \times \int_s \bar{\bar{G}} \cdot \vec{J} dx' = \hat{n} \times \vec{E}_i \text{ on } S_a.$$

$$= 0, \text{ on } S_0.$$

Dot multiplying eqn by $\vec{J}$ and integrating over the total surface S, we get:

$$\int_s \vec{J} \cdot \vec{E}_i dz = \int_s \int_s \vec{J} \cdot \bar{\bar{G}} \cdot \vec{J}' dz dx'.$$

The input impedance of the antenna at the aperture plane is equal to $-V \cdot I_i$. Hence we have:

$$Z_{in} = \frac{-1}{I_i^2} \int_s \int_s \vec{J} \cdot \bar{\bar{G}} \cdot \vec{J}' dz dx'.$$

I_i is the input current.

As the probe is assumed to be thin, and similar to a stub antenna above a conducting plane in free space, the current is assumed to be approximately sinusoidal. A current distribution of the form $I = I_1 sink_0(d - y) + I_2[1 - cosk_0(d - y)]$, is assumed. The current sheet approximating this probe is $J = I\delta$, where δ is the *impulse function or delta function.*

Evaluation of the integral gives us Z_{in} as a function of I_1 and I_2. To solve for the values of I_1 and I_2, we equate $\frac{\partial Z_{in}}{\partial I_1}$ and $\frac{\partial Z_{in}}{\partial I_2}$ to zero, which render the integral expression for Z_{in} stationary.

The field may be found in terms of a vector potential function $\vec{A}$ by means of the following equations:

$$\vec{E} = -j\omega\vec{A} + \frac{\nabla\nabla \cdot \vec{A}}{j\omega\epsilon_0\mu_0}.$$

$$\vec{B} = \nabla \times \vec{A}.$$

We define a Green's function $\bar{\bar{G}} = \hat{a}_y \vec{G} \hat{a}_y$, a solution of the following inhomogeneous equation:

$$\nabla^2 G + k_0^2 G = a_y a_y \delta(x - x')\delta(y - y')\delta(z - z'),$$

and satisfies the boundary conditions:

$G = 0$, at $x = 0, a$;

$\frac{\partial G}{\partial y}$, at $y = 0$.

The tangential electric field to be derived from $\bar{G}$ (corresponding to a vector potential from a unit y-directed current element) must vanish on the guide boundary.

For a uniform current distribution $\vec{J} = \hat{a}_y J_0 sink_0(d)$ on the SSL probe, the vector potential A is given by:

$\vec{A} = -\mu_0 \int_s \bar{G} \cdot \vec{J} da'$, where da' is an element of area on the SSL probe surface.

Integrating the complex Poynting vector over the SSL opening, we get:

$\frac{1}{2} V I_0^* sink_0 L = \frac{1}{2} V I_0 sink_0 L = \frac{1}{2} Z_{in} I_0^2 sink_0 L.$

as I_i at the base is real and equal to $I_0 sink_0 L$.

This should be the total power P_s plus the time average net reactive energy in the dielectric guide. The integral can therefore be interpreted as $\frac{-1}{2} \int_s \vec{J} \cdot \bar{G} \cdot \vec{J} da da'$ as giving the complex power,

$P_s + 2j\omega(W_m - W_e)$ into the guide.

To determine the power flow and rective energy in the field, we have to integrate and evaluate over the probe surface, $\frac{-1}{2} \int_s \vec{E} \cdot \vec{J} da$.

From the approximation that the probe is negligibly thin, and also $2\pi(\frac{1}{2} J_0) = I_0$, the total current on the probe, we have the real part giving the power radiated into the guide and the imaginary term gives the time-average reactive energy in the standing wave between the SSL probe antenna and the short circuited end of the guide.

The input impedance is given by, [16] :

$$Z_{in} = R + jX = \frac{P_s + 2j\omega(W_m - W_e)}{\frac{1}{2} I_0^2 \sin^2 k_0 L}.$$

3.4 Conclusion

A completely rigorous solution of SSL excited dielectric rod antenna boundary-value problem is just as difficult to obtain as the solution for antennas located in free space. Nevertheless, by making suitable approximations, solutions for a SSL probe in a dielectric rod waveguide can be obtained.

Chapter 4

Experimental Study of the Dielectric Rod Radiator

4.1 General

The scope of this study was mainly experimental, to study the effect of variation of the length of the probe in conjunction with the dielectric rod dimensions and the changes in input impedance, s11 characteristics, and the approximate radiation pattern.

4.2 Design approximation

The dielectric rod radiator was excited by a *suspended stripline*(SSL). Keeping in view the size compactness, and the test measurement equipment limitations, the gap between the either ground planes and the stripline dielectric substrate was kept to 0.1cm. The thickness, d of the substrate, RT-duroid, was $\frac{1}{32}$" :

This gave a b, gap between the ground planes, equal to 0.28cms (0.1+0.08+0.1). Using the data from [17] these values of b and d gave, for an input impedance of 50 Ohms (coaxial impedance) :

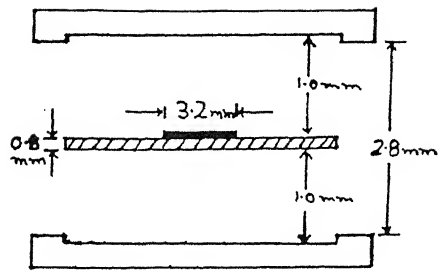

Figure 4.1: SSL Dimensions

$$b = 0.28\ cm$$

$$d = 0.08\ cm$$

$$\frac{d}{b} = 0.2857$$

$$\frac{w}{b} = 1.15$$

$$w = 0.322\ cm$$

$$for\ Z = 50.23\ ohms$$

$$\epsilon_f = 1.234$$

The dimensions of the ground planes(L) was taken as 5.0cms for compactness and easy handling, L>>w. The material used was Aluminium for easy machining.

The strip ($w = 0.32cms$) was cut on the Rubylith sheet of size 5.0cm square. This

was then printed on $\frac{1}{32}$" RT-duroid using photolithographic process. The strip was aligned on the centre line and upto the centre of the PCB square :

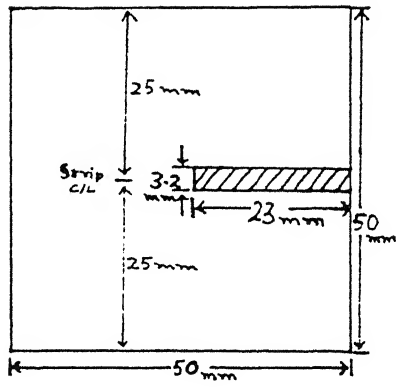

Figure 4.2: Strip Dimensions

4.3 Ground planes

The ground planes were selected of Aluminium (3mm thick) of 5.0cm square dimensions. To create the SSL structure each ground plane was milled on each side to a uniform thickness of 2.8mm, for flatness. A cavity of depth 0.1cm depth was created on one sideof each ground plane, leaving a border of 5.0mm to enable drilling and screw-nut tightening.

This created a hollow of 4.0cm square and 1.0mm depth on each plane. A channel was cut on one side of each plane for the stripline to pass through without touching either plane.

The substrate was sandwiched between the ground planes, with the stripline passing through the channel and a space of 5.0mm, from the strip centre, on each side. This structure was held together with screw and nuts through holes drilled along the sides. This also helped to align the stripline in the correct configuration.

4.4 Feed structure

To fix the coaxial connector on the assembly, a aluminium piece was machined to precise dimensions as shown in the figure 4.5. The hole was aligned accurately to ensure that the centre conductor was to lie on the precise centre of the stripline, making good eletrical contact. The dielectric between the centre conductor and the outer sleeve was not to protrude even a fraction of a millimetre to ensure flush fitting of the assembly with the radiator structure.

The SSL can be fed by standard in-line coaxial connectors at microwave frequencies. In this case the ground plane spacing is generally larger than the inner diameter of the outer conductor the coaxial connector with the result the fringing field of the SSL gets intercepted by the outer conductor of the coaxial line.

This was fixed to the lower ground plane by screws, thus, enabling the top ground-plane to be easily slid out/in for changing the dielectric rods and varying the stripline length.

4.5 Dielectric Rods

By the equation [6], the diameter, D_{max} of the dielectric rod at the feed end was given by :

$$D_{max} = \frac{\lambda_0}{\sqrt{\pi(\epsilon_r - 1)}}$$

for a design wavelength of $\lambda_0 = 3cms$, this gave a D_{max} of $1.53cms$.

As a compromise and mathematical simplifications, the diameter was kept at 1.0cms. A step of 0.5mm at the feed end was made to ensure a tight fit of the rod on the stripline, whatever be the measurement plane orientation.

A hole of dimension 1.0cm diameter, at the top ground plane centre, was drilled through which the rod could be passed and kept in a fixed plane.

A disc, of thickness 1mm, and diameter 1.0cm, was machined to be kept between the lower ground plane and the stripline substrate. This was aligned to the precise centre of the lower ground plane and fixed permanently by adhesive.

Three rods of similar diameter, using Teflon, but of varying lengths 1.0cm, 2.0cm, and 3.0cm were fabricated. The constraint of time in the machining restricted the use of more lengths or diameters.

4.6 Testing

For various lengths of the dielectric rod radiators, using varying stripline lengths, s11 magnitude measurements and input-impedance calculations were made using the

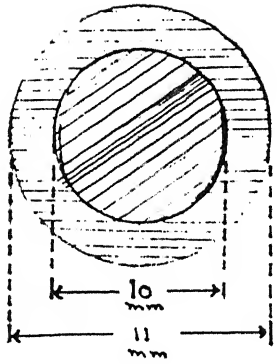

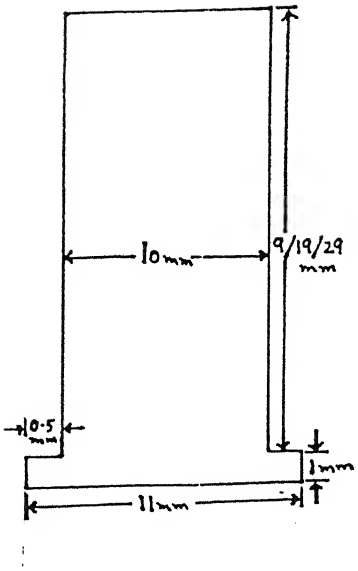

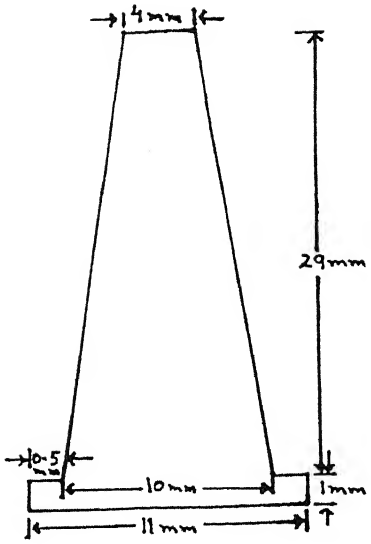

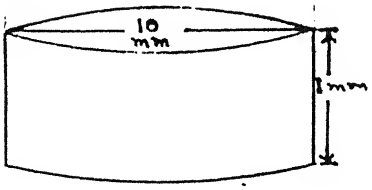

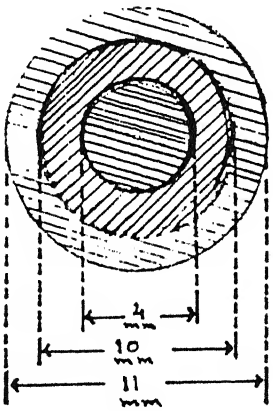

Cylindrical Tapered

Dimensions : Dielectric Rods

Network analyzer.

For a particular fixed length of the stripline, the s11 magnitude and phase measurements were made, using dielectric rod radiators of varying lengths. This enabled to arrive at the appropriate and optimum length of the stripline. The stripline length was reduced in steps of 0.5mm .

4.7 Radiation pattern : experimental setup

In the absence of an anechoic chamber, a makeshift but effective arrangement was made for plotting the approximate radiation pattern of the *SSL excited dielectric rod antenna.*

The experimental setup, figure 4.7, consisted of the antenna mounted on a rod, in the center of a rotary table. The antenna could be aligned in the E - plane or the H - plane. The rod, with a pointer at the base, could be moved in steps of, minimum, 1^0.

This radiating system was fed by a Wavetek microwave source(8.2 to 12.4 GHz) through a coaxial line.

The receiving end (at a distance of 1meter) consisted of a standard X-band horn antenna, also mounted on a rod. This horn was kept stationary and connected to a spectrum analyzer (SA).

Centers of the rod antennas and the horn antenna were aligned and kept at the same height from the tabletop.

Both the transmitting and the receiving systems were switched ON and the rod antenna rotated slightly, in the horizontal plane, to get a peak on the SA. This was taken as the 0^0 alignment.

The relative power received, with respect to the peak, was noted as a function of angle, 0^0 *to* 180^0 and 0^0 *to* -180^0.

A set of readings having been taken in the E-plane, the rod antenna was affixed in the H-plane and the above procedure repeated.

4.8 Problems

The fabrication, testing and measurements brought to light a wide sphere of problems, the most pressing of which were :

1. The time taken in fabrication: Keeping in view the precise and accurate machining dimensions, a lot of time was wasted during the workshop phase. Upto a fortnight in case of the connector fixture. This limited the variations of the other dimensions.

2. Radiation pattern measurement: This part having to be conducted in the microwave laboratory itself, took upto 3 days for a set of readings, for any one structure. The movement of persons in the lab used to create wide fluctuations in the readings. Added to this was the reflection from the walls, the equipment in the lab, proximity of the walls, the feed assembly and the reader itself. The asymmetry in the patterns brings this out.

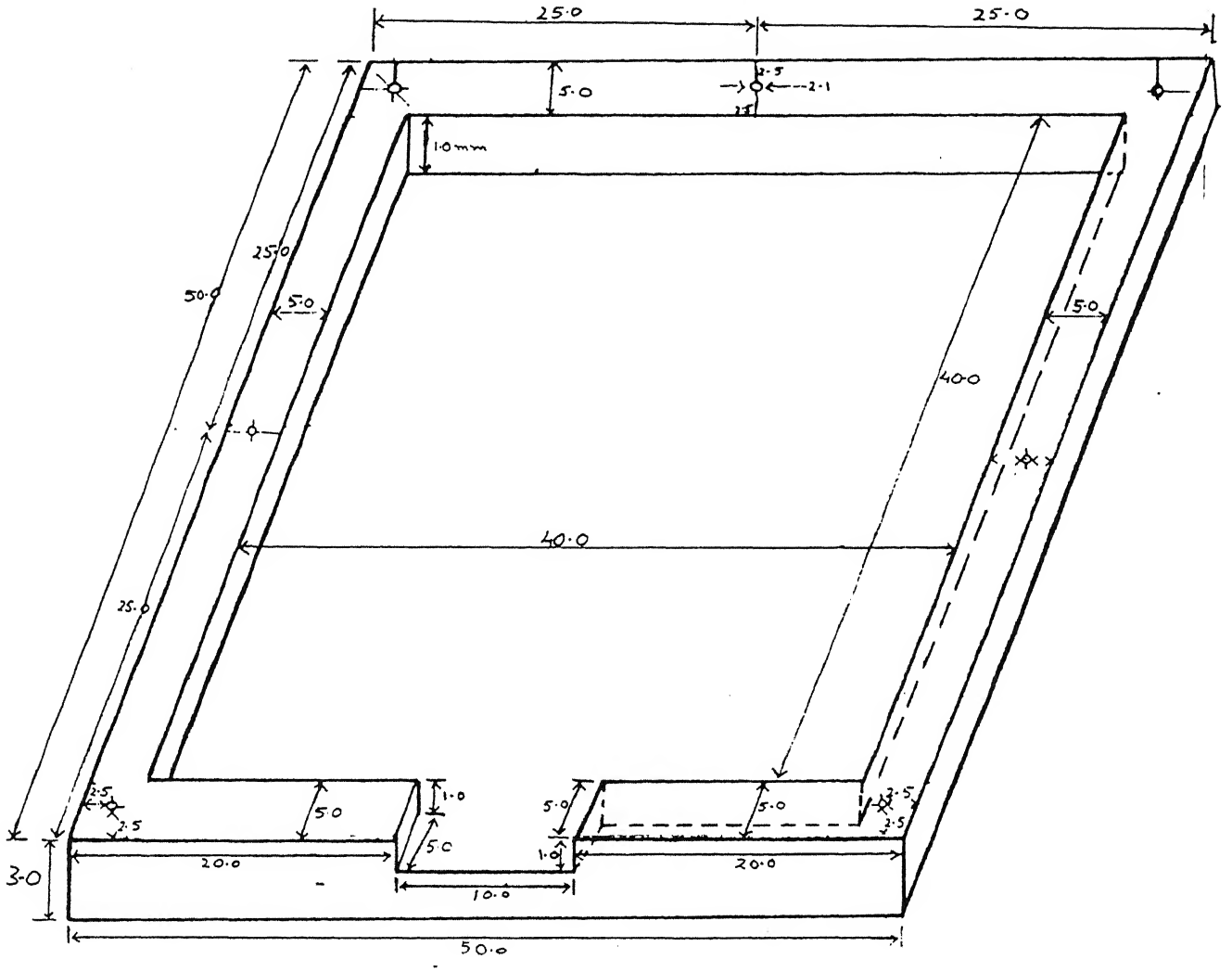

Figure 4.3: Ground plane Dimensions

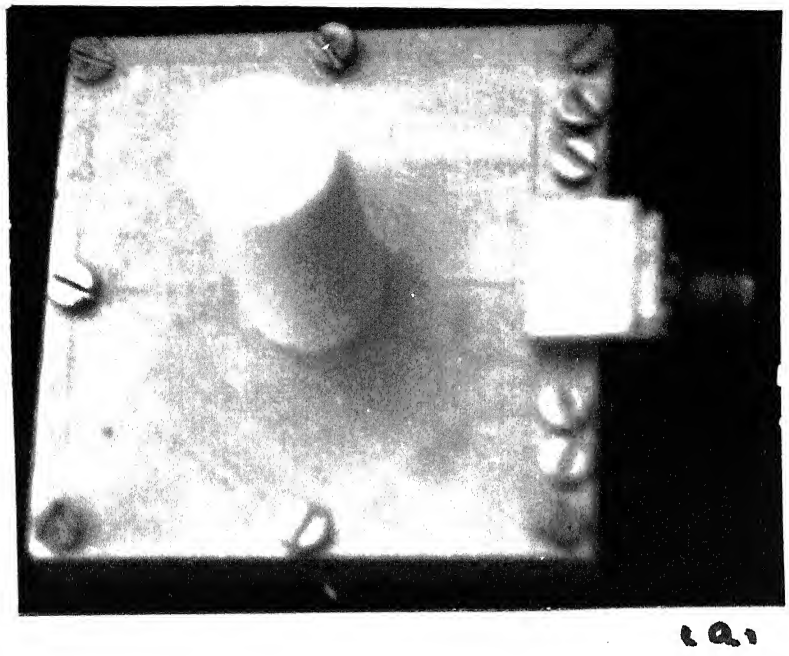

(a)

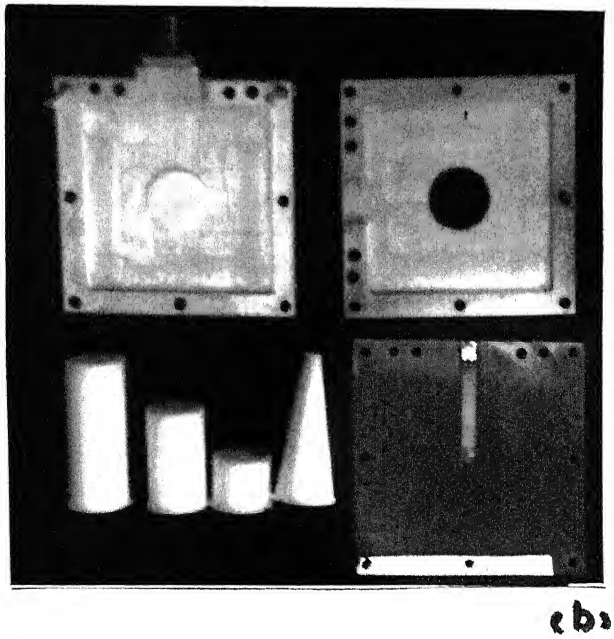

(b)

Figure 4.4: a. Assembled Antenna; b. Disassembled Antenna

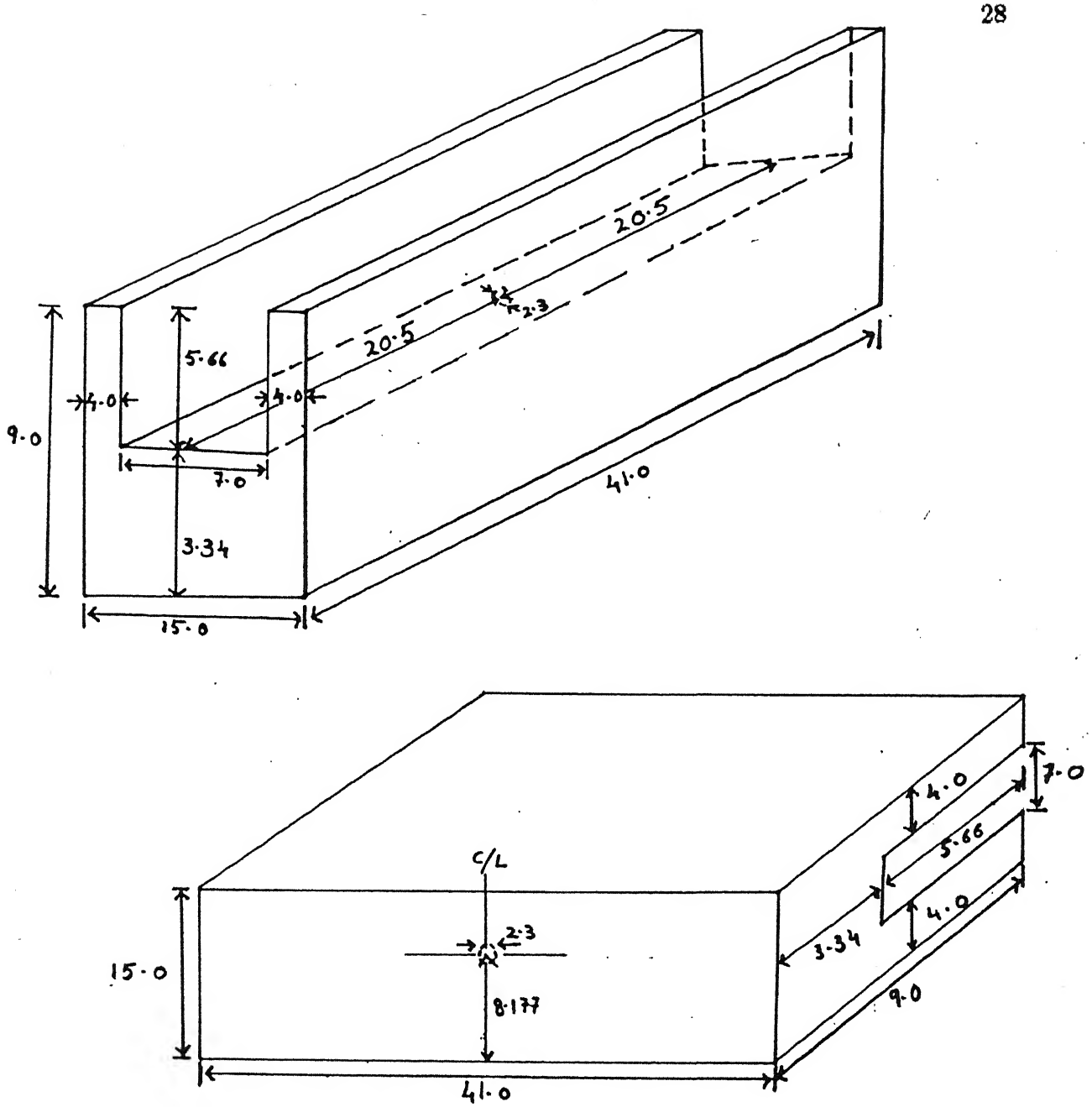

Figure 4.5: Coax connector block

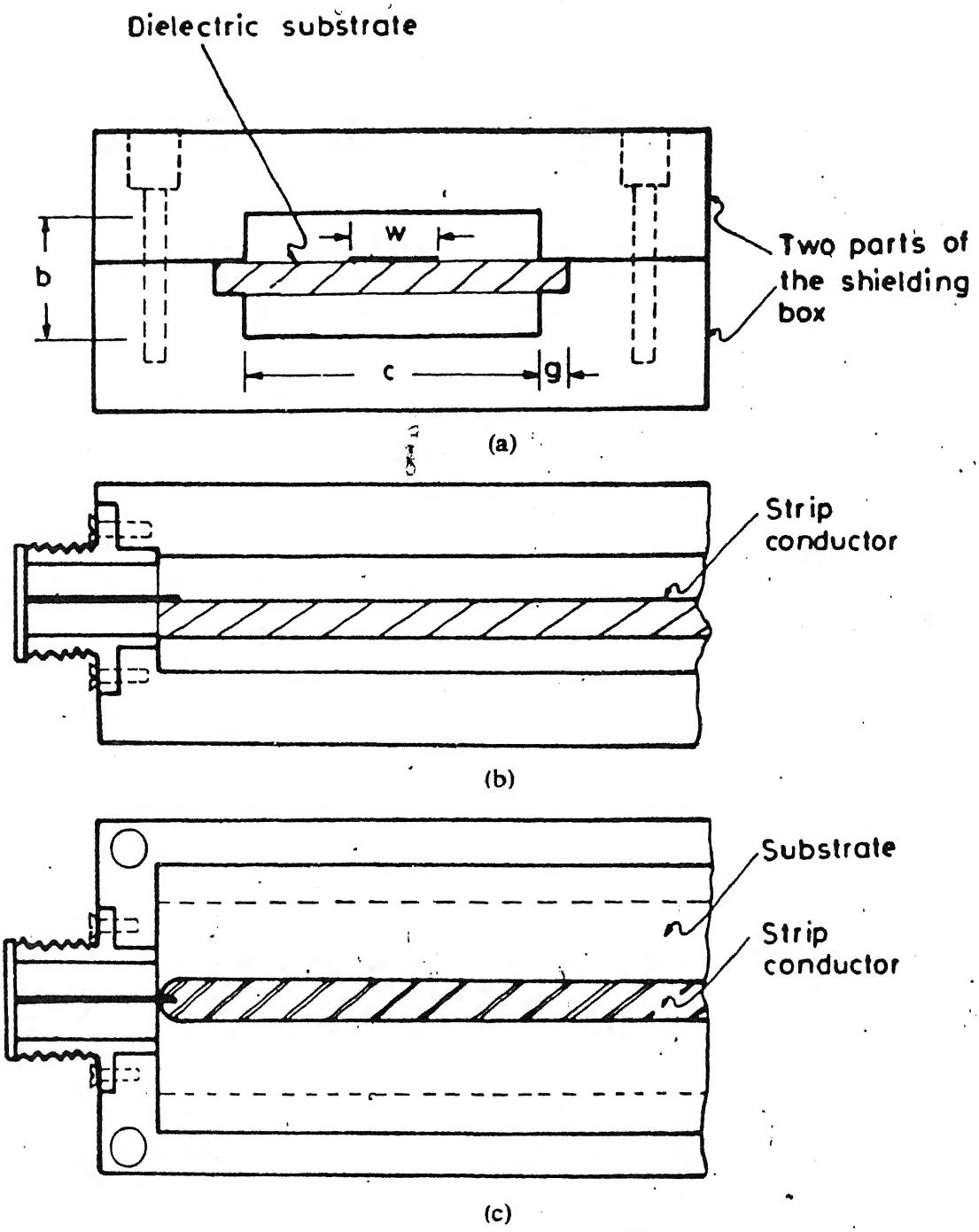

(a) Cross-sectional view of suspended stripline (b) Coaxial to suspended stripline launcher—side cross-sectional view (c) View of the launching end with top portion of the housing removed.

Figure 4.6: Coaxial to SSL transition

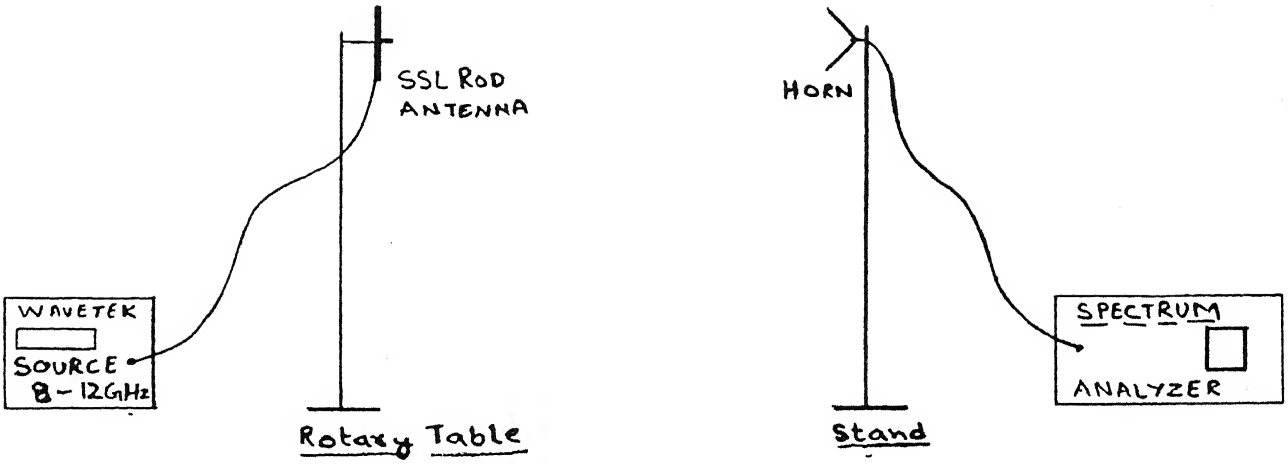

Figure 4.7: Radiation pattern measurement: setup

Chapter 5

Experimental Results and Conclusion

5.1 Introduction

This chapter analyses the data collected on the basis of tests and meausrements carried out on the dielectric rod antenna, and to establish a working model for the same.

5.2 S11 Measurement

The s11 measurements on the dielectric rod antenna commenced with a SSL length of 25mm, from the feed point. This brought the free end to the center of the dielectric rod. The test was initiated on the 30mm rod and also repeated on the 20mm and 10mm rods,to study the variation of s11 with dielectric rod lengths. The results were plotted and are presented in the graphs 1 to 4.

Phase was measured for each frequency reading separately and having obtained the s11 and phase parameters the impedance calculations were made with the Fortran program at appendix 'A'.

These set of readings were repeated for varying lengths of the stripline $\cdots$ the

stripline length was reduced in steps of 0.5mm, upto 22mm, i.e. the edge of the rod. For each length of the strip line the readings were taken for the three different dielectric rod lengths.

Here, only 4 sets of readings, for stripline lengths of 25mm, 24.5mm, 23.5mm and 23mm are presented.

The results of these set of *graphs* is as follows :

5.2.1 25/10,20,30

The SSL length was 25mm, thus terminating in the center of the rod. This set of readings were repeated for the 10, 20, and the 30mm rod. From graphs 1,2,3, and 4 it is seen that the best match is available at 9.8GHz. The other s11 dips, not consistent frequency-wise for all rods, could probably be due to the cavity effects or the termination effects of the SSL. The best s11 magnitude recorded was -20 dB for the 25/20 (graph 2).

Graph No. 4 has been plotted as comparison plot for the 3 different rod lengths.

5.2.2 24.5/10,20,30

The SSL was shortened in length, from the free end side, in steps of 0.5mm. This set of graphs 9 to 12, for a SSL of 24.5mm shows that the match frequency is 9.75GHz, with a s11 of -30dB for 24.5/20.

5.2.3 23.5/10/20/30

For the SSL of 23.5 mm, and the 3 rod lengths gave a best match at 9.82GHz and s11 of -22dB. The set of graphs 17 to 20 shows that the other s11 dips also become

consistent,frequency-wise, as the SSL was shortened.

5.2.4 23/10,20,30

Graphs 25 to 28 were plotted for a SSL of 23mm. It is seen that the best match is available at frequency 0.73GHz but with a s11 of only -12dB.

The entire set of readings above, were recorded with no measures having been taken to nullify the side radiations. These side radiations arise due to the field in the dielectric substrate. To counter this, the edges of the SSL substrate were covered with aluminium foil. This arrangement, when tightened between the two ground planes, reduced the side radiation to a large extent.

The above experimental procedure was repeated and plotted as graphs 33 to 36.

5.2.5 s23/10,20,30

Here 's' denotes the short between the two ground planes by the aluminium-foil. It is seen, from graph 36, that the frequency match is available at 9.86GHz with a s11 of -32dBs.

This structure provides a +10dB bandwidth of 0.3GHz.

From the above is evident that the best frequency matches are available for the 20mm rod. This needs to be analyzed and elaborated upon in the future studies.

5.3 Side Radiation

The above arrangement of using aluminium foil to remove the side radiations, due to the field through the SSL substrate,works out fine, easy, and neat for a single element. In the case of an array, however, this arrangement is not feasible. For an

array, a suggested way of susuppressing this radiation could be the use of shorting pins, interspaced $< \frac{\lambda}{8}$, around the rods as shown, figure 5.1 :

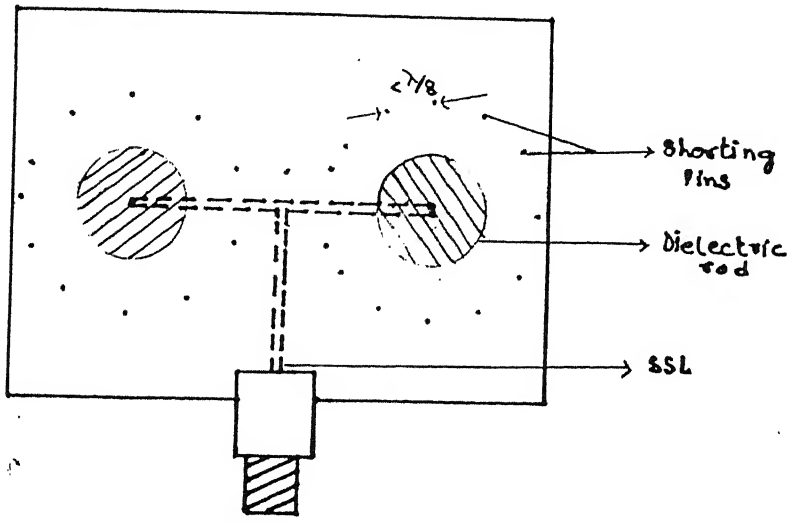

Figure 5.1: Shorting pin arrangement: Two rod array

5.4 Impedance and Phase measurements

Phase was measured for each varying structure at the various frequency readings separately. With the available values of phase and s11, the input impedance was calculated utilising the Fortran program at appendix 'A'. These set of graphs are plotted as 8,16, 24, 32, 40, and 42. From an input impedance value of 34 ohm (graph32), the best match to the coaxial line impedance(50ohm) is available at 49.73ohm (graph40) for the s23 set of readings.

A relative comparison of graph32 and graph40 (same SSL length but aluminium foil in the latter) gives the distinct advantage of having used the shorting arrange-

ment.

5.5 Tapered rod

Whole of the observations above and the deductions is based upon the circular cylindrical rods. A variant, circular conical dielectric rod (30mm) was also fabricated and tested. The set of graphs 41 to 44 covers the s11, phase and impedance characteristics as a function of the frequency. In this case the SSL length was maintained at a constant 23mm, with the aluminium foil in position.

The s11 plot (graph41) shows that the best frquency match was available at 9.78GHz and provides a s11 of -28dB. The input impedance (graph42) gives us an input impedance of 47.5ohm at the frequency 9.78GHz.

5.6 Cylinder vs Tapered rod

An analysis of the recordings and deductions brings out the fact that the best match was presented by the 23mm SSL for the 20mm rod, with the aluminium foil in position. However, the variations are not very significant. Various other shapes, e.g. spherical end, stepped rod, etc need to be studied to arrive at a conclusive deduction.

5.7 Radiation Pattern

In the absence of an anachoic chamber and a proper arrangement for making the radiation pattern measurement, a modified radiation pattern measurement arrangement (chapter 4, sec 4.7) was made in the microwave laboratory.

This set of graphs is plotted as graphs 41 to 53 . Both E- and H-plane radiation patterns were plotted. It is seen that the H-plane radiation patterns are narrower

than the E-plane. This is due to the asymmetric nature of the HE_{11} mode.

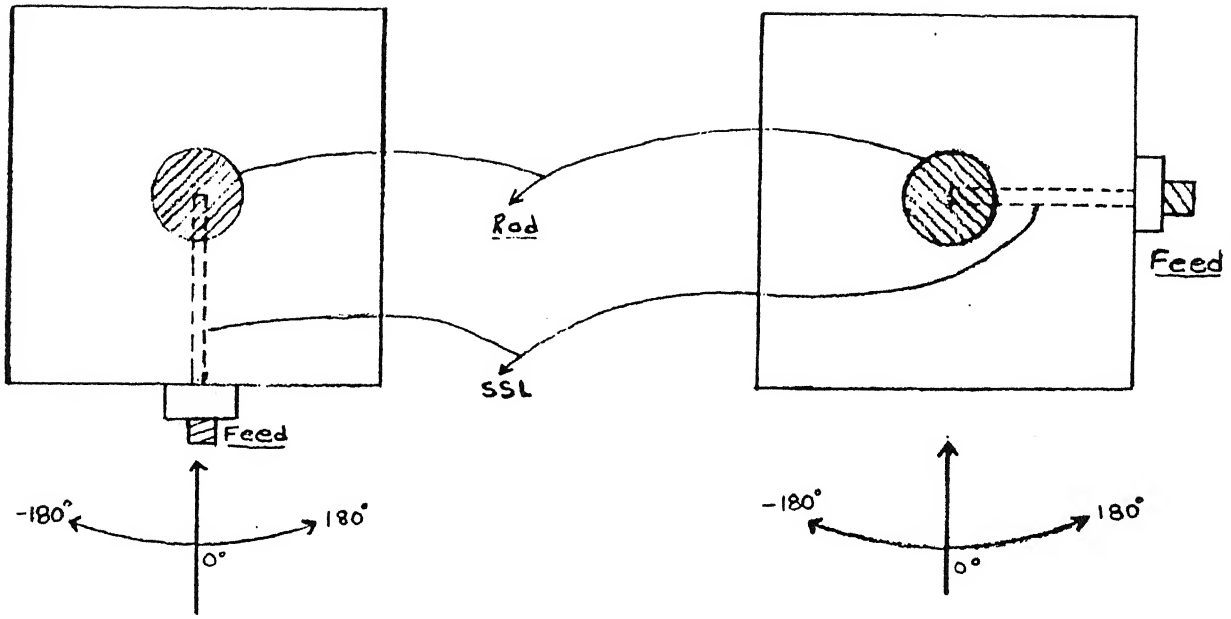

Figure 5.2: E - plane H - plane

The pattern measurements commenced with the tapered rod (30mm) in the E-plane, and also in the H-plane. The readings are plotted as graphs 45 and 46 and for comparison as graph 47.

The pattern asymmetry between 0^0 to 180^0 and 0^0 *to* -180^0 has arisen, probably, due to the measurement equipment not being located centrally (equal distances from all sides) and also, probably, due to the other equipment. This pattern includes the radiations of the microwave source and the feed coaxial.

Graphs 48 to 50, for 20mm rod and SSL of 23mm length show that the E-plane half-power beamwidth is 40^0 and for the H-plane is 95^0.

A set of readings for the 20mm cylindrical rod and the 30mm tapered rod (SSL length of 23mm) was repeated but with the aluminium foil, covering the SSL substrate

edges, removed. These are plotted as graphs 51 to 53. It is seen, on comparison with graphs 45 to 50, that there are lots of side lobes, which were otherwise suppressed by the foil.

Simple gain calculations using the formula,

$G(dBs) = 10\log_{10}(\frac{41000}{\Theta^E_{HP}\times\Theta^H_{HP}})$,

gave a gain of 15dB for the 30mm tapered rod and a gain of 11dB for 20mm cylindrical rod.

5.8 Theoretical verification

Modes higher than the fundamemntal HE_{11}, [18], mode cannot propagate provided $\frac{d(diameter\,of\,rod)}{\lambda_0} < \frac{0.628}{\sqrt{\epsilon}}$. The first two higher modes, TE_{01} and TM_{01}, produce a null in the end-fire direction.

Gain and Beamwidth : The gain of a antenna is the product of the directivity and the radiation efficiency. The maximum gain of a antenna occurs, 100

$\beta - k_0 L = \pi$, and the gain is given by,

$G = 4\zeta\frac{L}{\lambda_0}$, where the gain factor ζ is, $\zeta \simeq 1.8 + 0.4\frac{Lambdao}{L}$.

If the length of the rod antenna is increased, the gain will monotonically increase and the beamwidth will decrease, but the side-lobe level will go up.

The half-power beamwidth of a maximum gain design is given by, $\Theta_{BE} = \Theta_{BH} \simeq 55\sqrt{\frac{\lambda_0}{L}}$ degrees.

Beamwidths narrower than about 20^0 are difficult to realize in practice, [18], with a single dielectric rod. For narrower beams, a linear array of rod radiators may be used. Since the radiating elements are of the surface wave type, mutual coupling

must be taken into consideration while analyzing.

5.9 Scope for future work

This experimental study has been studied only in terms of variations of rod lengths (upto λ) and stripline lengths. Future studies could be carried out on the following:

- Effect of cavity backing, on radiation characteristics.
- Effect of moisture on the radiator surface.
- Antenna characteristics as a function of the dielectric rod *diameter*.
- Effect of *dielectric constant* on the antenna characteristics, keeping other physical dimensions same.
- antenna arrays, linear and rectangular.

5.10 CONCLUSION

This thesis has presented an experimental study of a dielectric rod radiator characteristics as a function of the dielectric rod lengths, shapes, and stripline lengths. The salient features of the SSL excited dielectric rod radiator are :

- All rods, but one, are of cylindrical shape.
- Only one tapered rod was used as a comparative study.
- The effect of shorting out the side radiation was studied both in impedance tests and radiation patterns.
- the antenna has a compact and mechanically robust construction.

- ideally suited for array applications, however this has to be studied and confirmed.

References

[1] A.A. Kish and Lotfollah Shafai, *Radiation characteristics of the Short Dielectric Rod Antenna : A numerical solution*, *IEEE trans AP*, vol. AP35, pp:139-146, Feb 1987.

[2] Arthur D. Yaghijan and Edward T. Kornhauser, *Modal Analysis of the Dielectric Rod Antenna Excited by the HE_{11} Mode*, *IEEE trans AP*, vol. AP20, pp:122-128, Mar 1972.

[3] K. Mahdjoubi and C. Terret, *An Analysis of Piecewise Homogeneous Dielectric Rod Antennas*, *IEEE trans AP*, vol. AP34, pp:599-601, Apr 1986.

[4] O.F. Halliday and D.G. Kiely, *Dielectric Rod Aerials*, *JIEE*, vol. 94, pp:610-618, 1947.

[5] Kiely D.G., *Dielectric Aerials*, *John Wiley and Sons Inc*, New York, 1953.

[6] Prof. R. Chatterjee, *Dielectric and Dielectric-Loaded Antennas*, *John Wiley and sons inc.*, New York, 1985.

[7] J. Brown , *The Radiating Properties of End-Fire Aerials*, *IEE proc.*, vol-100, Part B, pp:27-34, 1957. ock *IEE proc.*, vol-100, PtIII, 1953.

[8] J. R. James, *Theoretical Investigations of Cylindrical Dielectric Rod Antennas*, *IEE proc.*, vol-114 , pp:309-319, 1967.

[9] A.Z. Fradin, *Microwave Antennas, Pergammon Press*, 1961.

[10] D.Marcuse, *Theory of Dielectric Waveguides, Academic Press*, New York, 1974.

[11] Marcateli E.A.J. and Schmeltzer R.A. , *Hollow Metallic and Dielectric Waveguides for Long Distance Optical Transmission and Lasers, Bell Tech Syst Journal*, vol-43, pp:1783-809, 1964.

[12] N.S. Kapany, *Fibre Optics, Academic Press*, New York, 1967.

[13] D.D. King, *Properties of Dielectric Image Lines, IRE trans MTT.*, vol-3,i pp:75-81, 1965.

[14] Goswami J.C. , *Analysis and Design of SSLA array element, Thesis submitted for M. Tech. to the deptt of E.E., I.I.T. kanpur*, April 1989.

[15] Horton C.W., Karal F.C. and Mckinney C.M., *On the Radiation Patterns of Dielectric Rods of circular Cross section - the TM_{01} Mode, J. Appl. Phys.*, vol. 21, pp:1279-83, 1950.

[16] Robert E. Collin, *Field Theory of Guided Waves*, McGraw Hill Book Company Inc., 1960.

[17] Bharathi Bhatt and Shiban K Kaul, *Stripline like Transmission Lines for Microwave Integrated Circuits, Wiley Eastern Co. ltd.*, 1989.

[18] P. Bhartia and I.J. Bahl, *Millimeter Wave Engineering and Applications, John Wiley and Sons*, 1984.

```
      complex s11(30), z1(30)
      integer i, nmax
      real mag(30), magdb(30),pha(30)
      real freq(30), z0
      open(unit = 10, file = 'infile.for')
      open(unit = 20, file = 'outfile.for')
      read(*,*)nmax
      do i = 1, nmax
      read(10,*)freq(i),magdb(i),pha(i)
      end do

      q = 3.1415927 / 180.0
      z0 = 50.0
      do i = 1,nmax
      mag(i)= 10**(magdb(i) / 20.0)
      x = cos(q*pha(i))
      y = sin(q*pha(i))
      s11(i)=mag(i)*cmplx(x,y)
      z1(i)=z0*(1.0+s11(i)) / (1.0-s11(i))
      write(20,30)freq(i),z1(i)
      end do
30    format(f9.3,5x,f10.4,2x,f10.4)
      stop
      end
```

S11 PLOT: 25/10

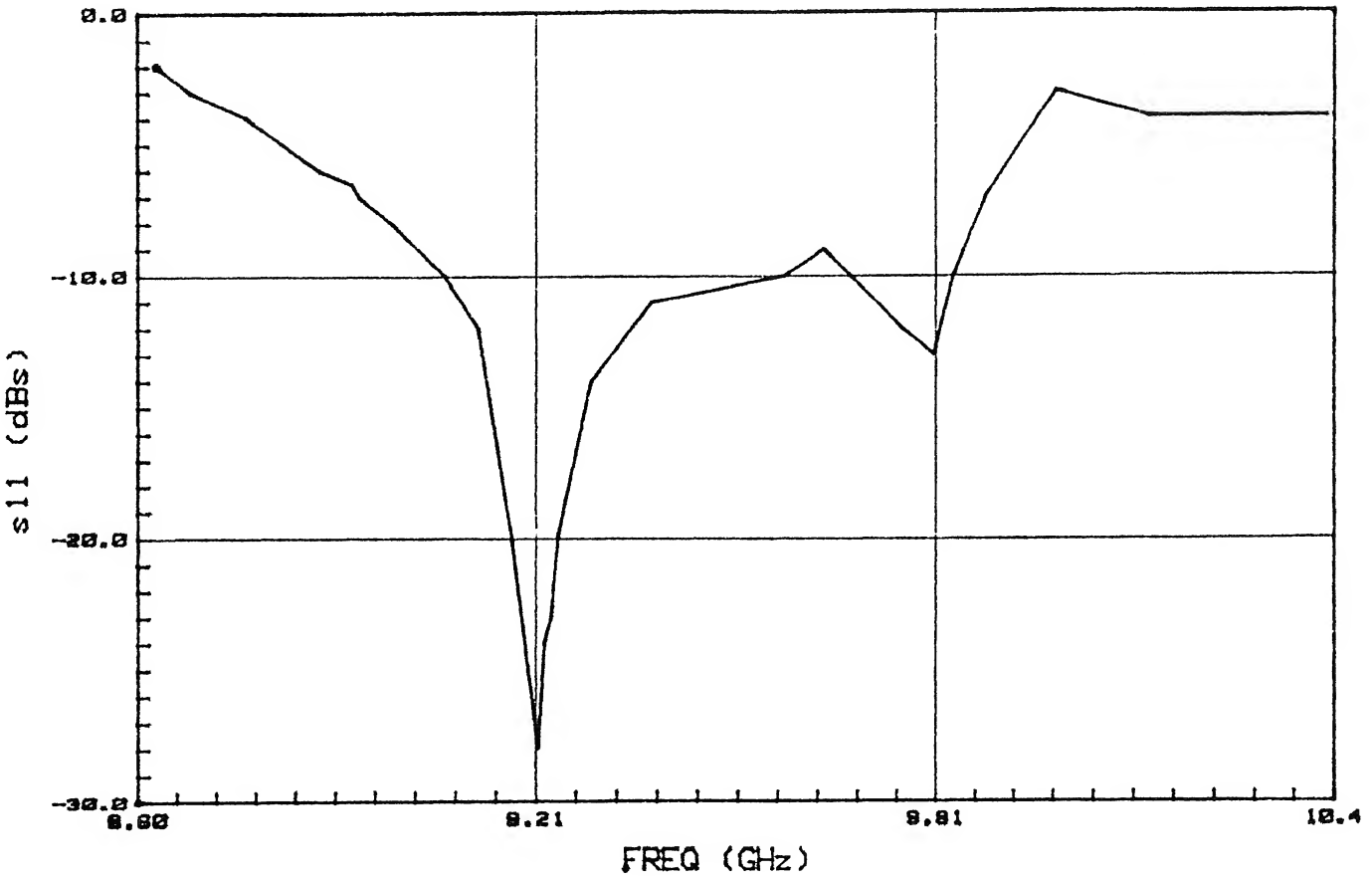

S11 PLOT: 25/20

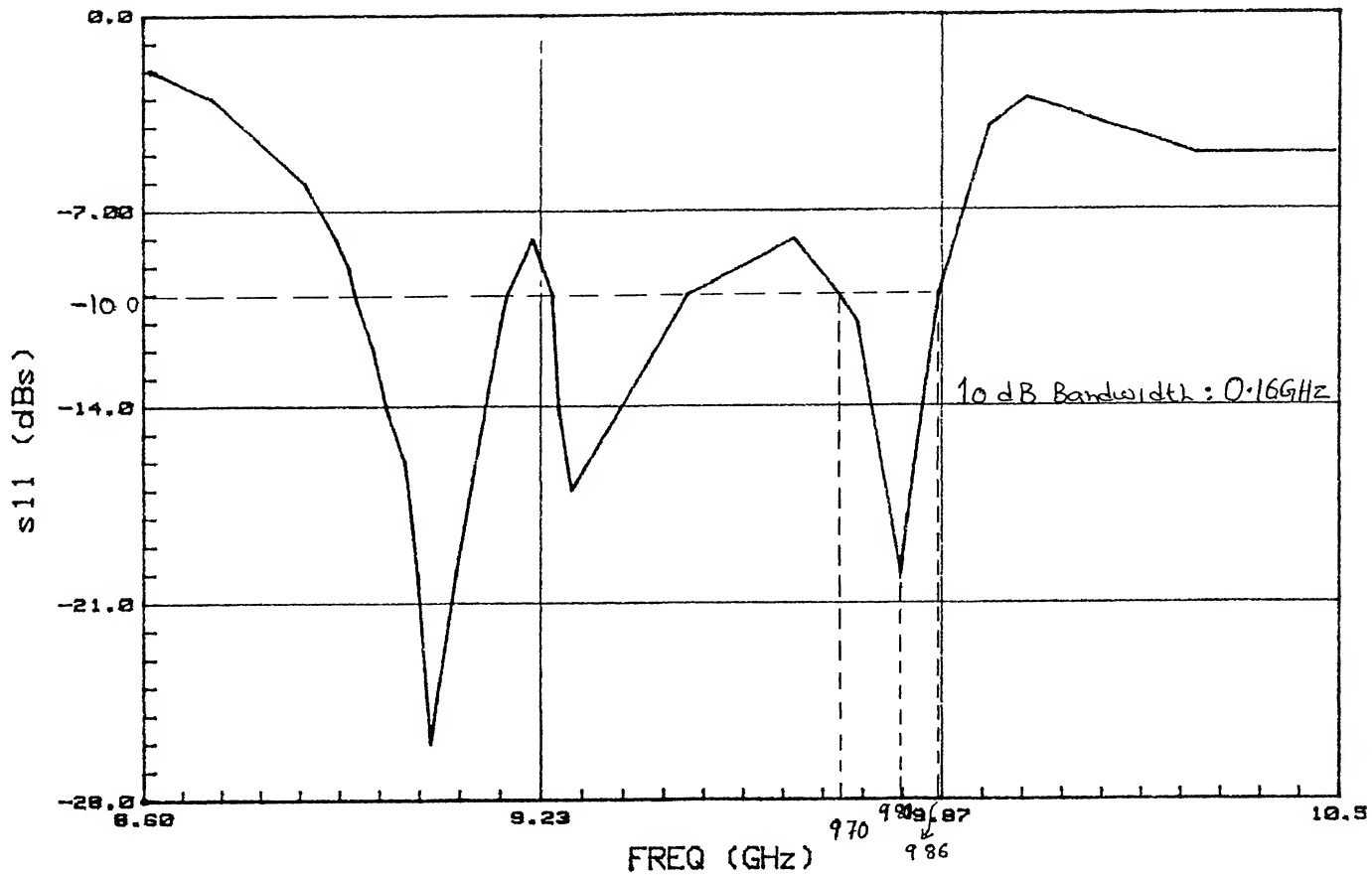

S11 PLOT: 25/30

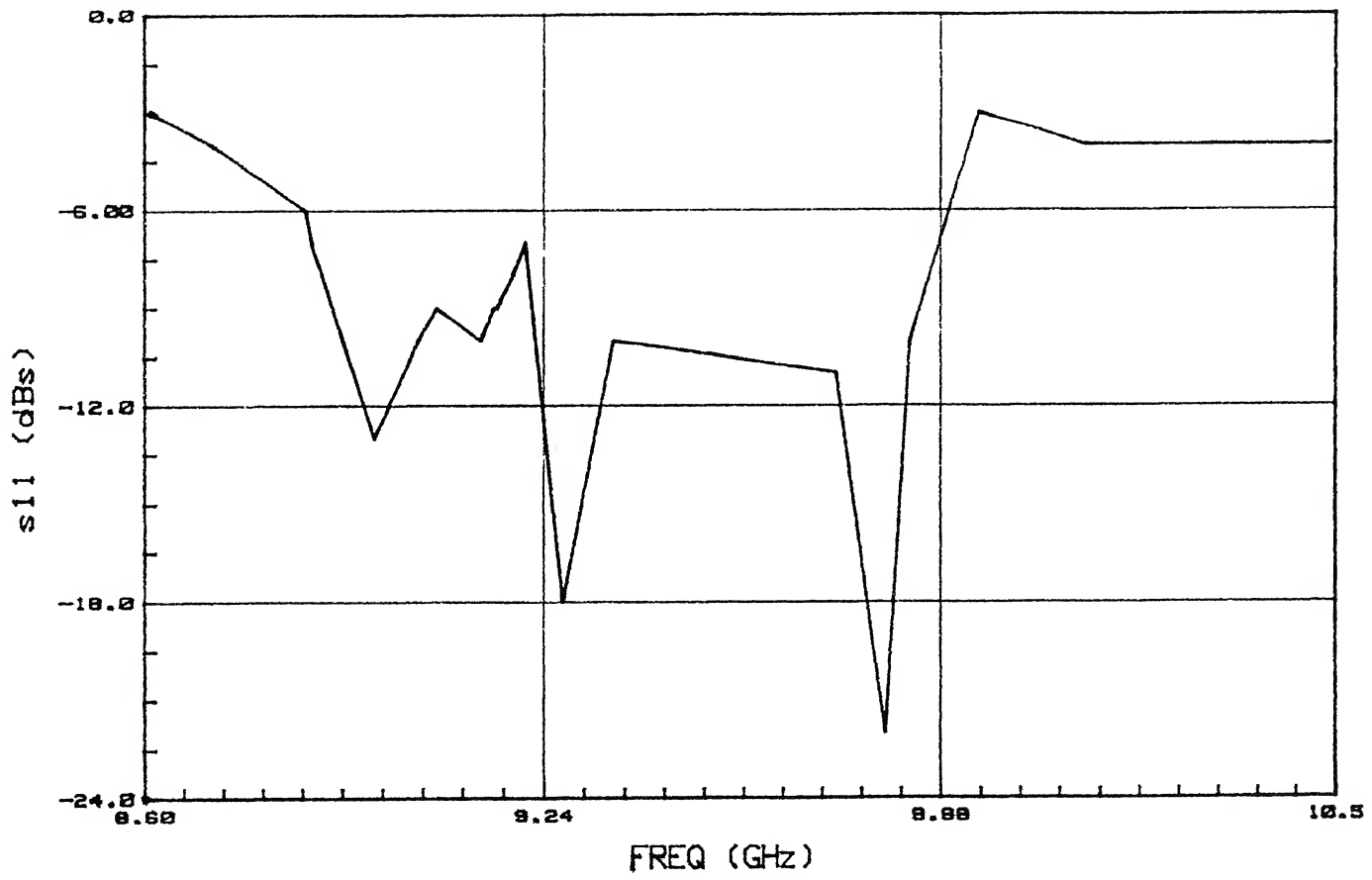

S11 PLOT: 25/10,20,30

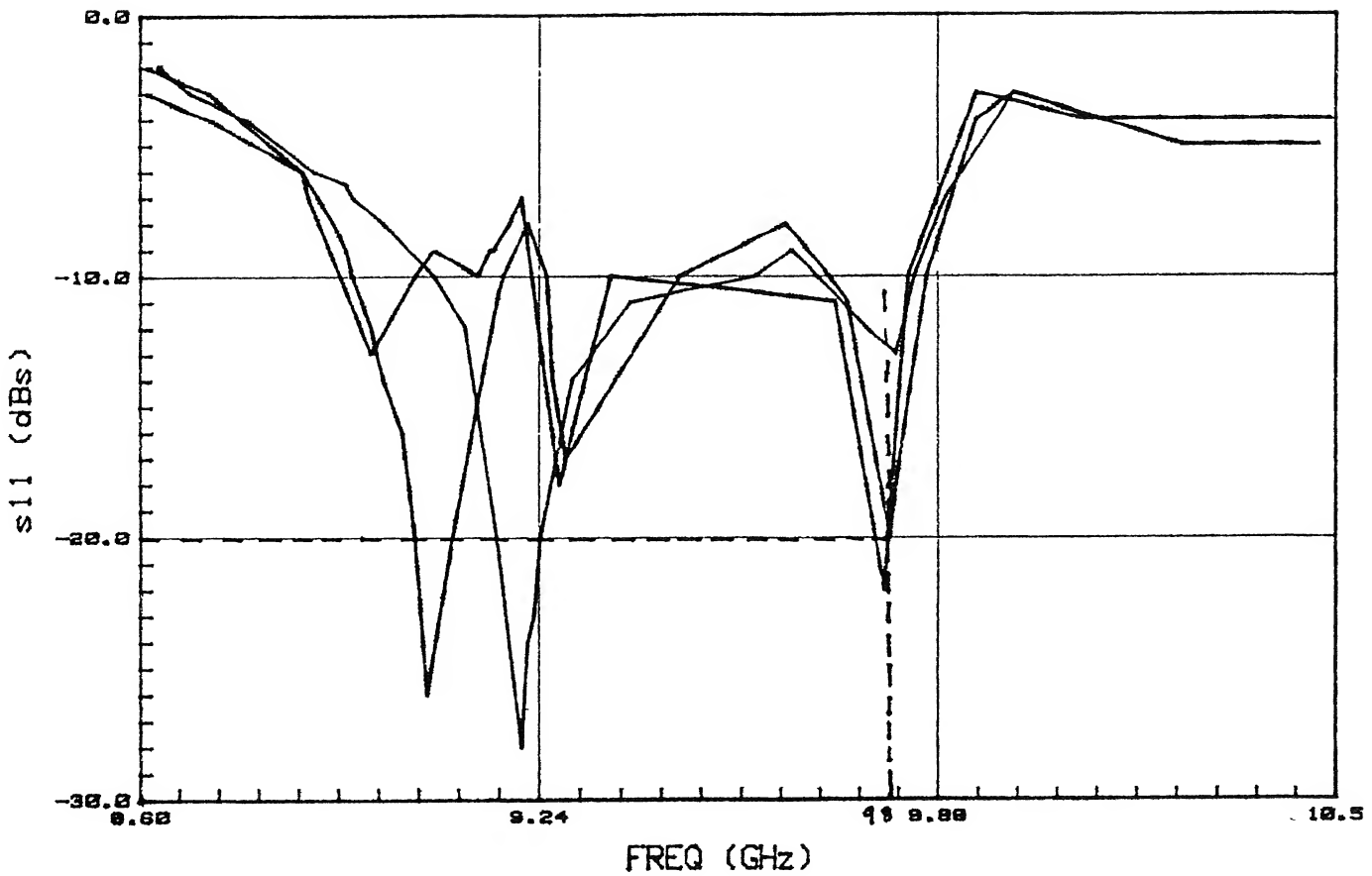

IMPEDANCE PLOT: 25/10

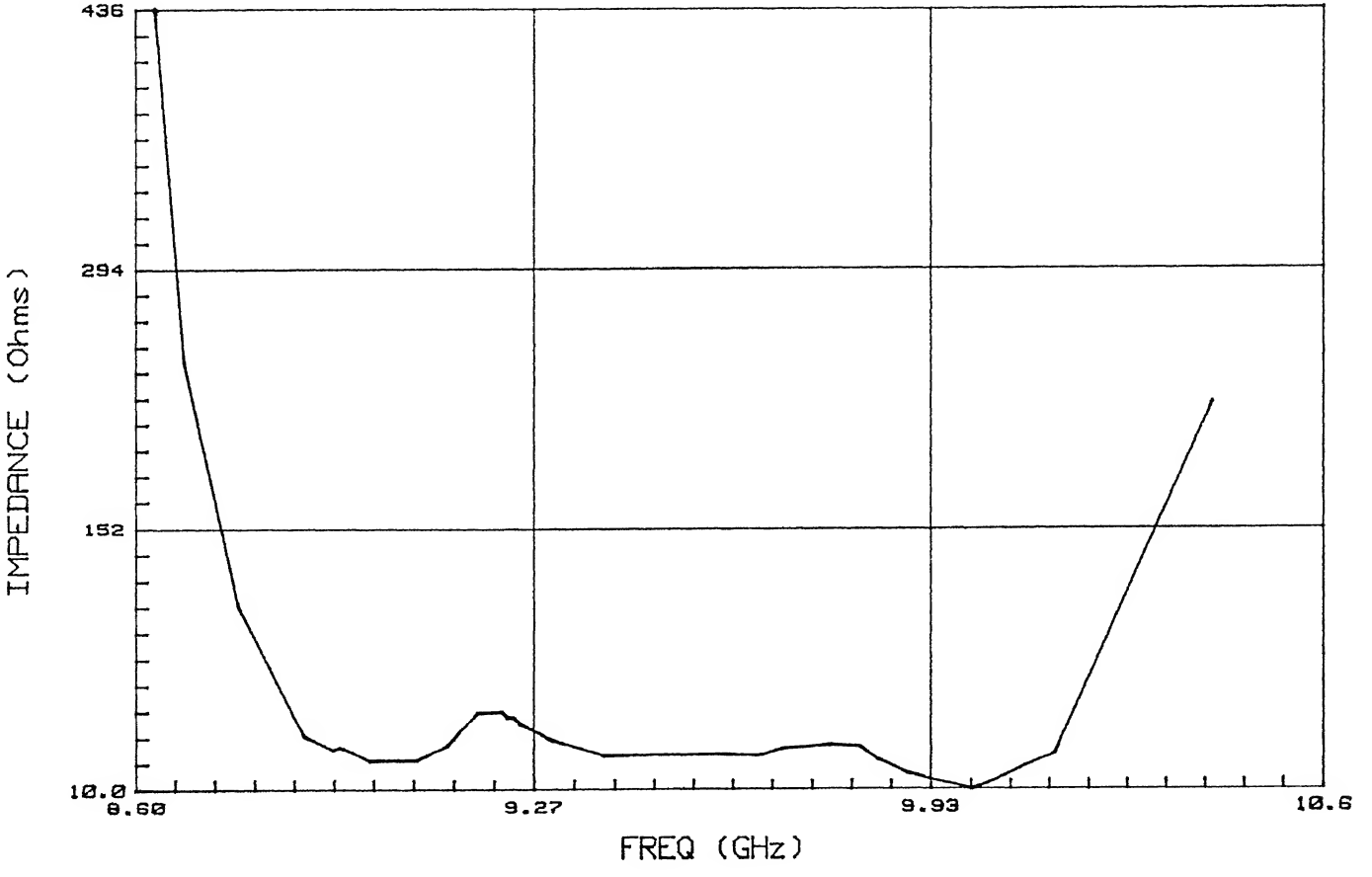

IMPEDANCE PLOT: 25/20

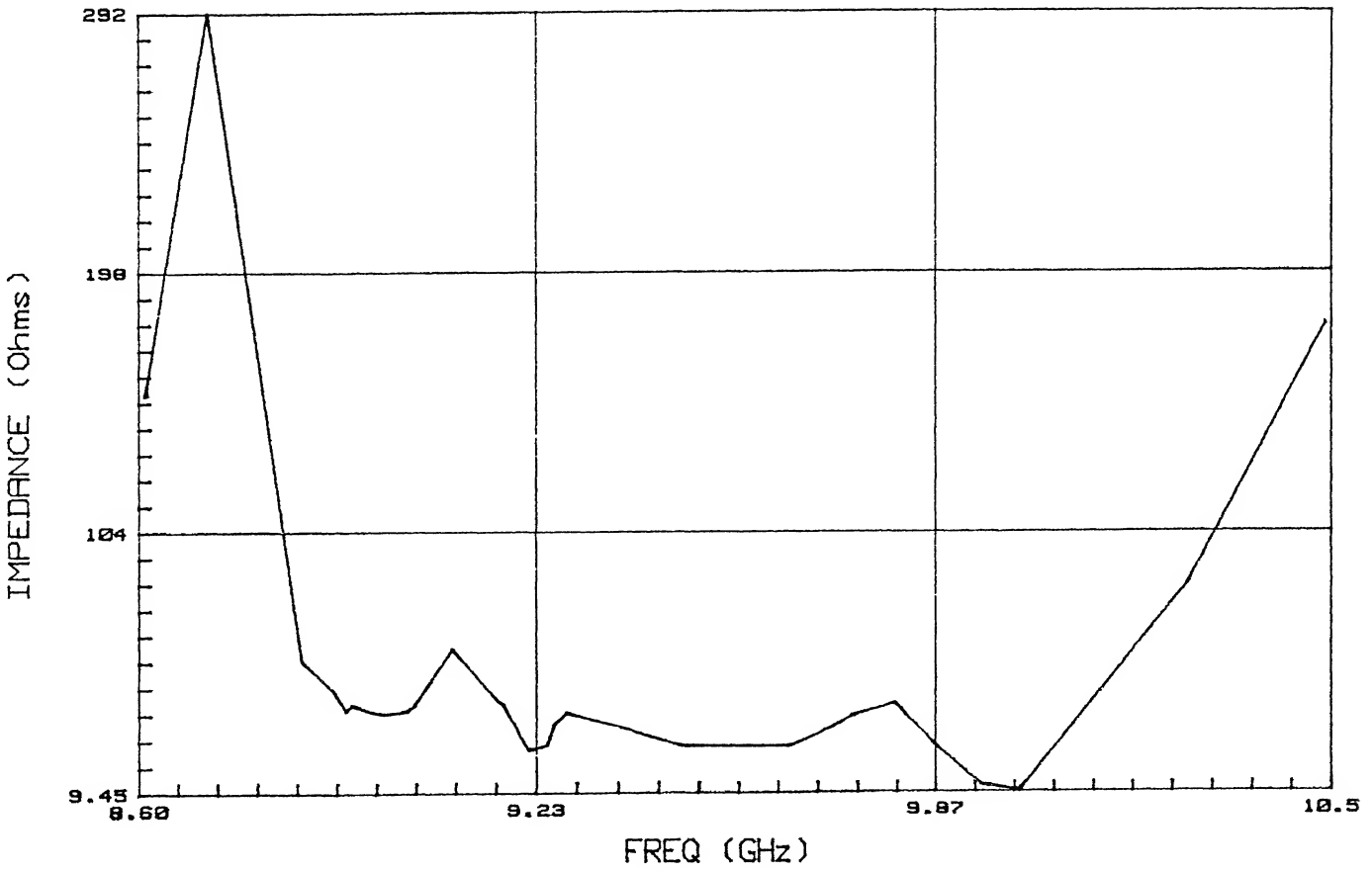

IMPEDANCE PLOT: 25/30

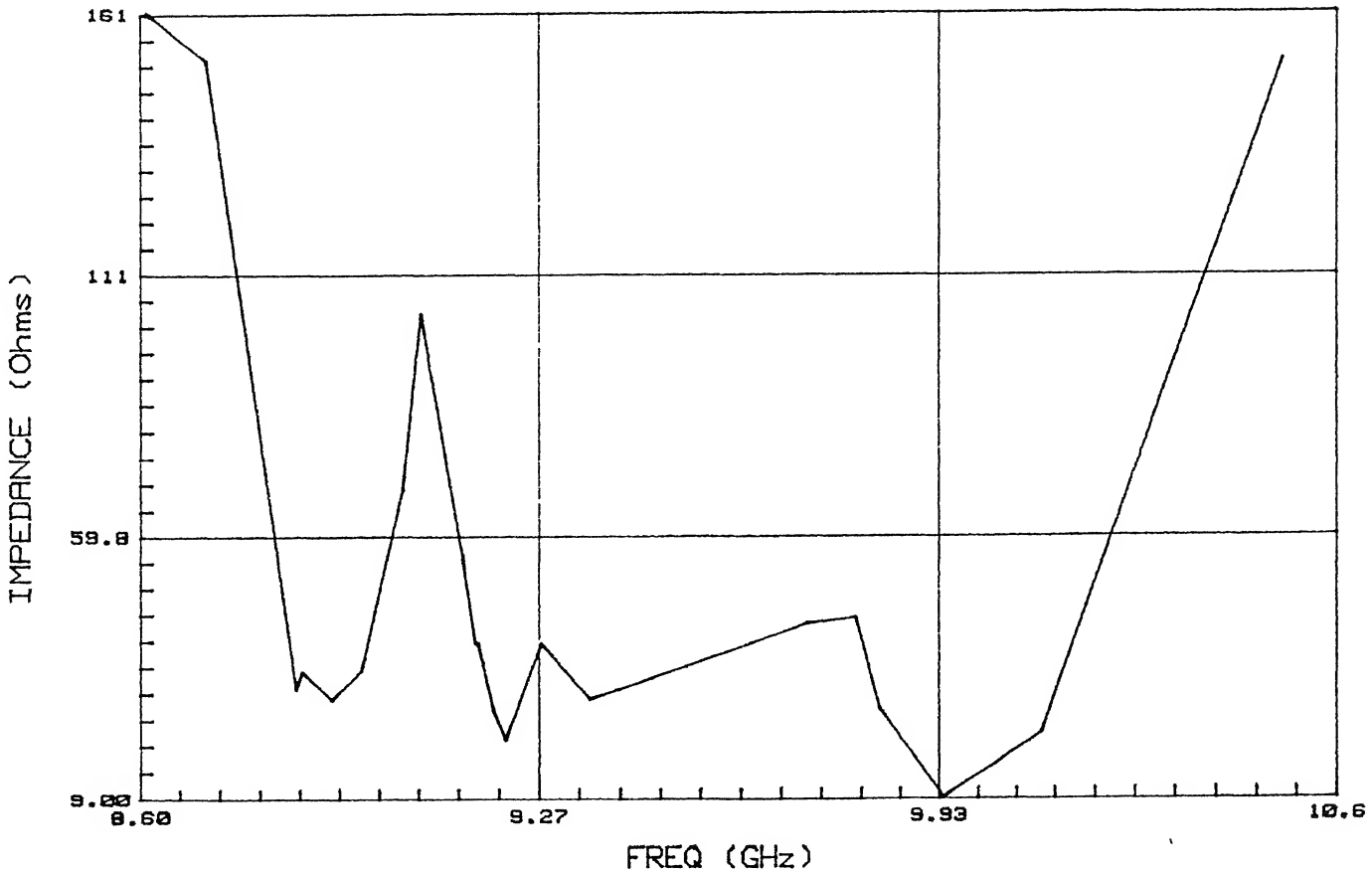

IMPEDANCE PLOT: 25/10,20,30

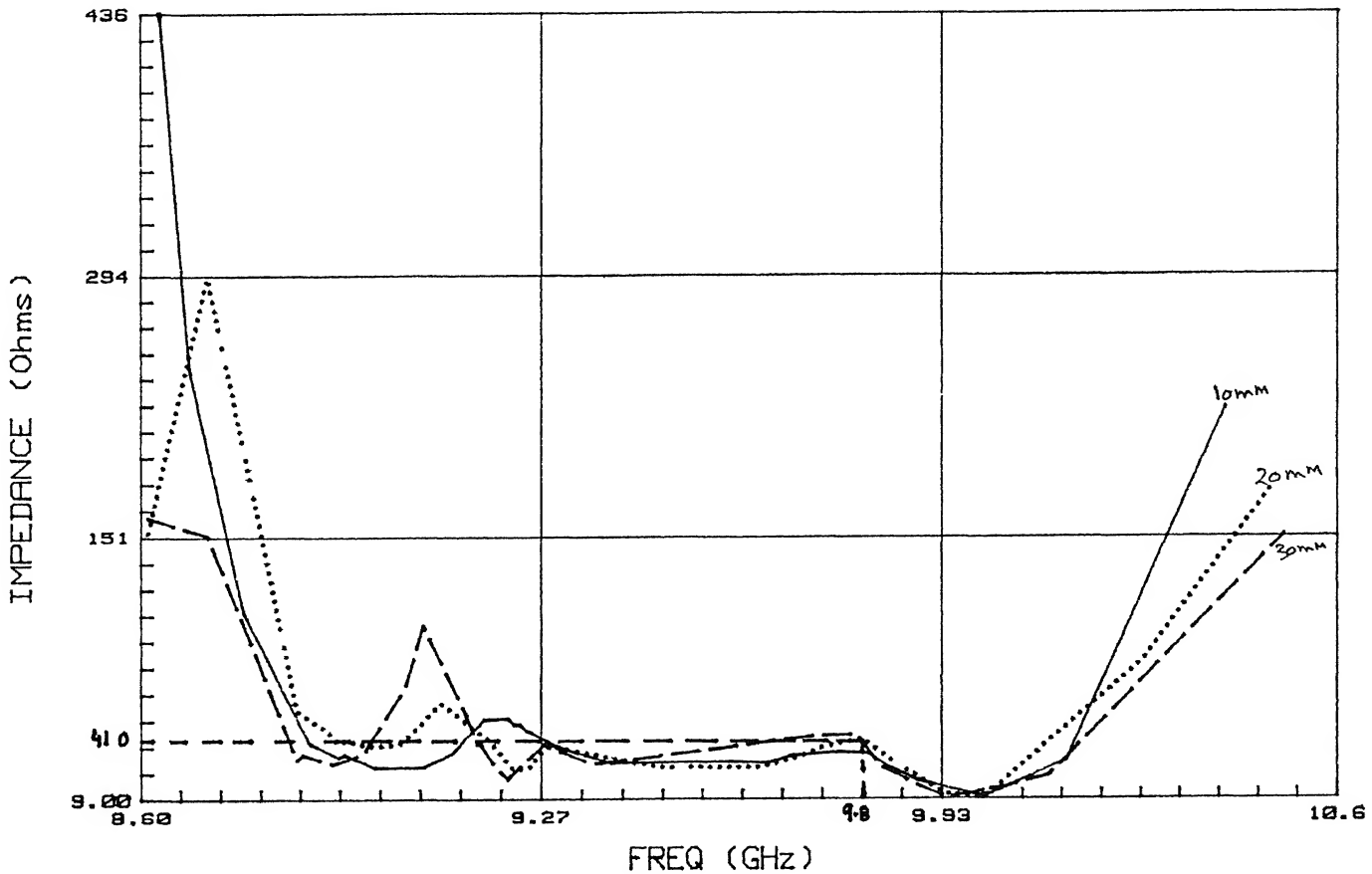

S11 PLOT: 24.5/10

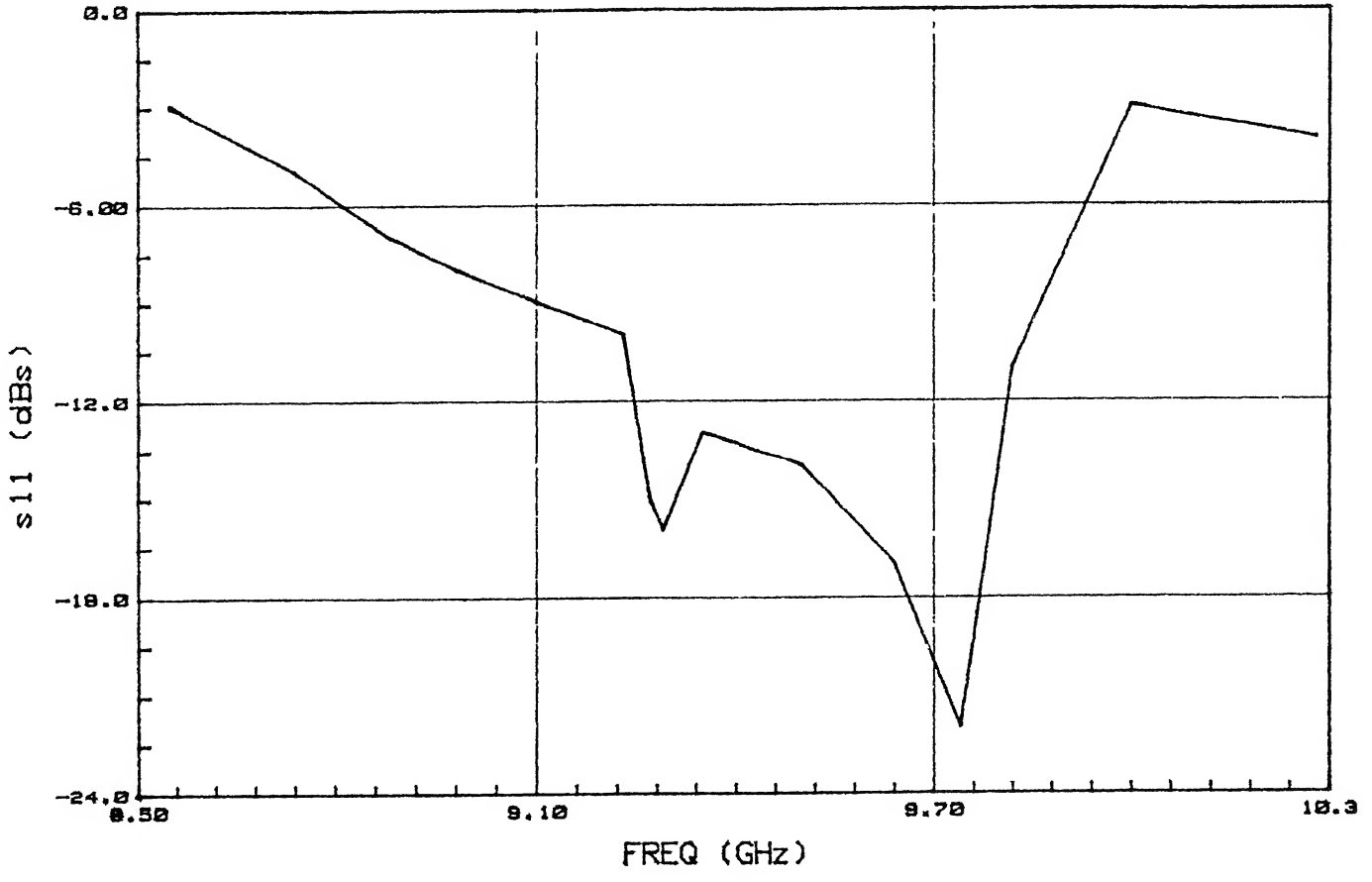

S11 PLOT: 24.5/20

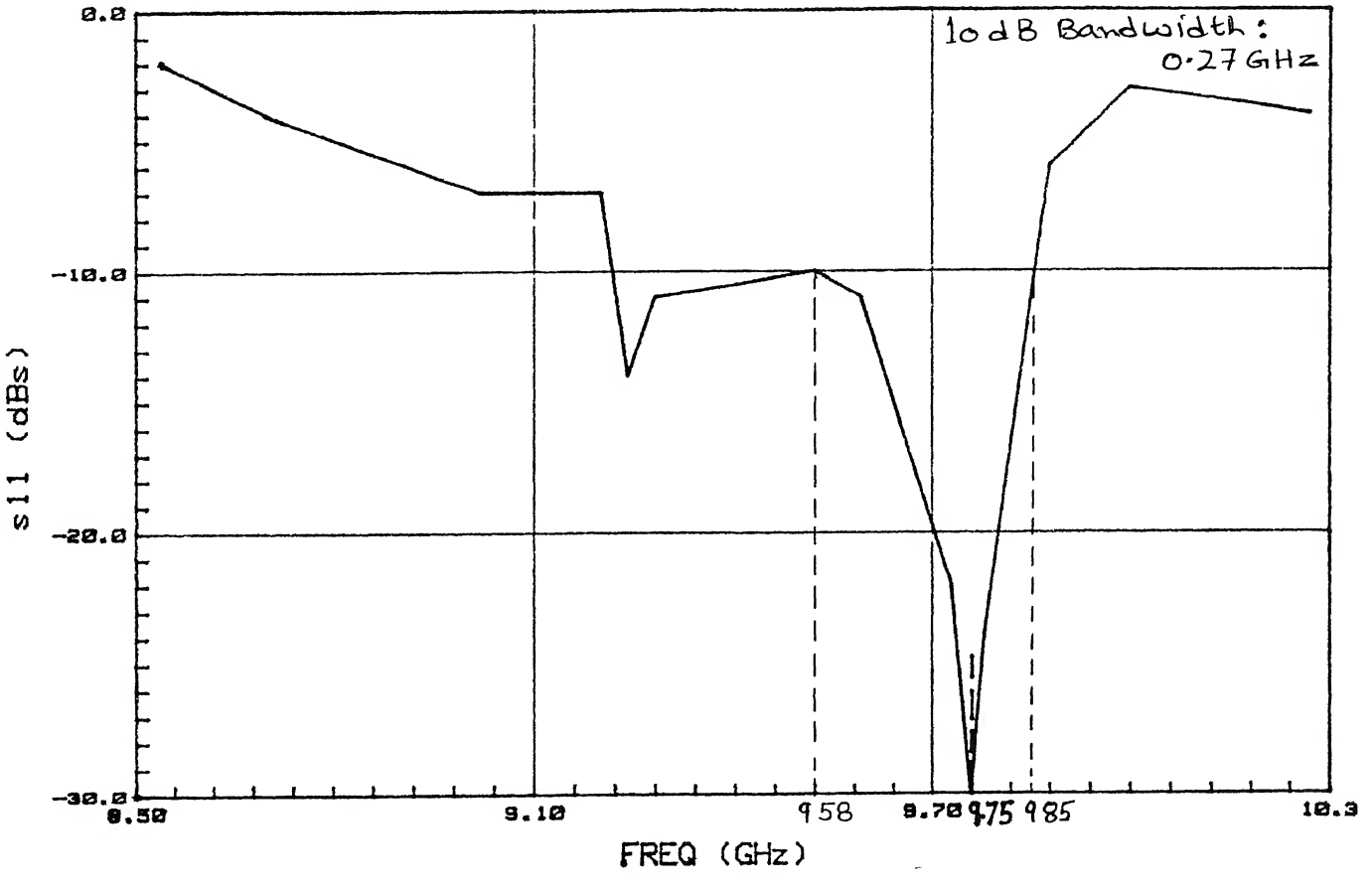

S11 PLOT: 24.5/30

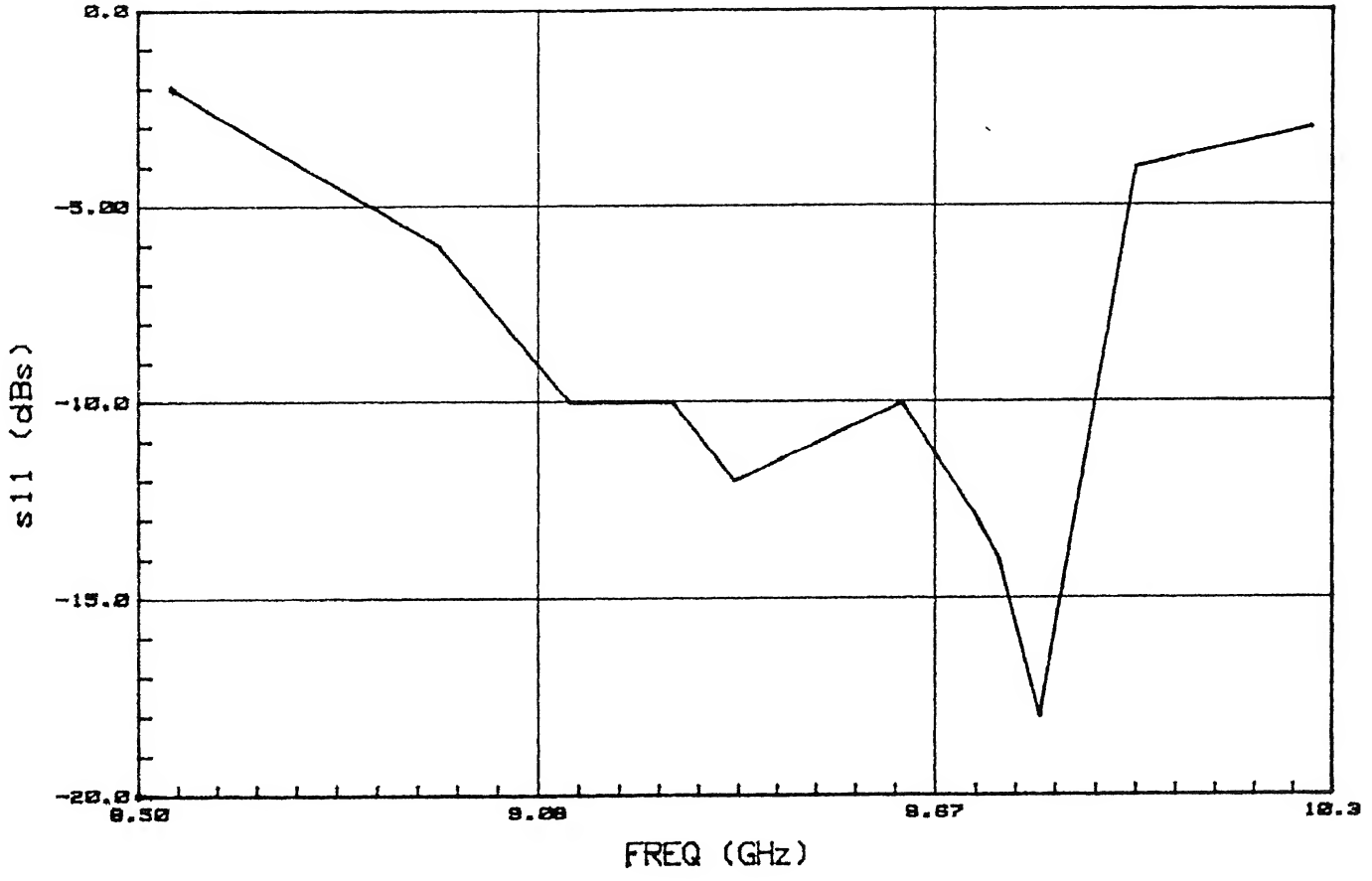

S11 PLOT: 24.5/10,20,30

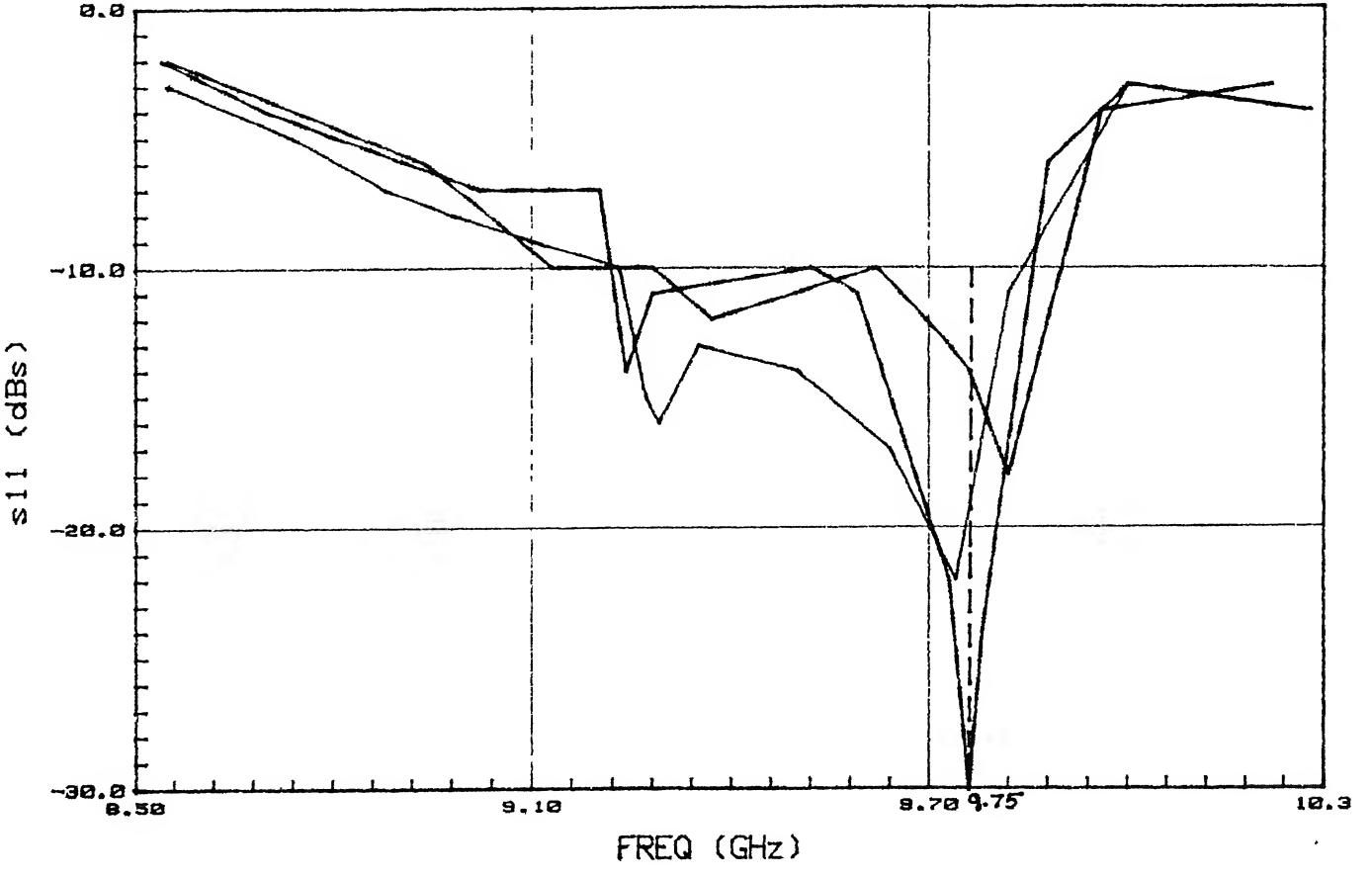

IMPEDANCE PLOT:24.5/10

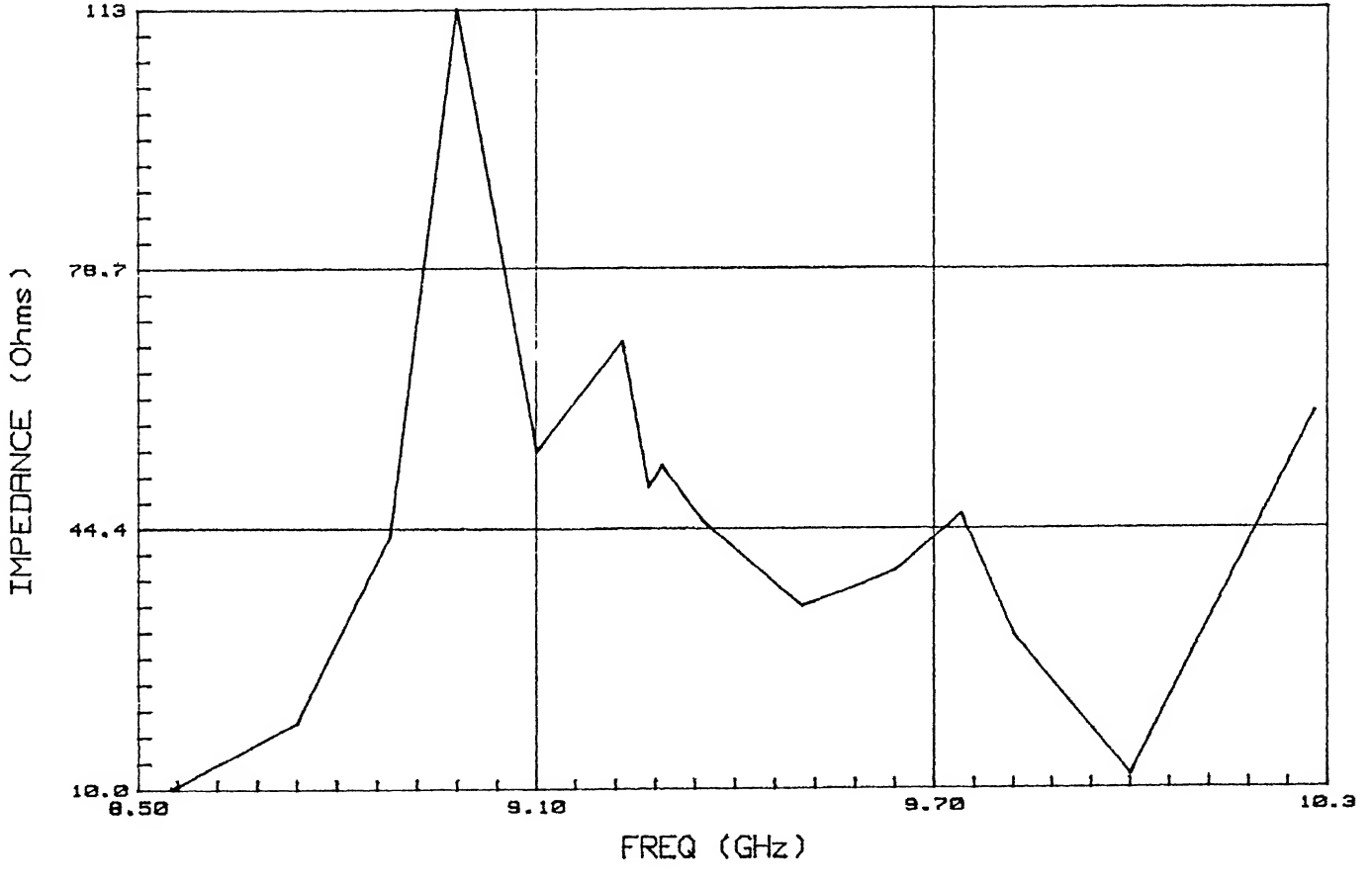

IMPEDANCE PLOT:24.5/20

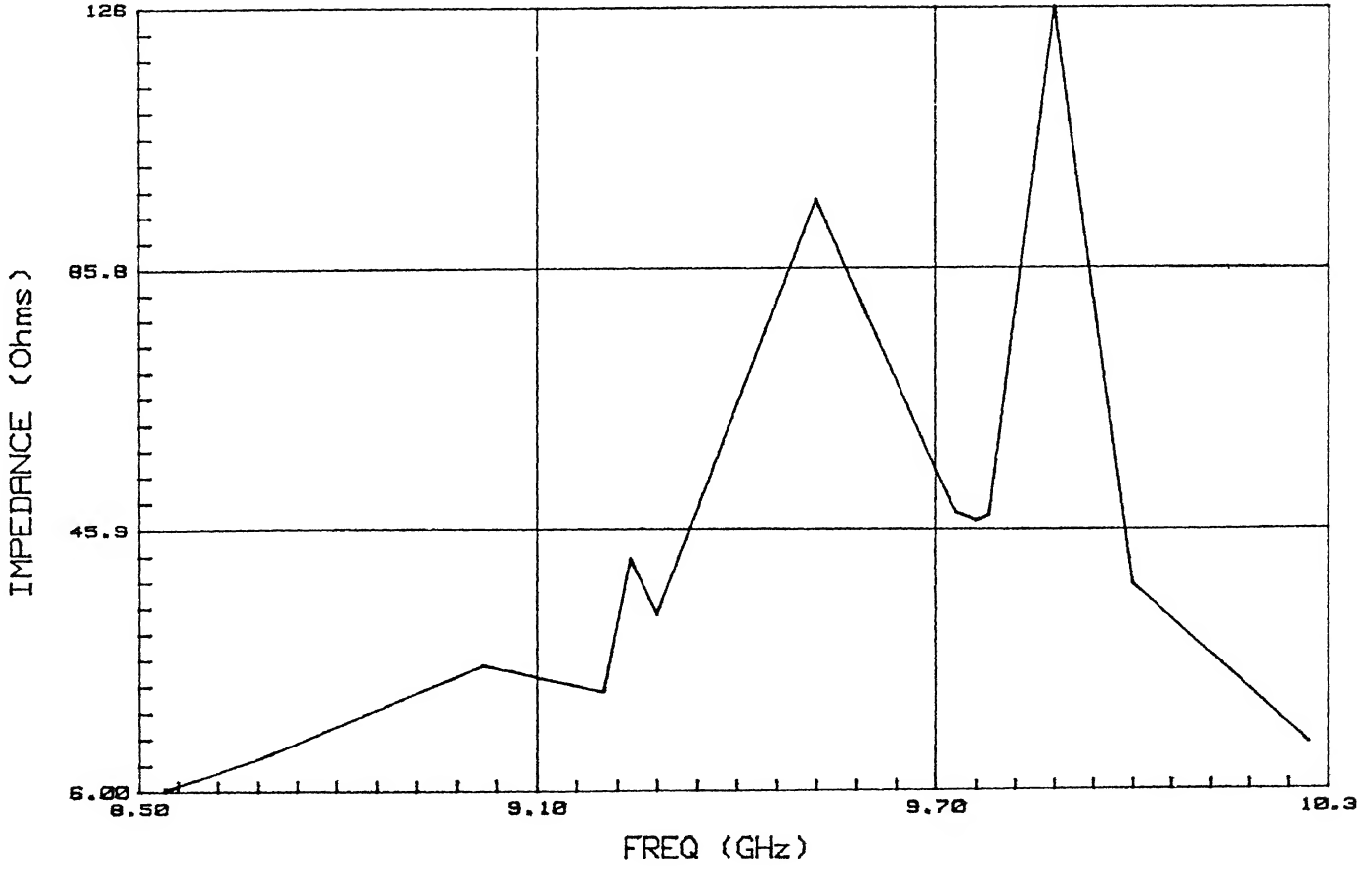

IMPEDANCE PLOT:24.5/30

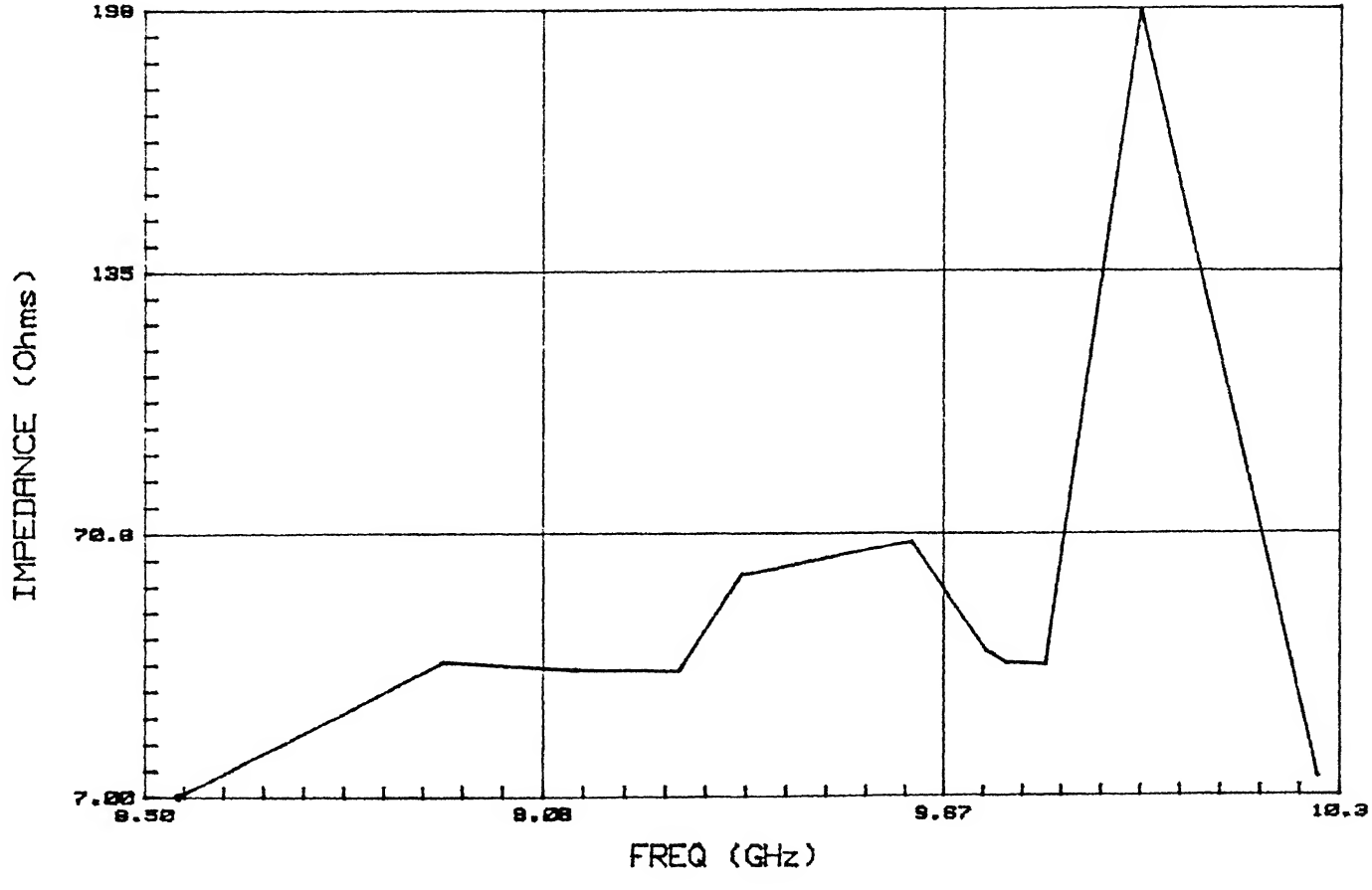

IMPEDANCE PLOT: 24.5/10,20,30

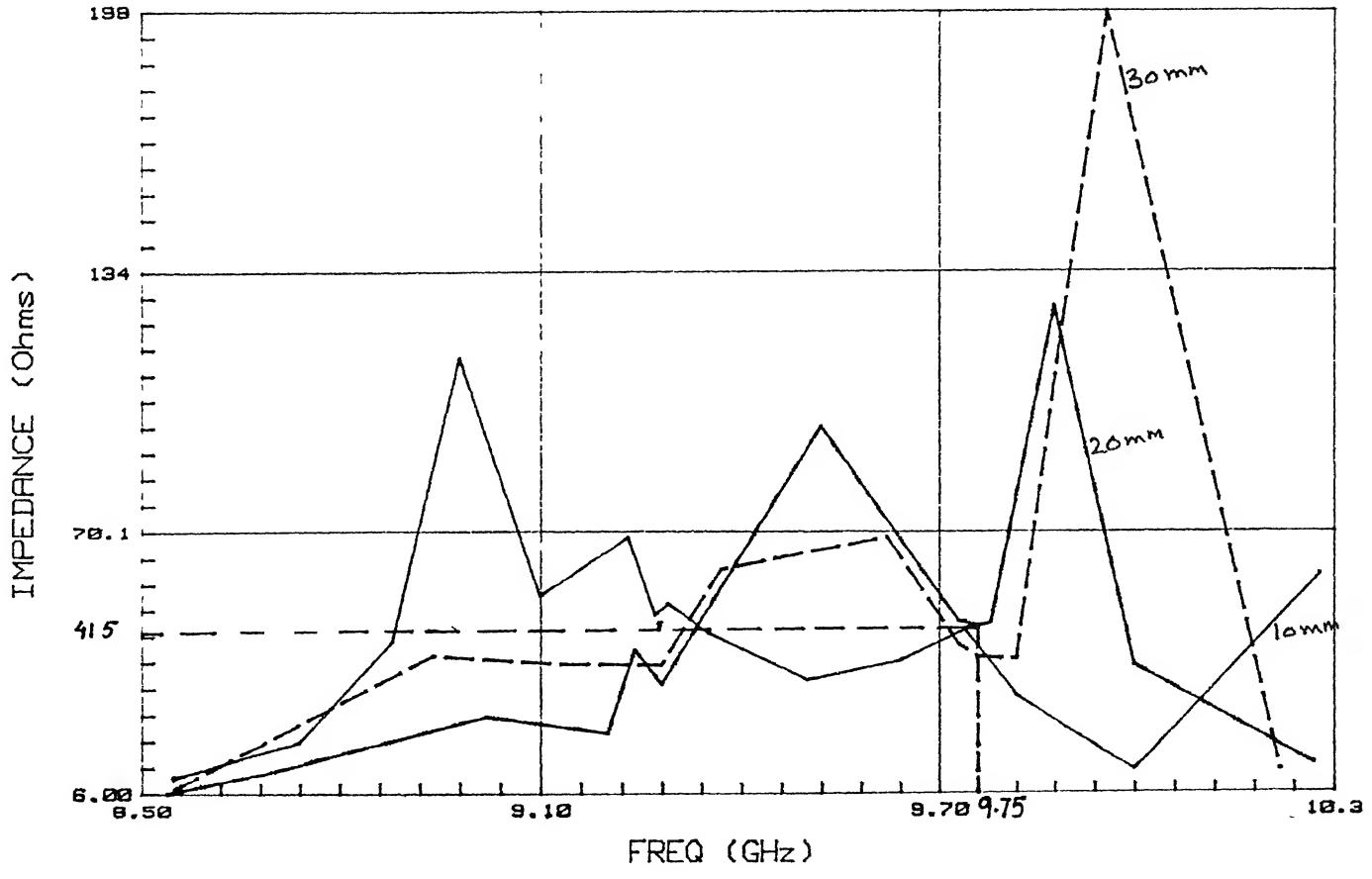

S11 PLOT: 23.5/10

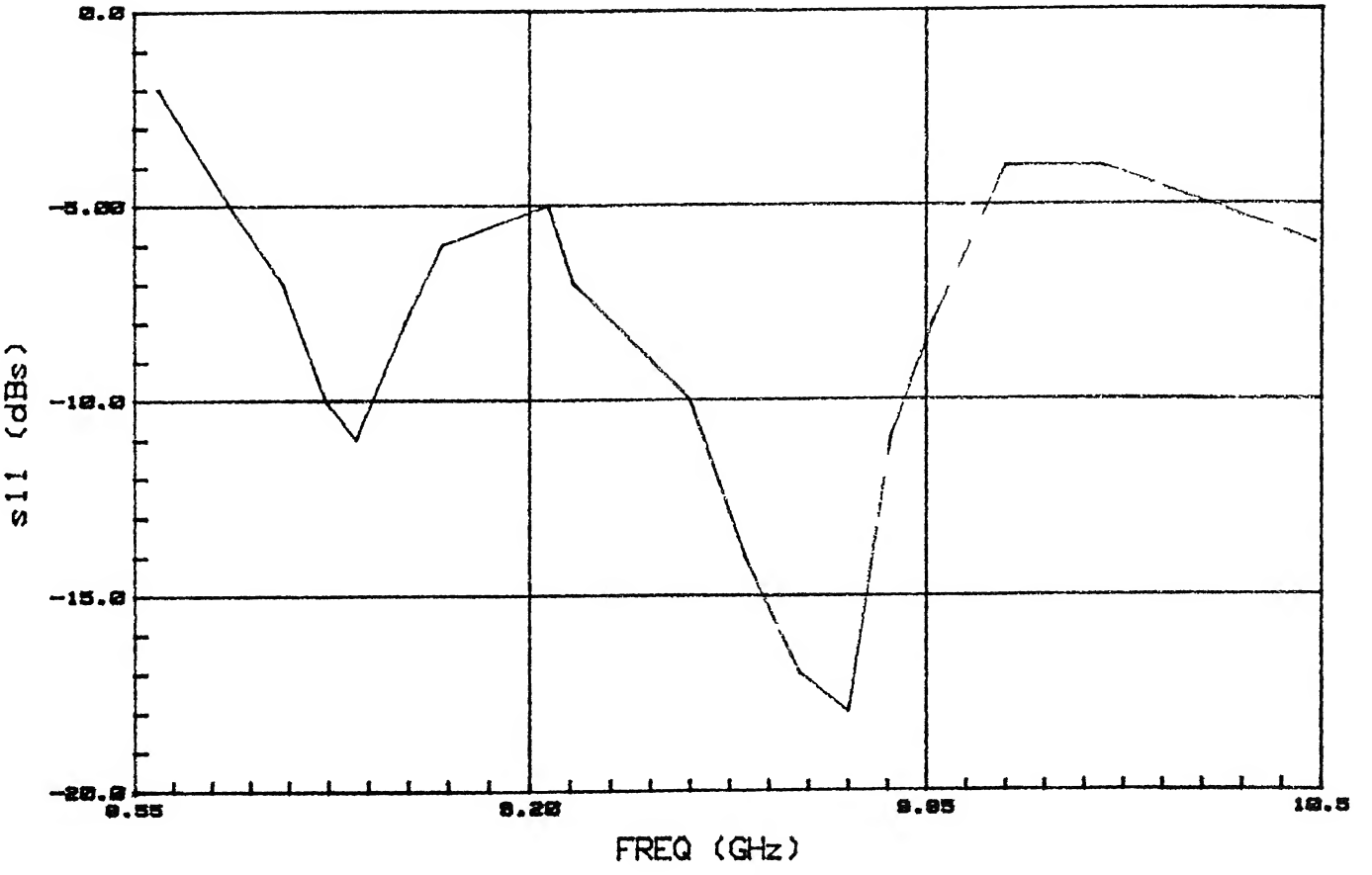

S11 PLOT: 23.5/20

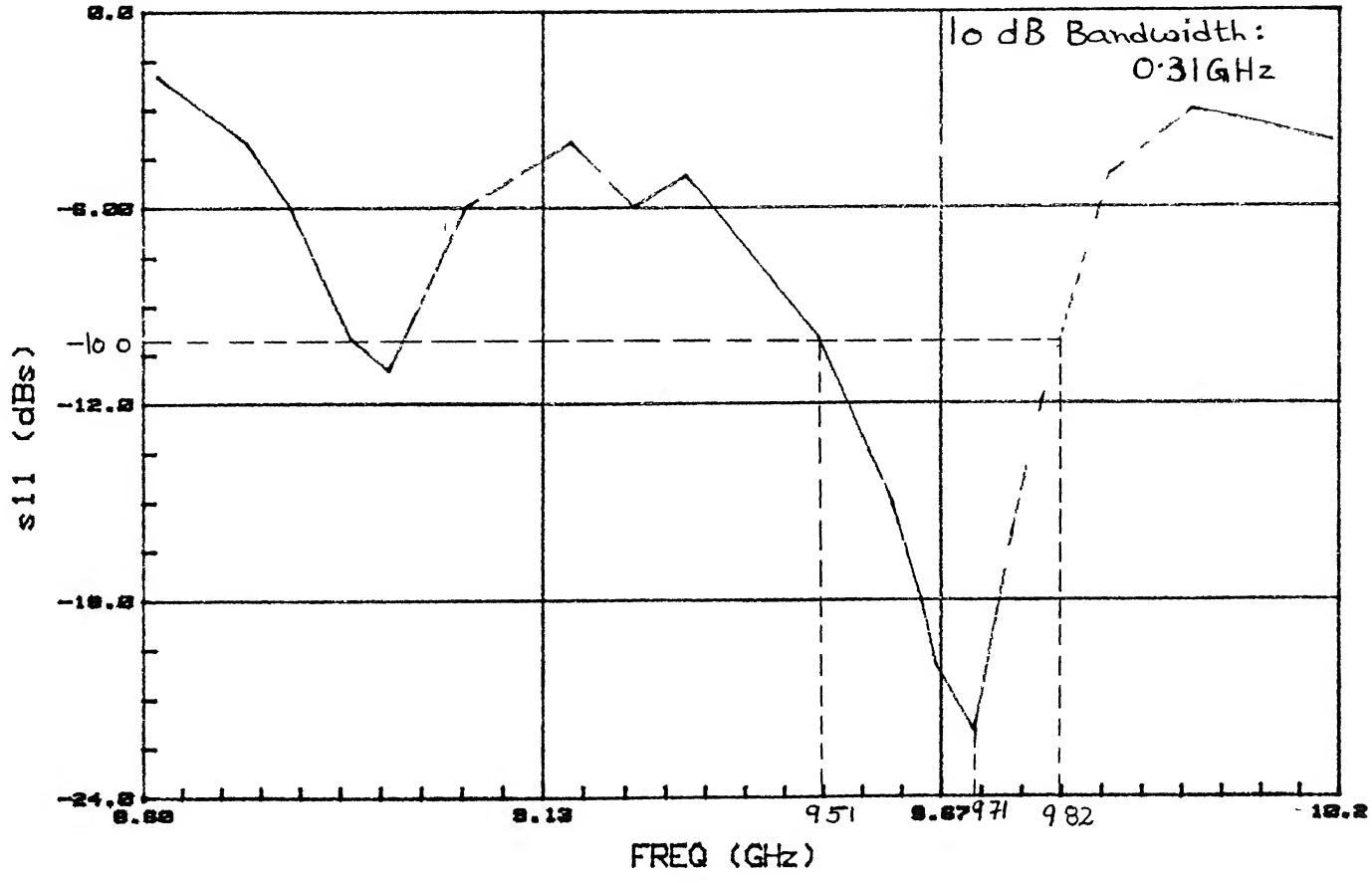

S11 PLOT: 23.5/30

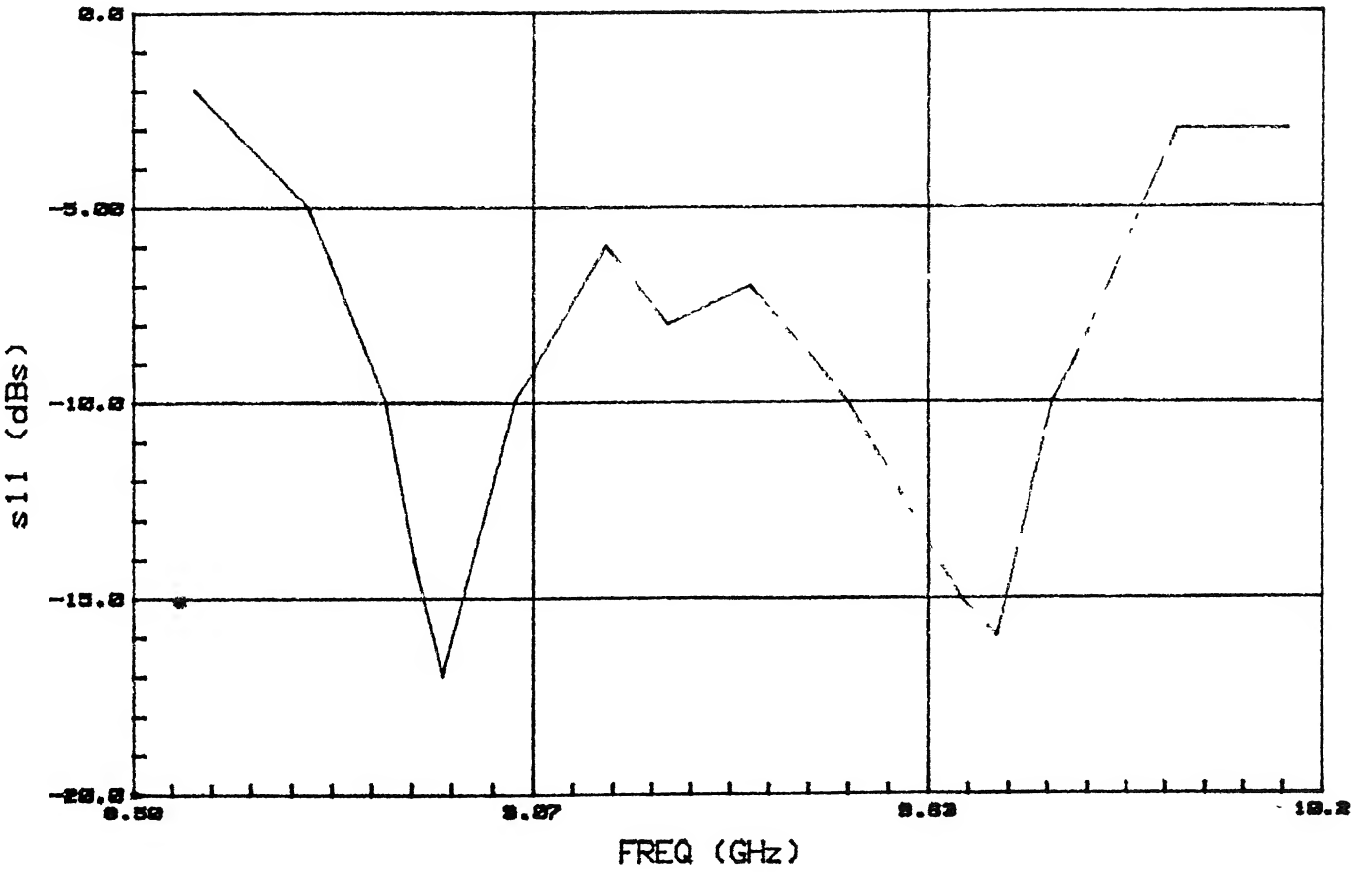

IMPEDANCE PLOT:23.5/10

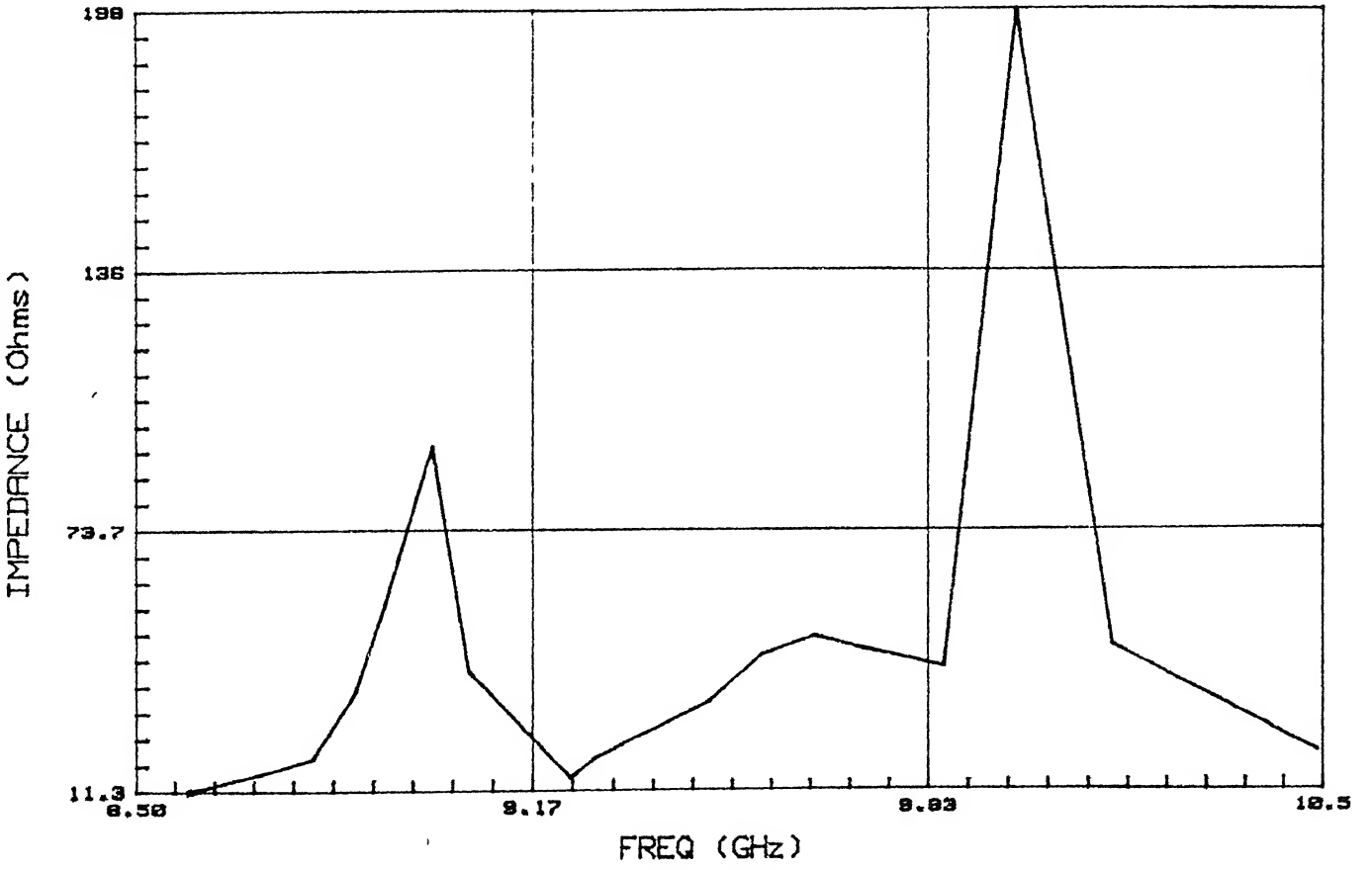

IMPEDANCE PLOT:23.5/20

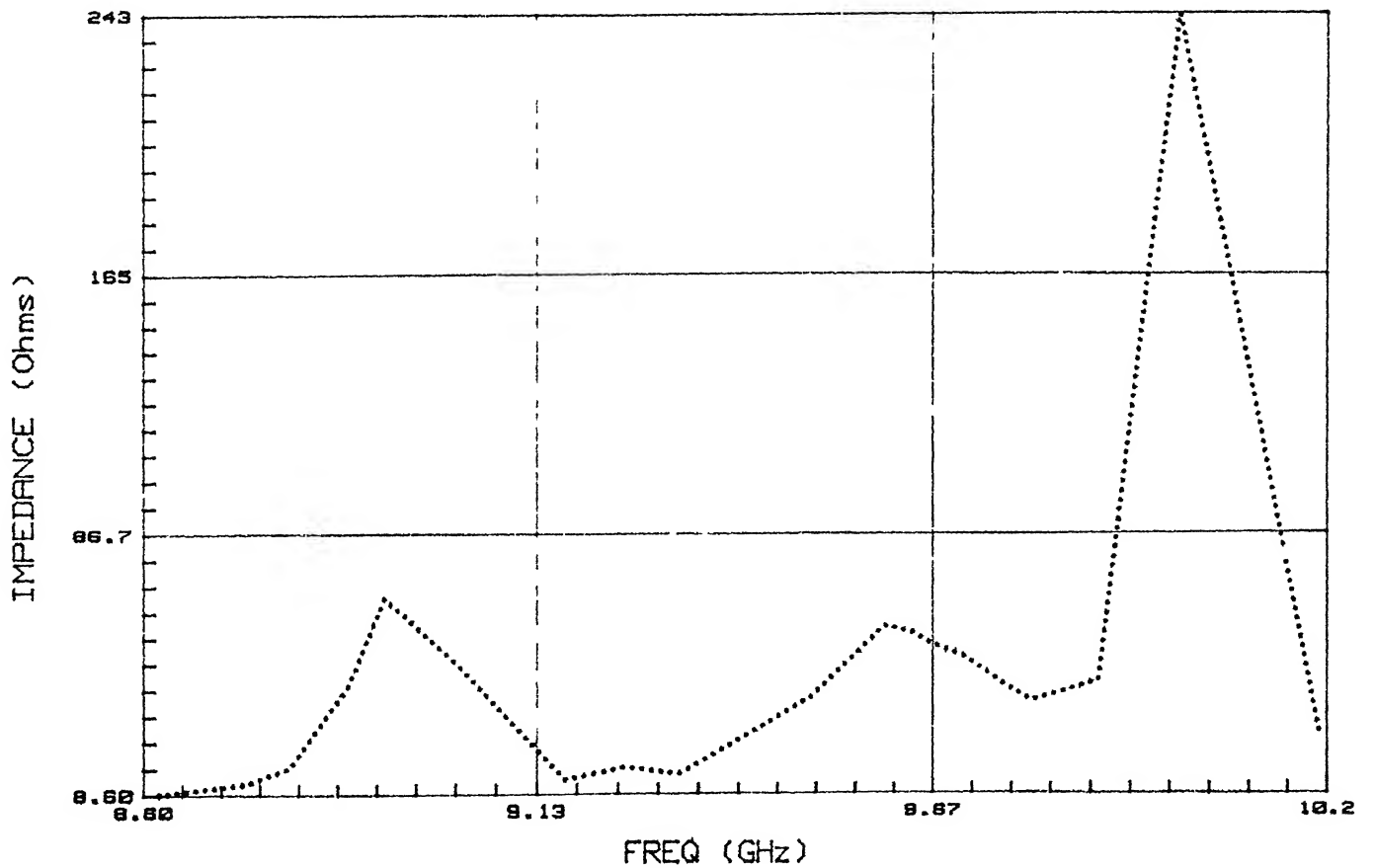

IMPEDANCE PLOT:23.5/30

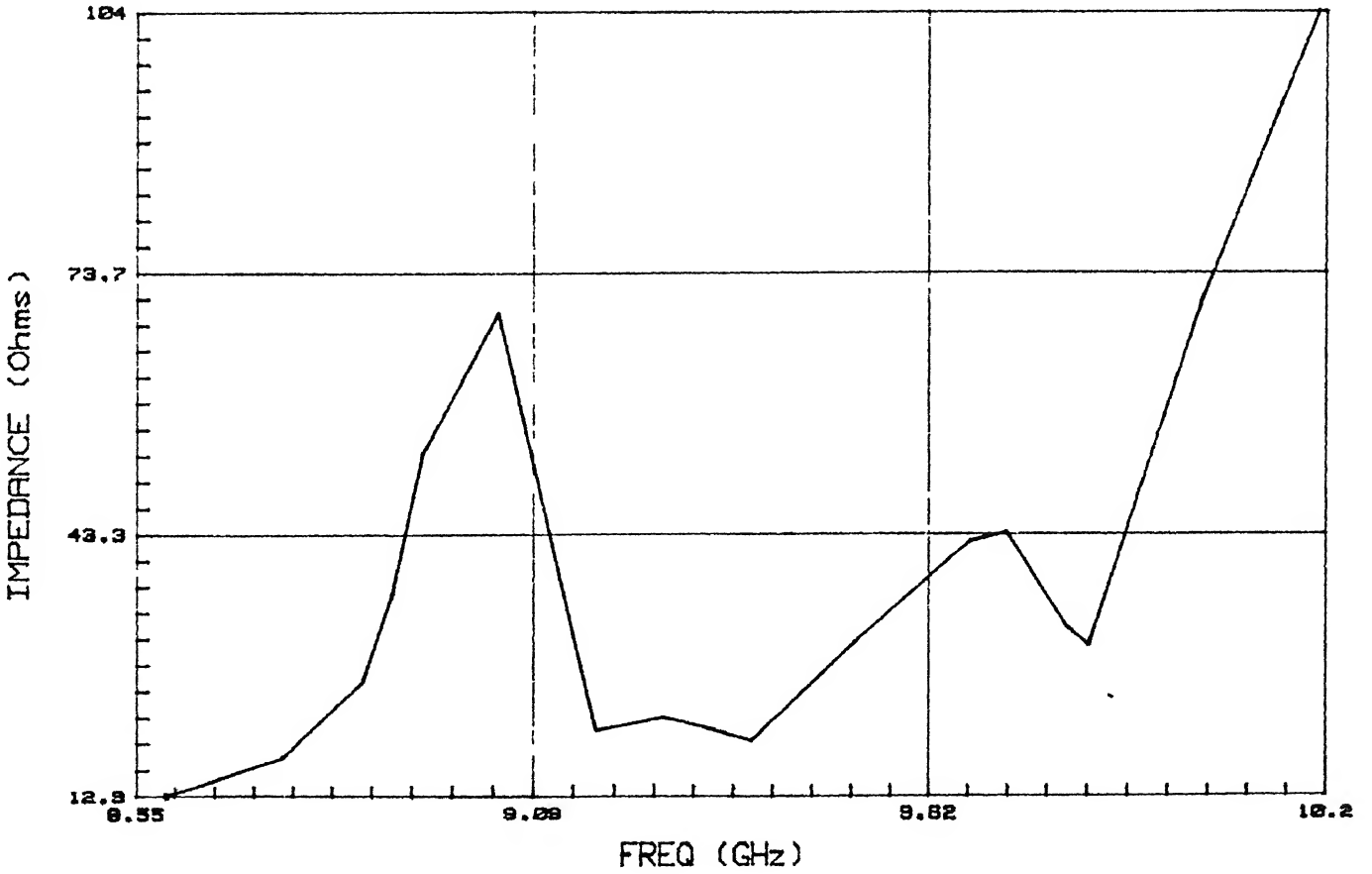

IMPEDANCE PLOT:23.5/10,20,30

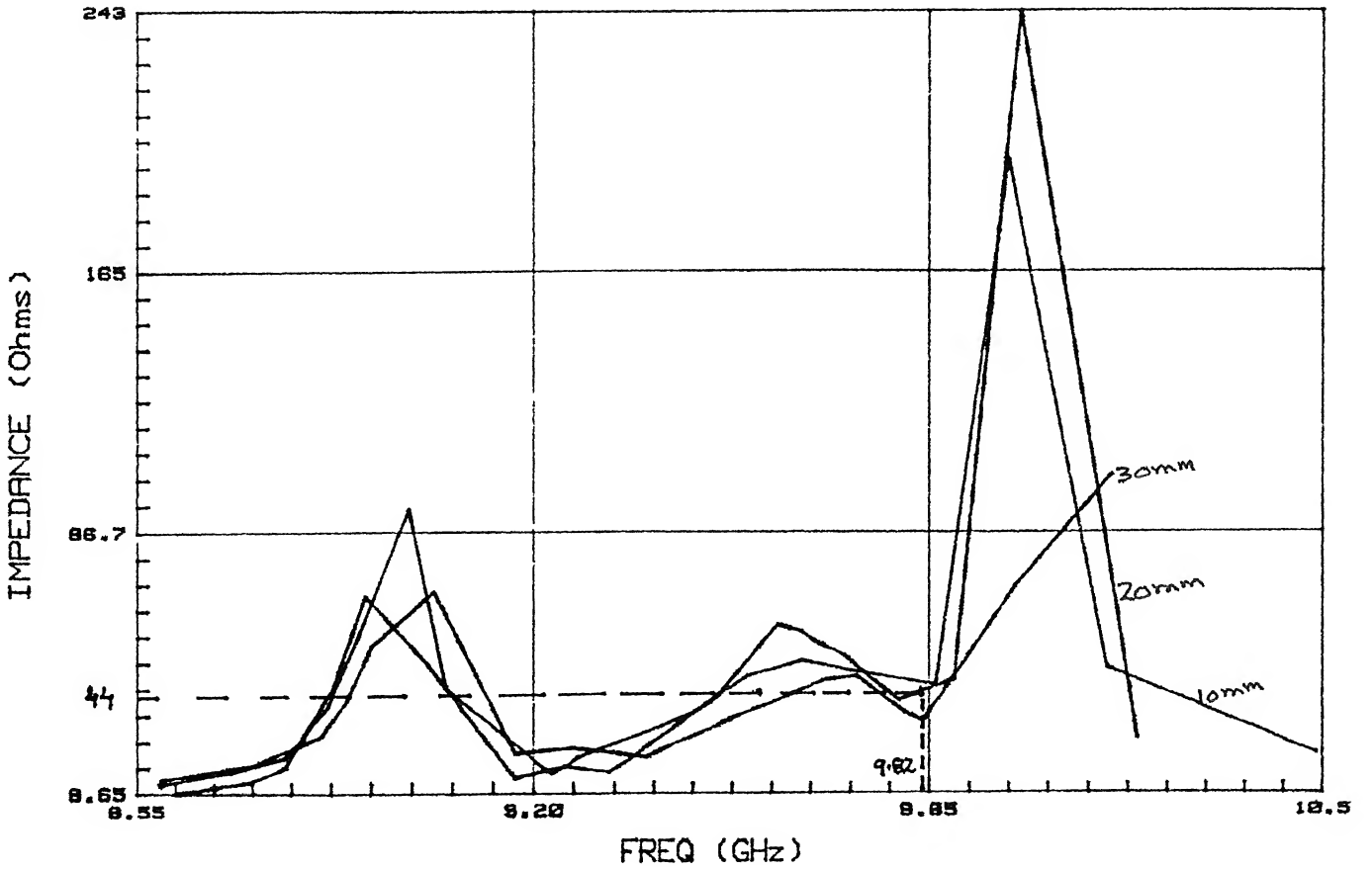

S11 PLOT: 23/10

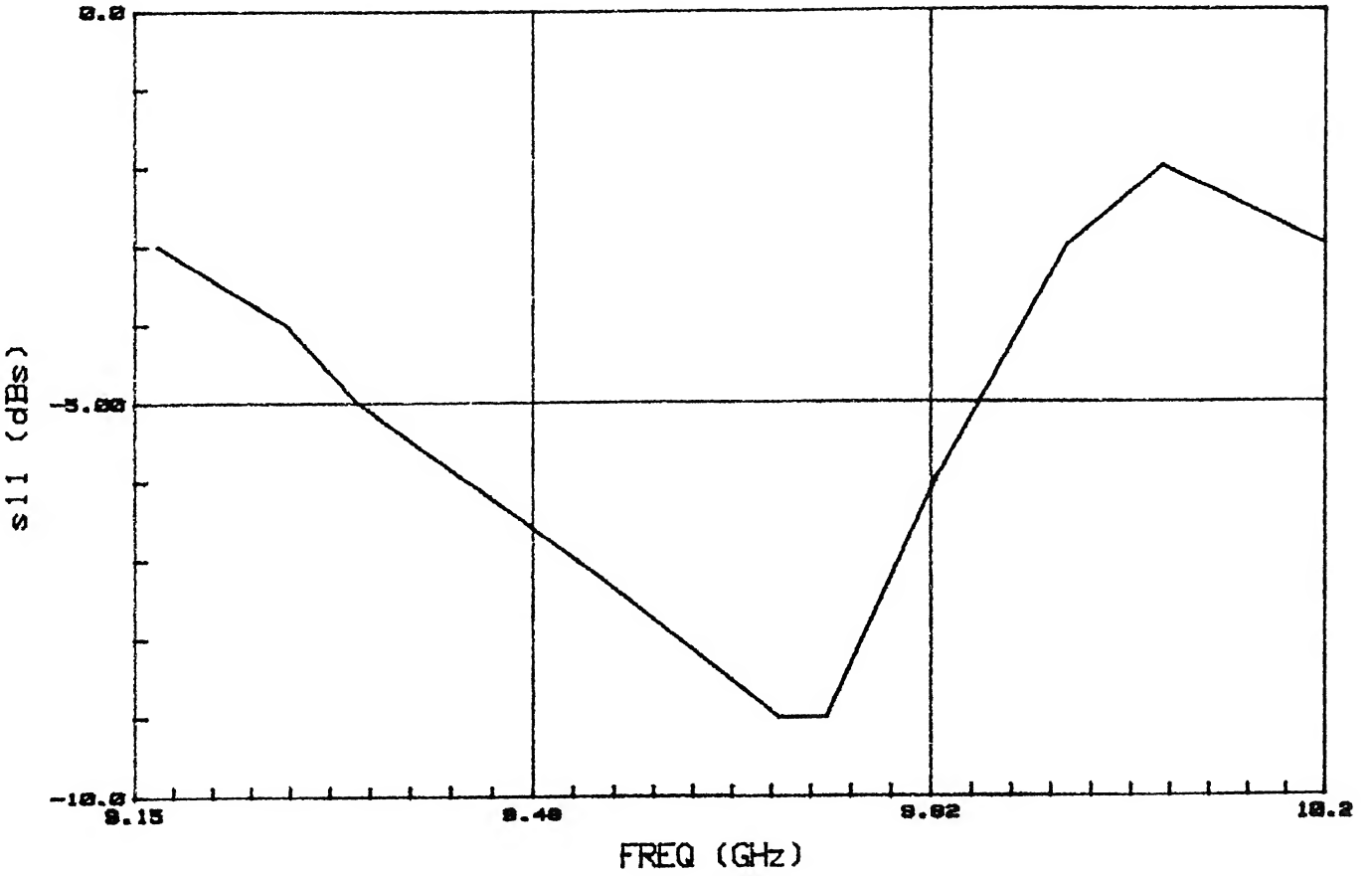

S11 PLOT: 23/20

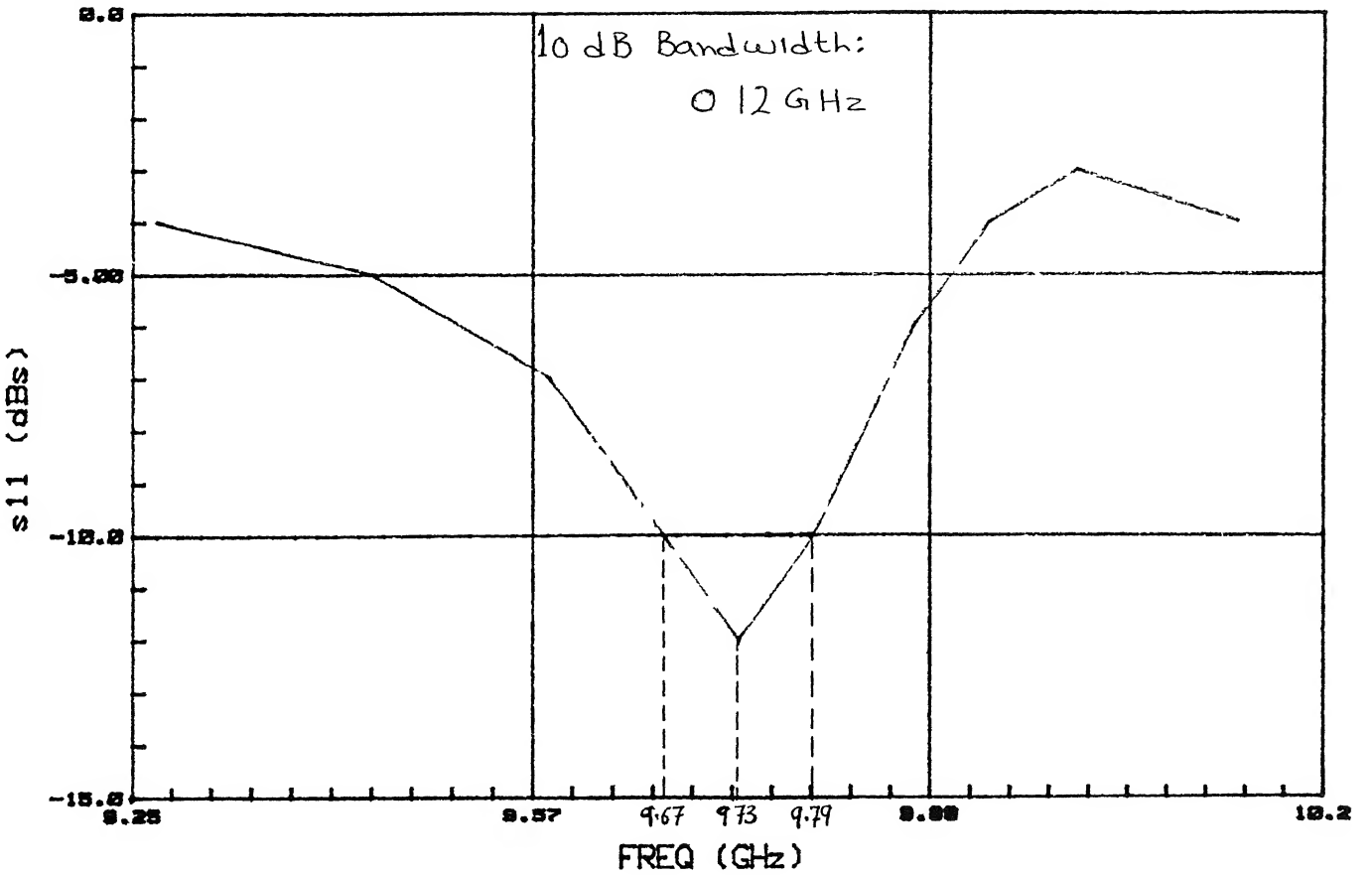

S11 PLOT: 23/30

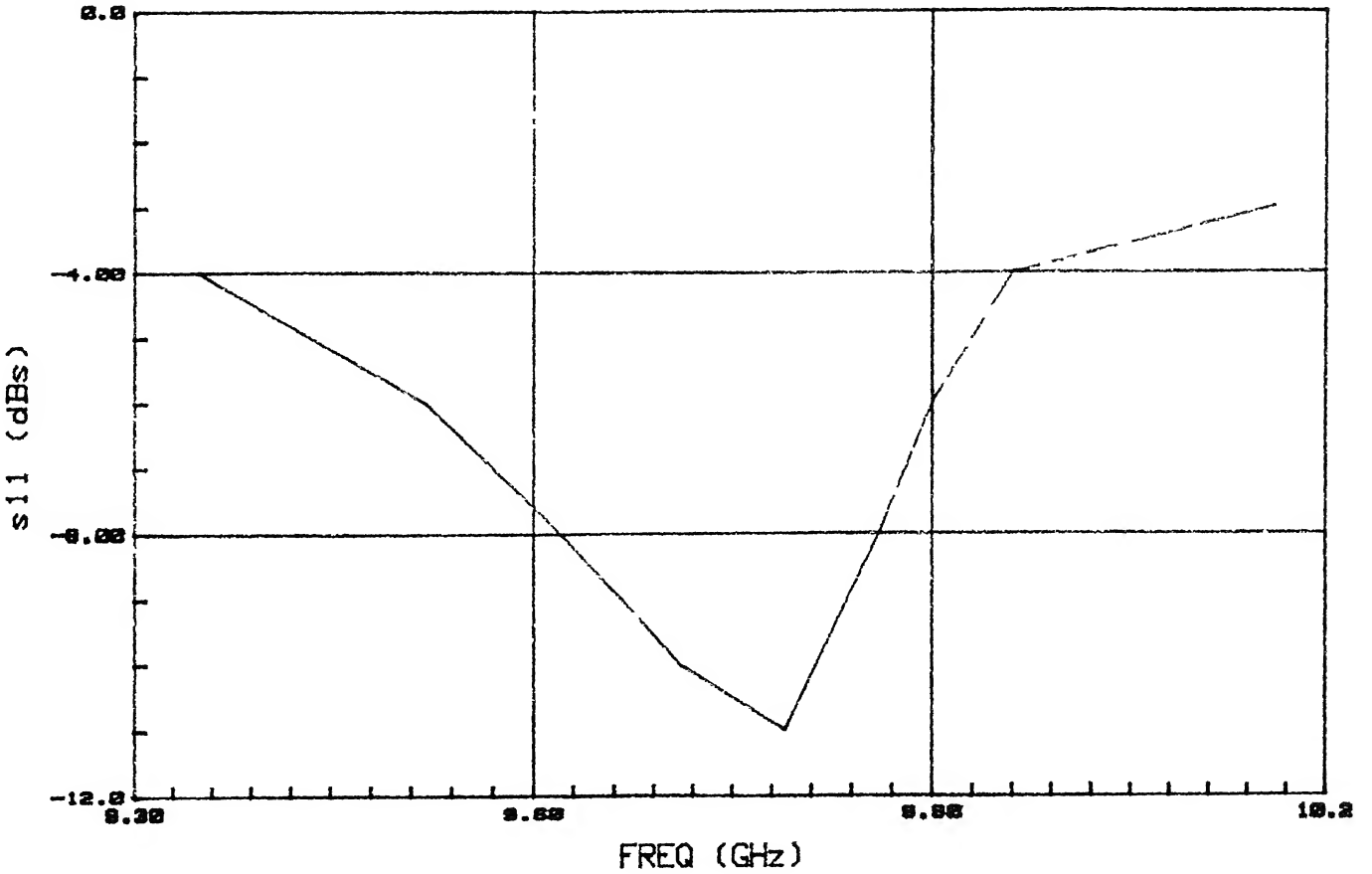

S11 PLOT: 23/10,20,30

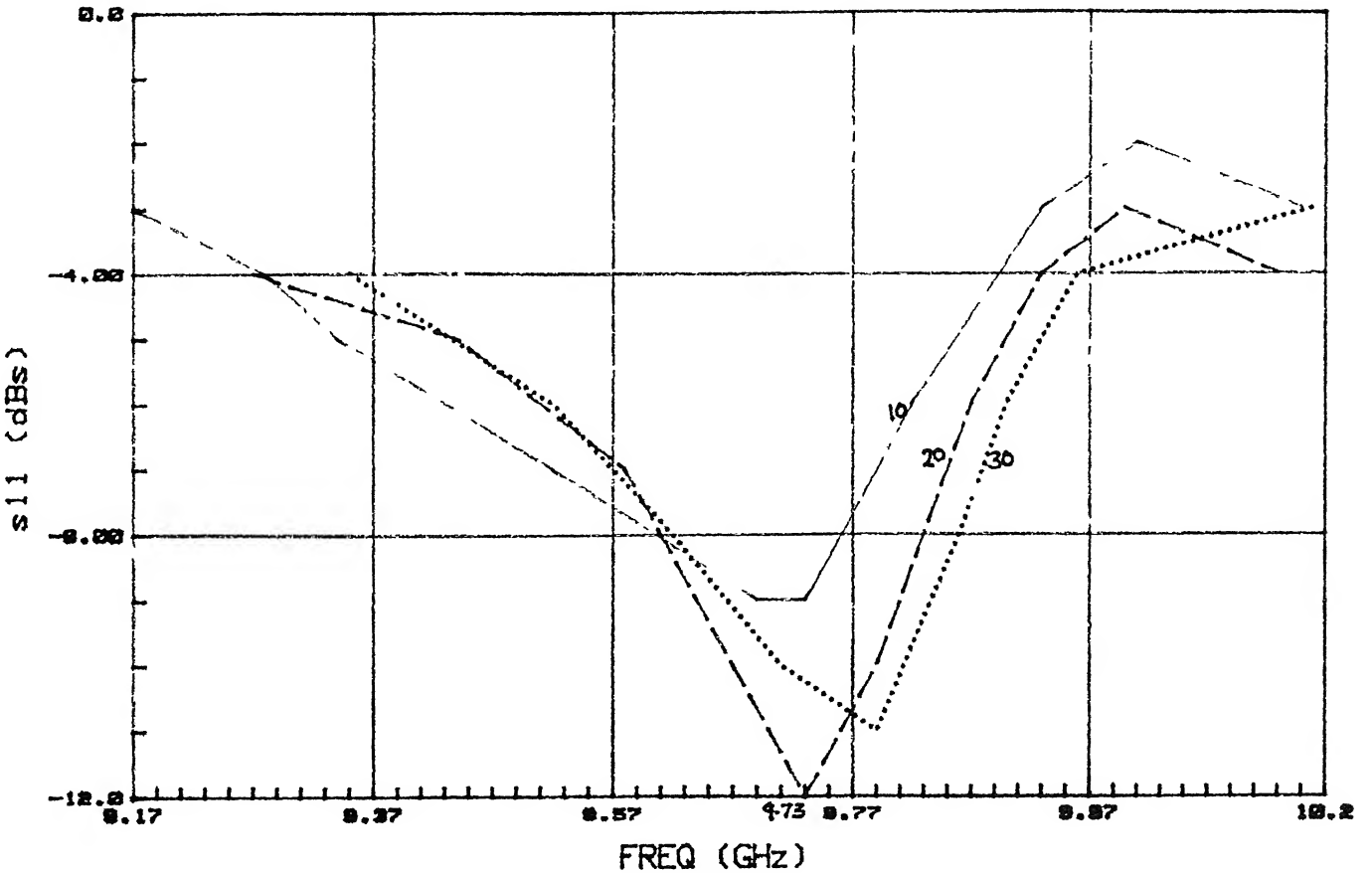

IMPEDANCE PLOT:23/10

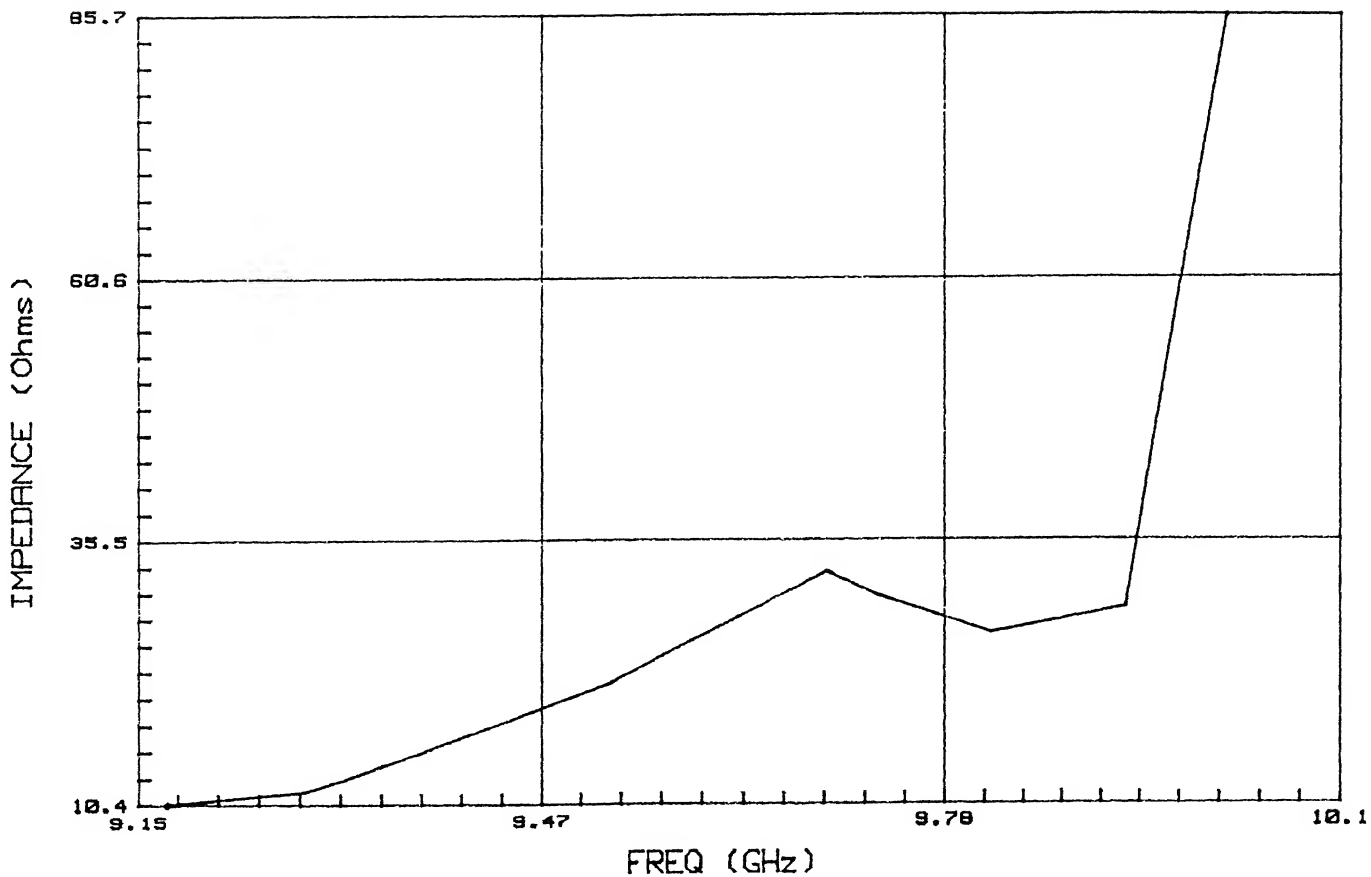

IMPEDANCE PLOT: 23/20

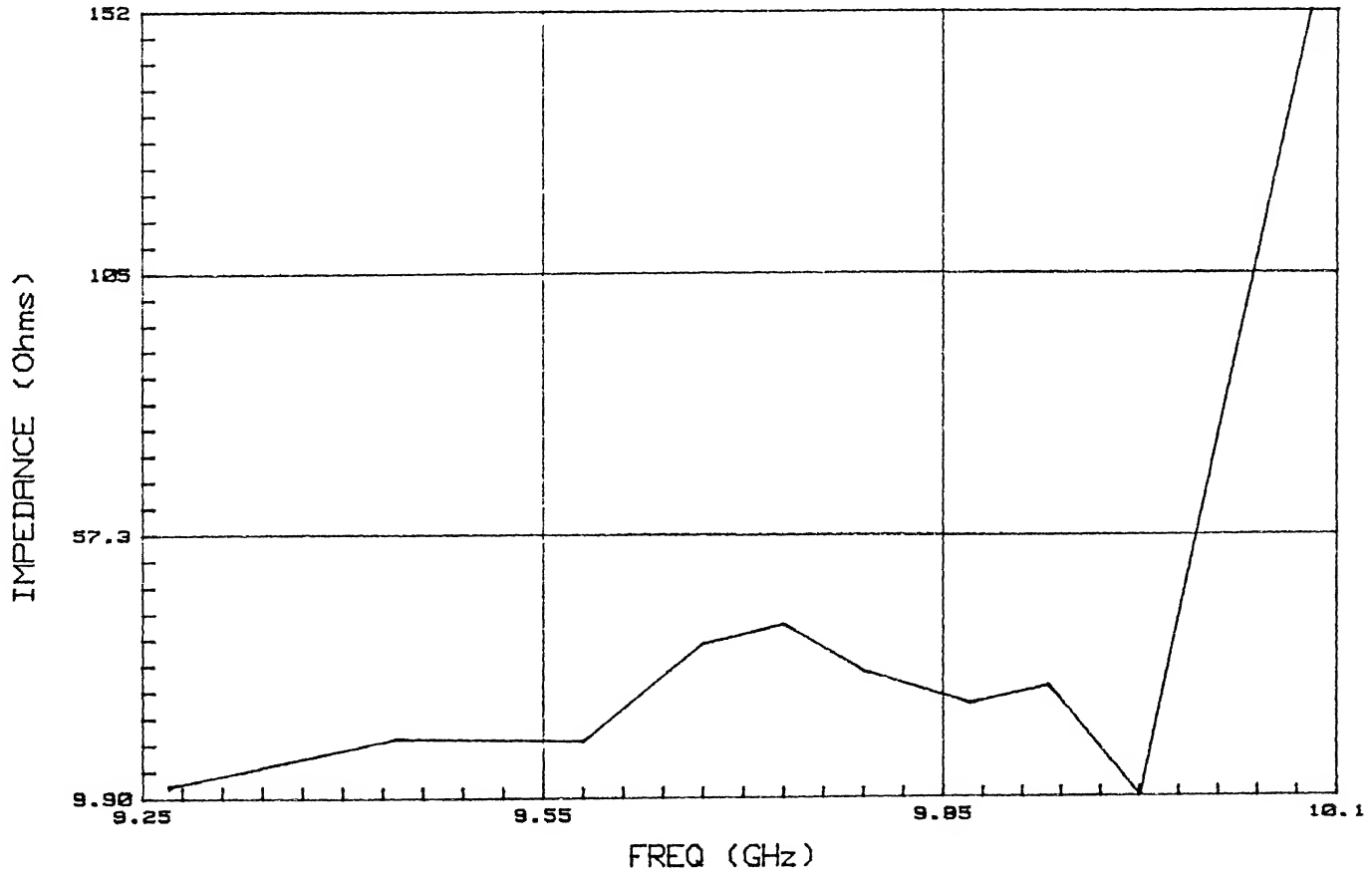

IMPEDANCE PLOT: 23/30

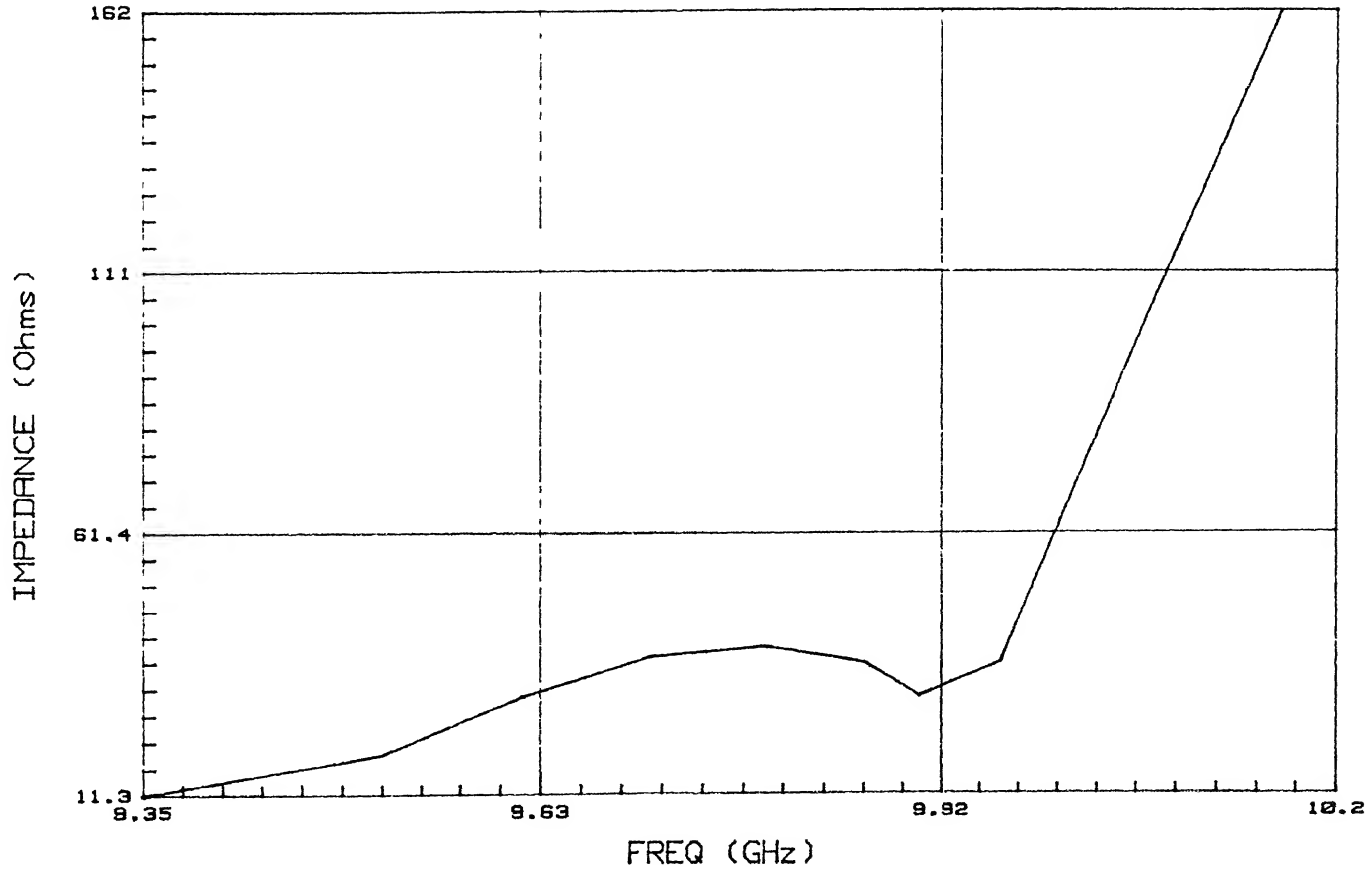

IMPEDANCE PLOT: 23/10,20,30

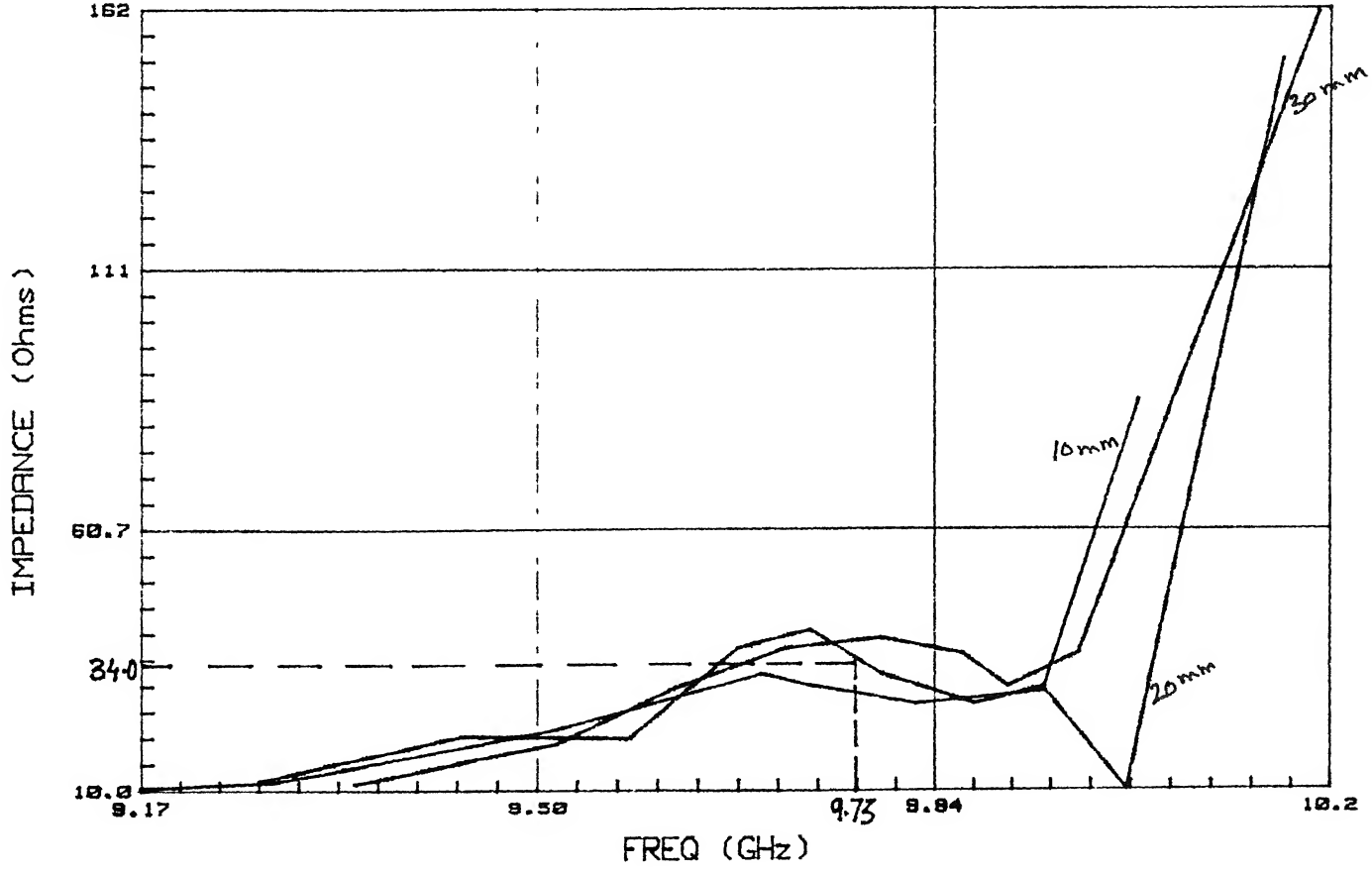

S11 PLOT:s23/10

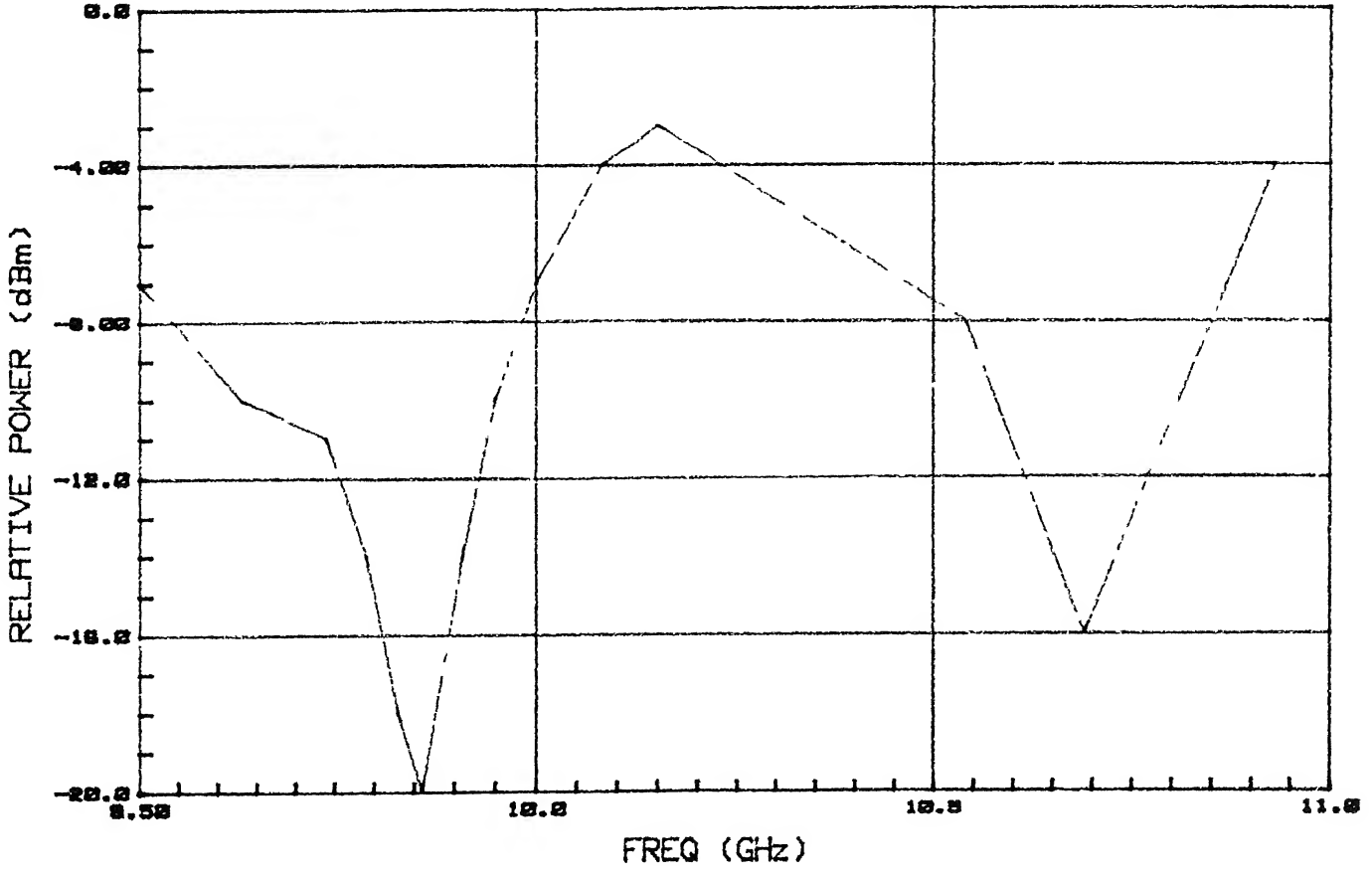

S11 PLOT: s23/20

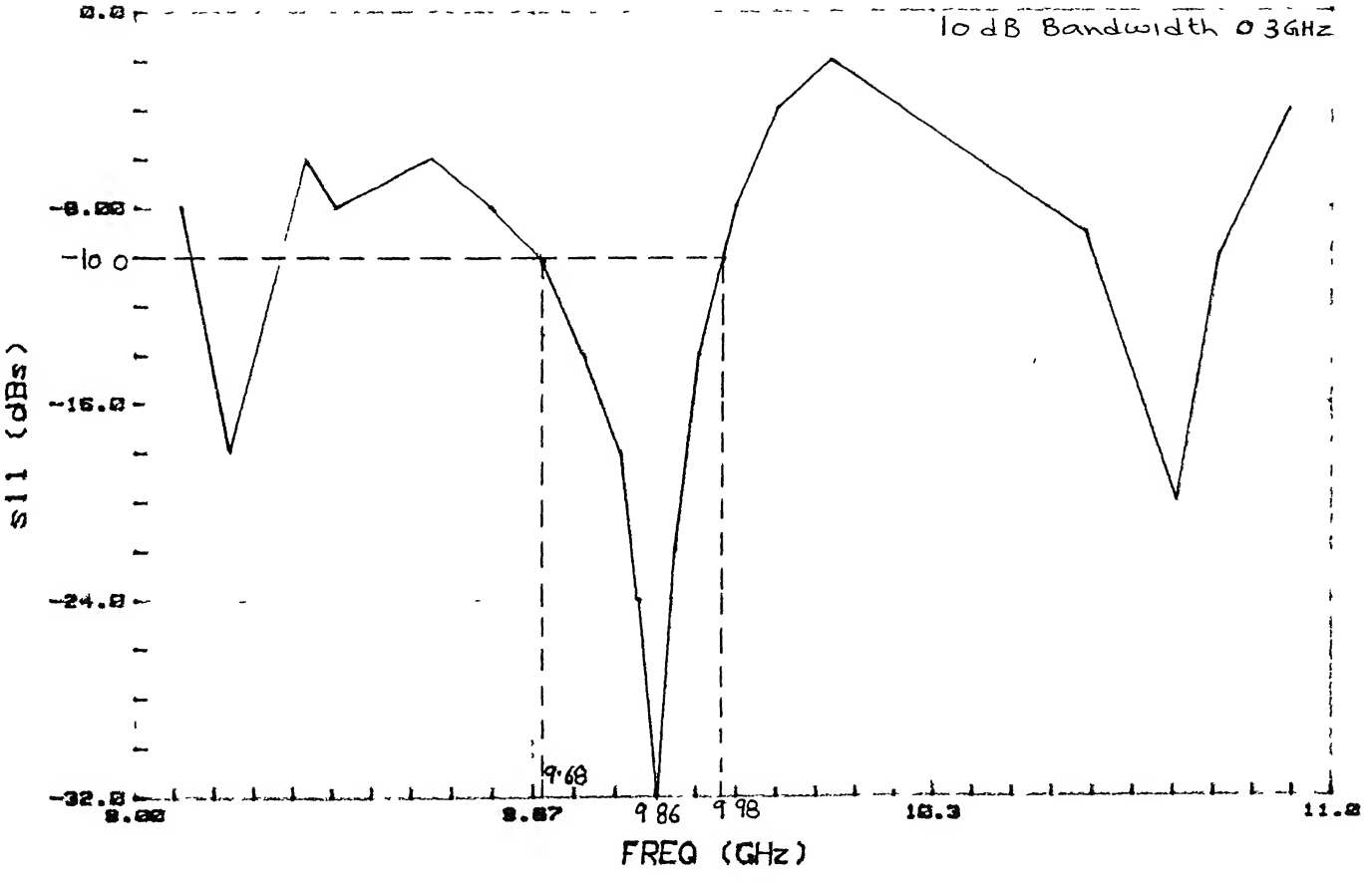

PLOT: s23/30

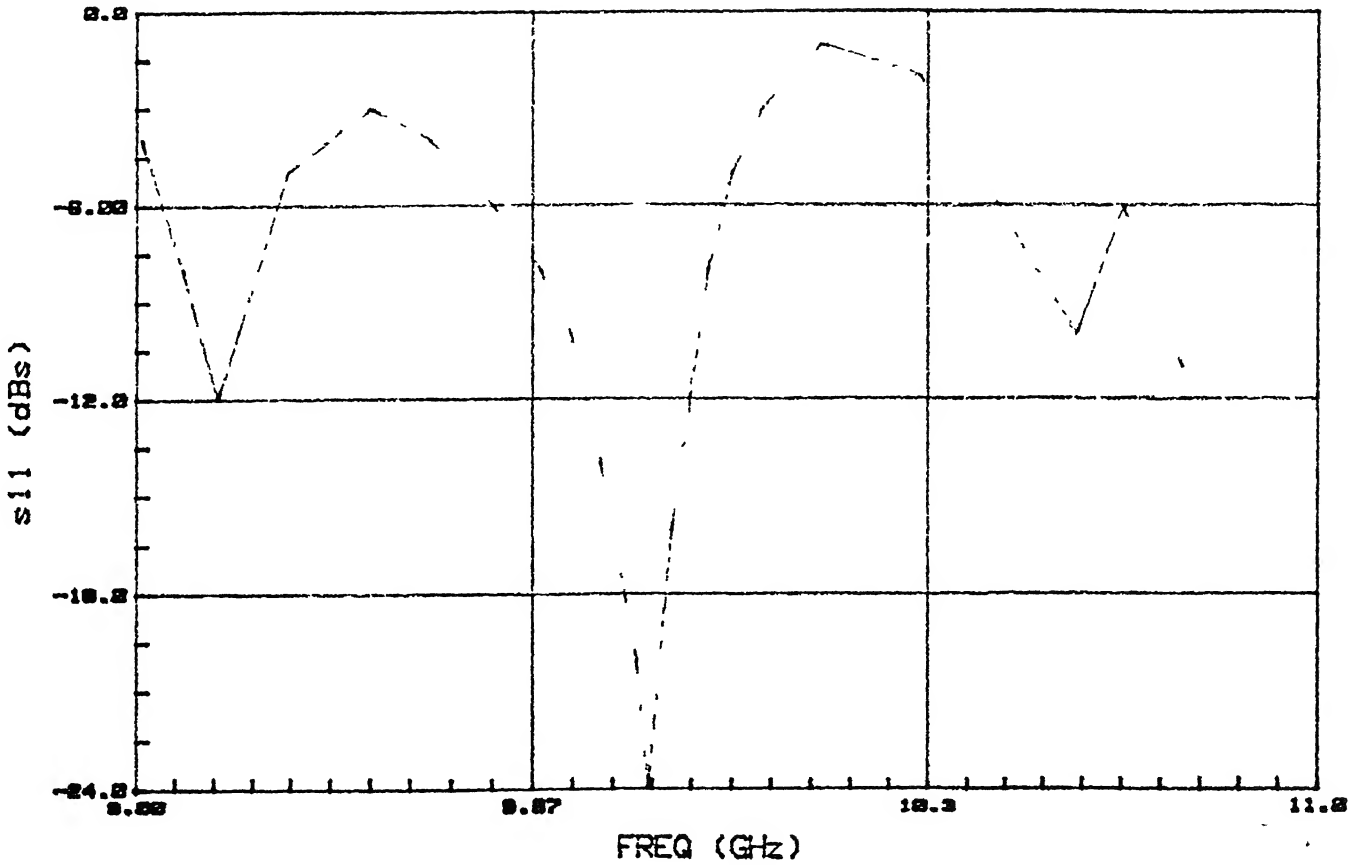

S11 PLOT: s23/10,20,30

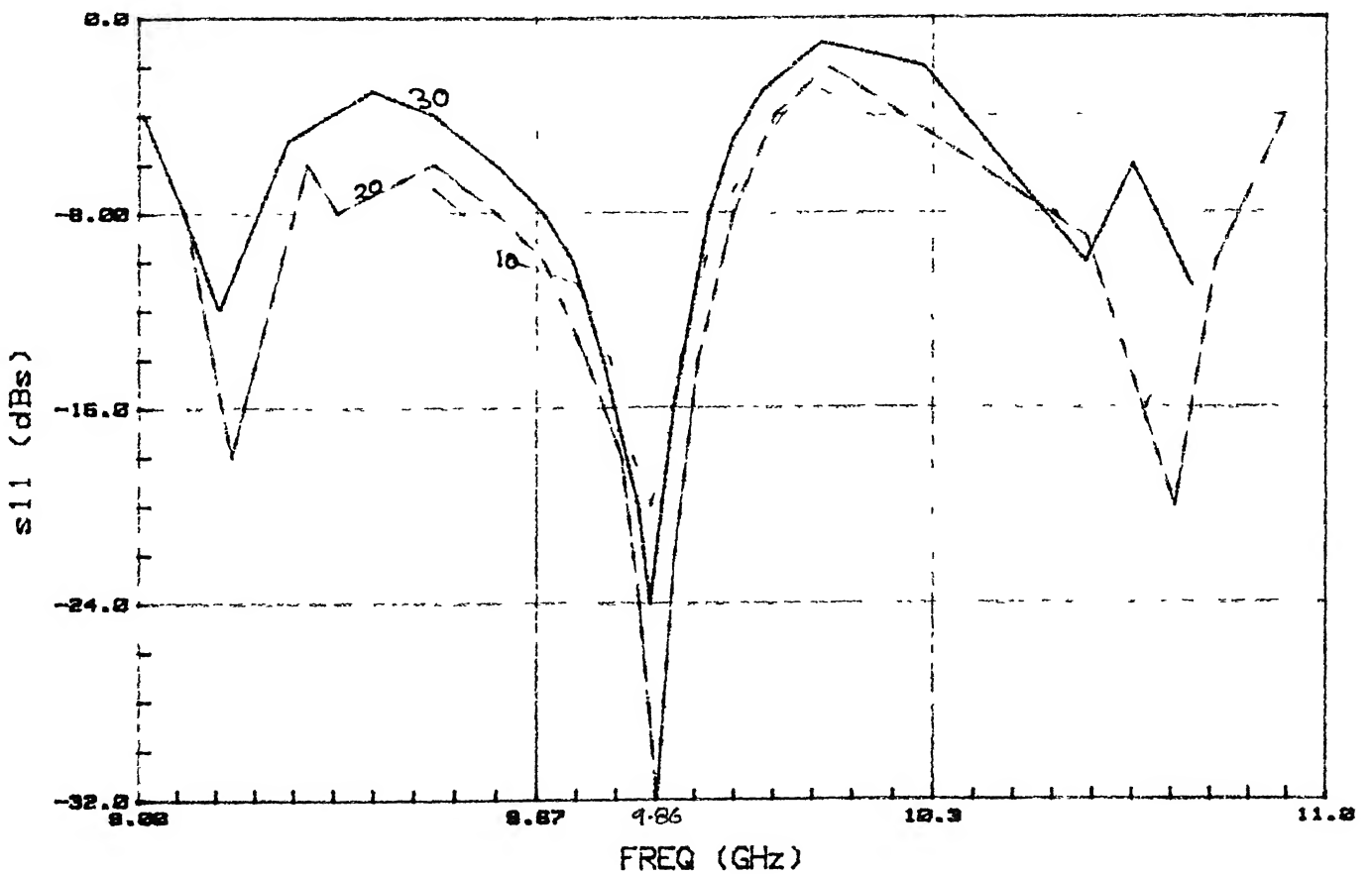

IMPEDANCE PLOT: S23/10

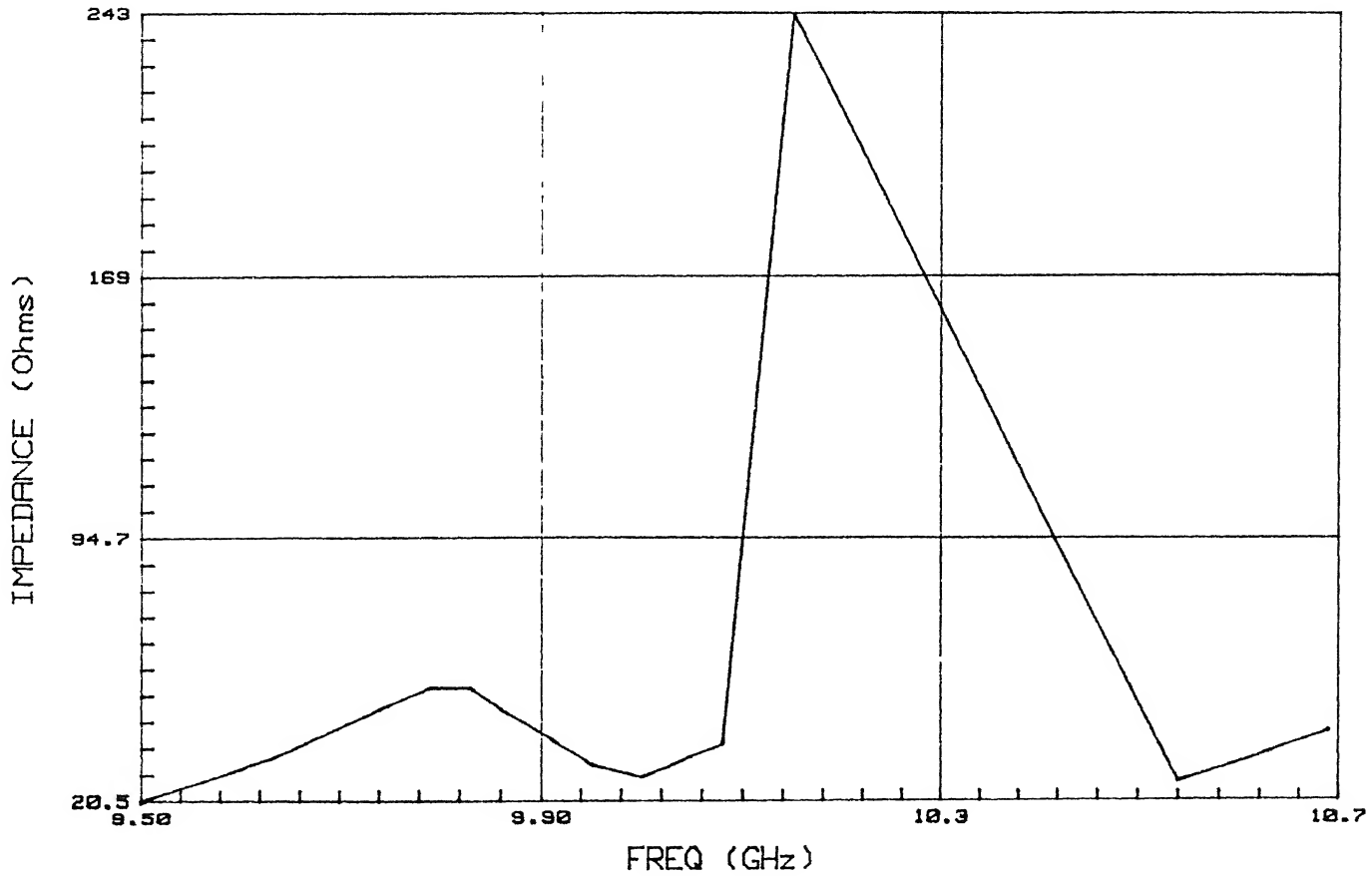

IMPEDANCE PLOT: S23/20

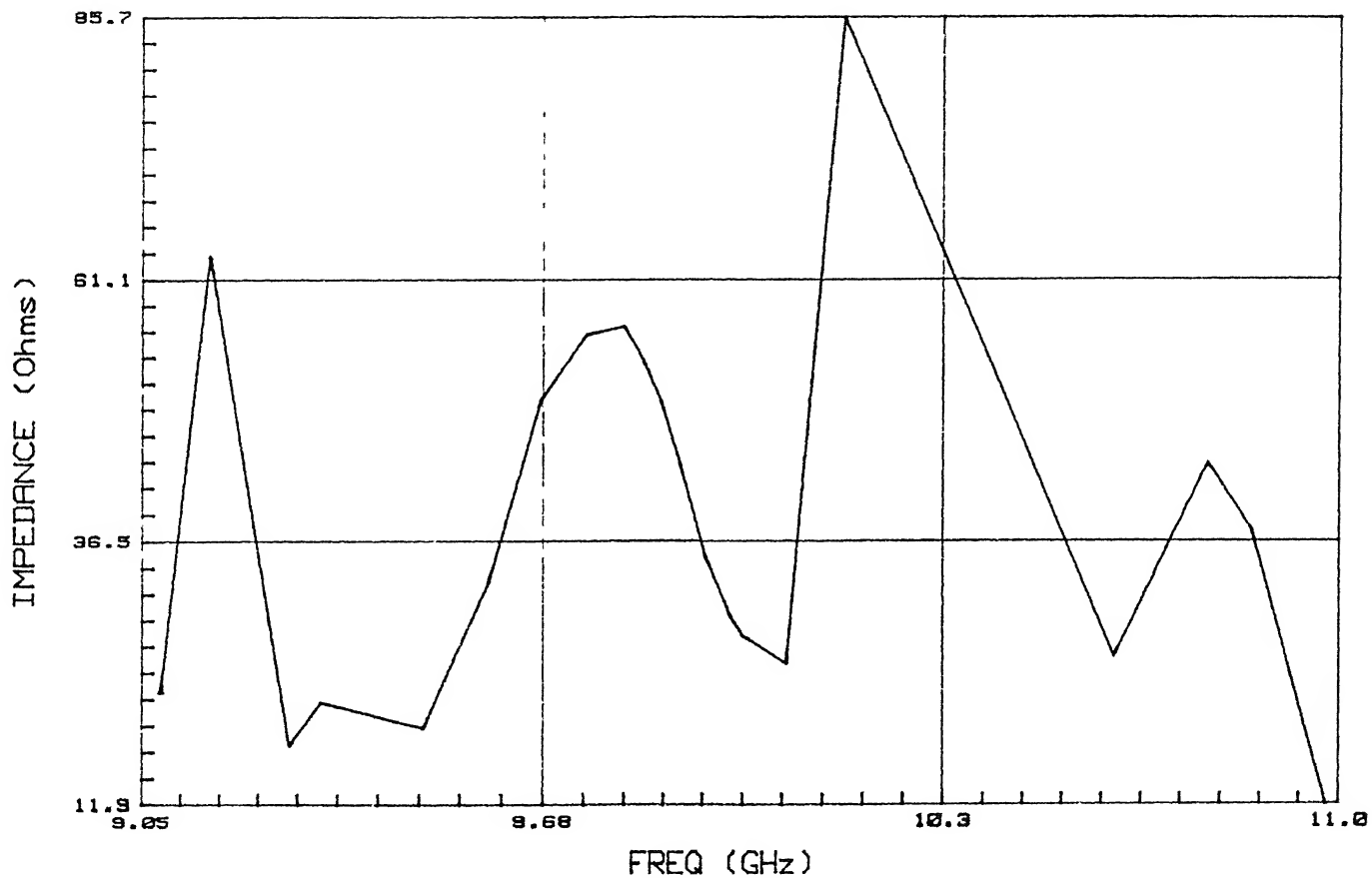

IMPEDANCE PLOT: S23/30

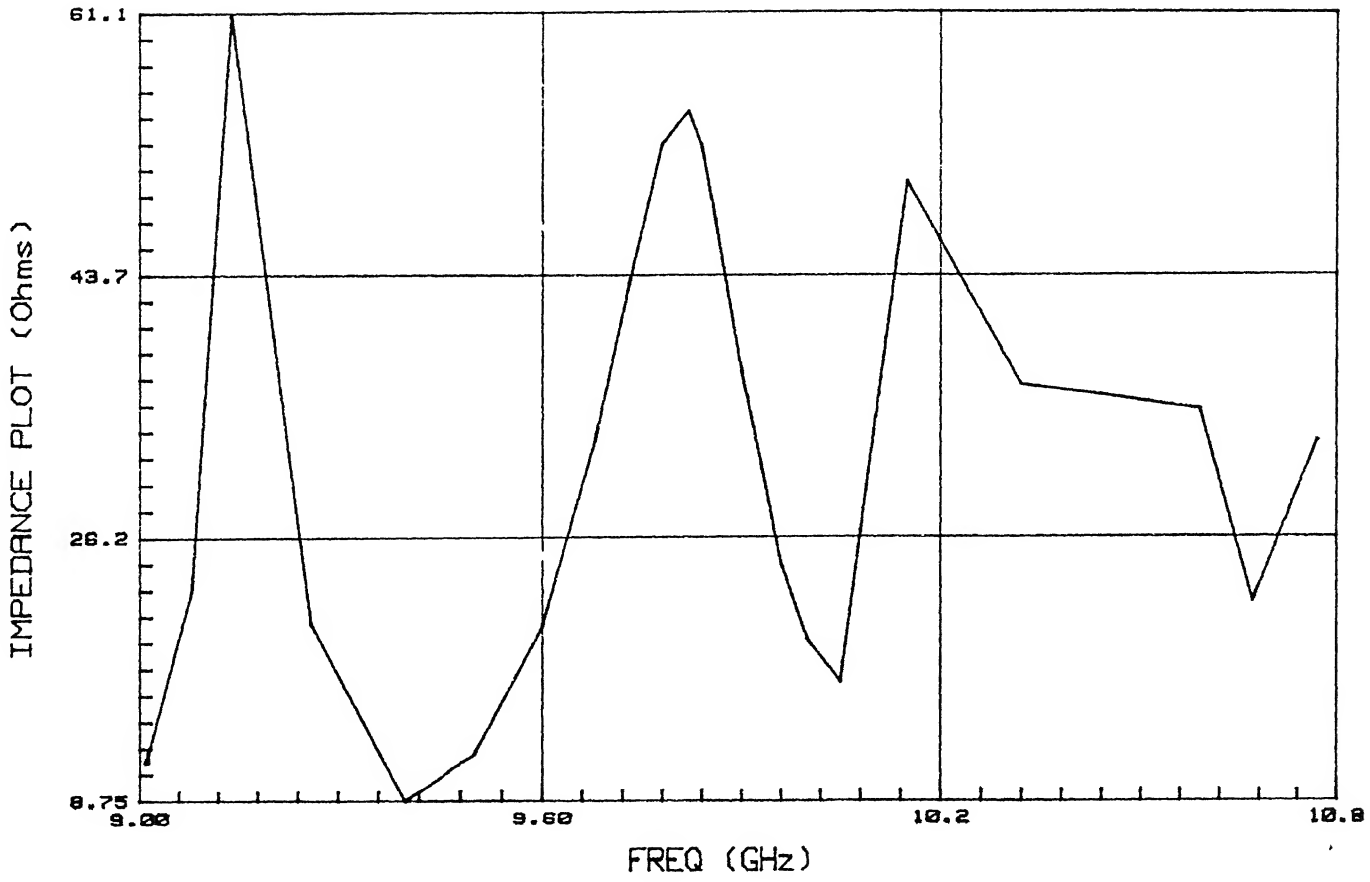

IMPEDANCE PLOT: S23/10,20,30

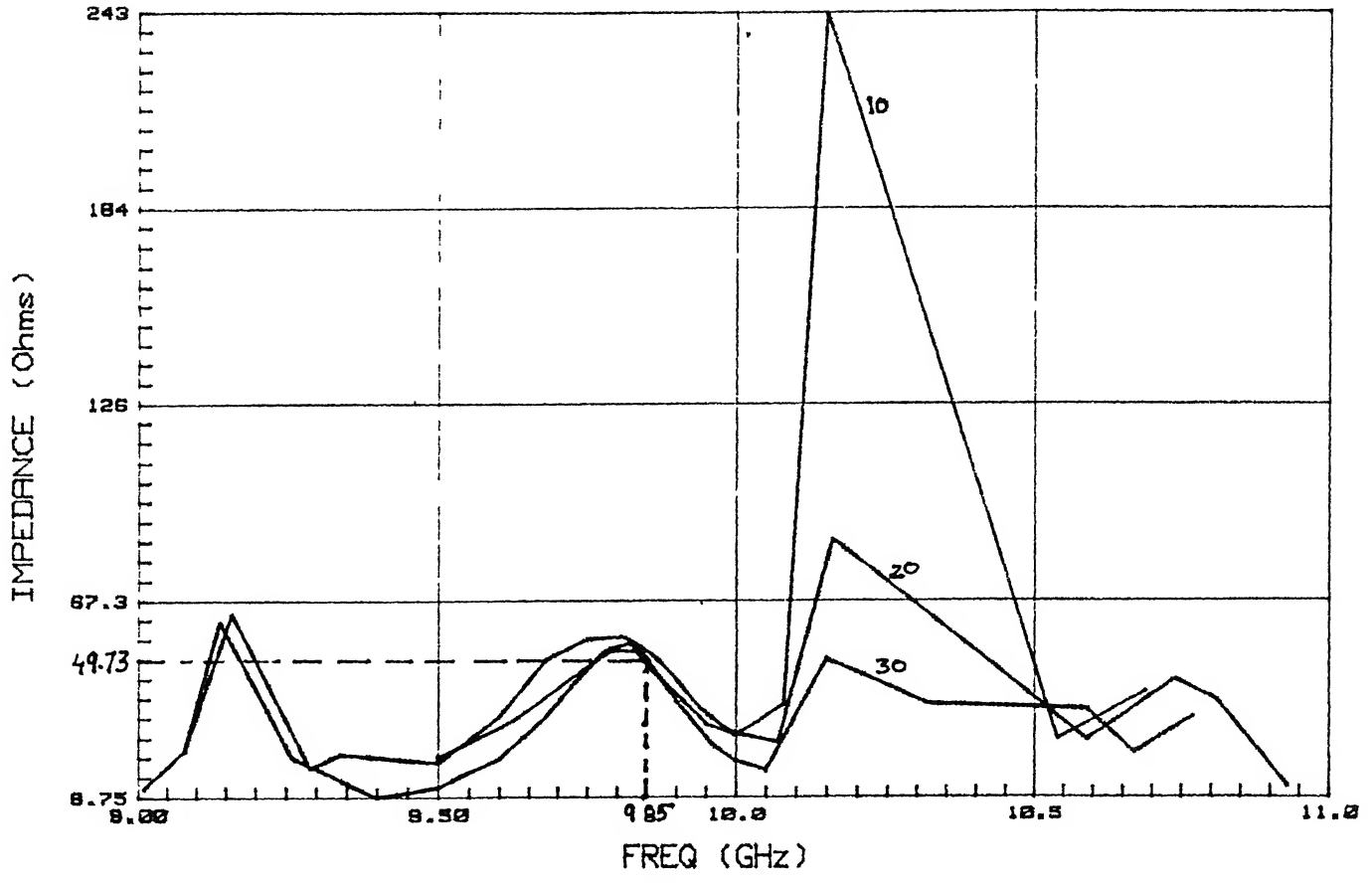

S11 PLOT: TAPER 23/30

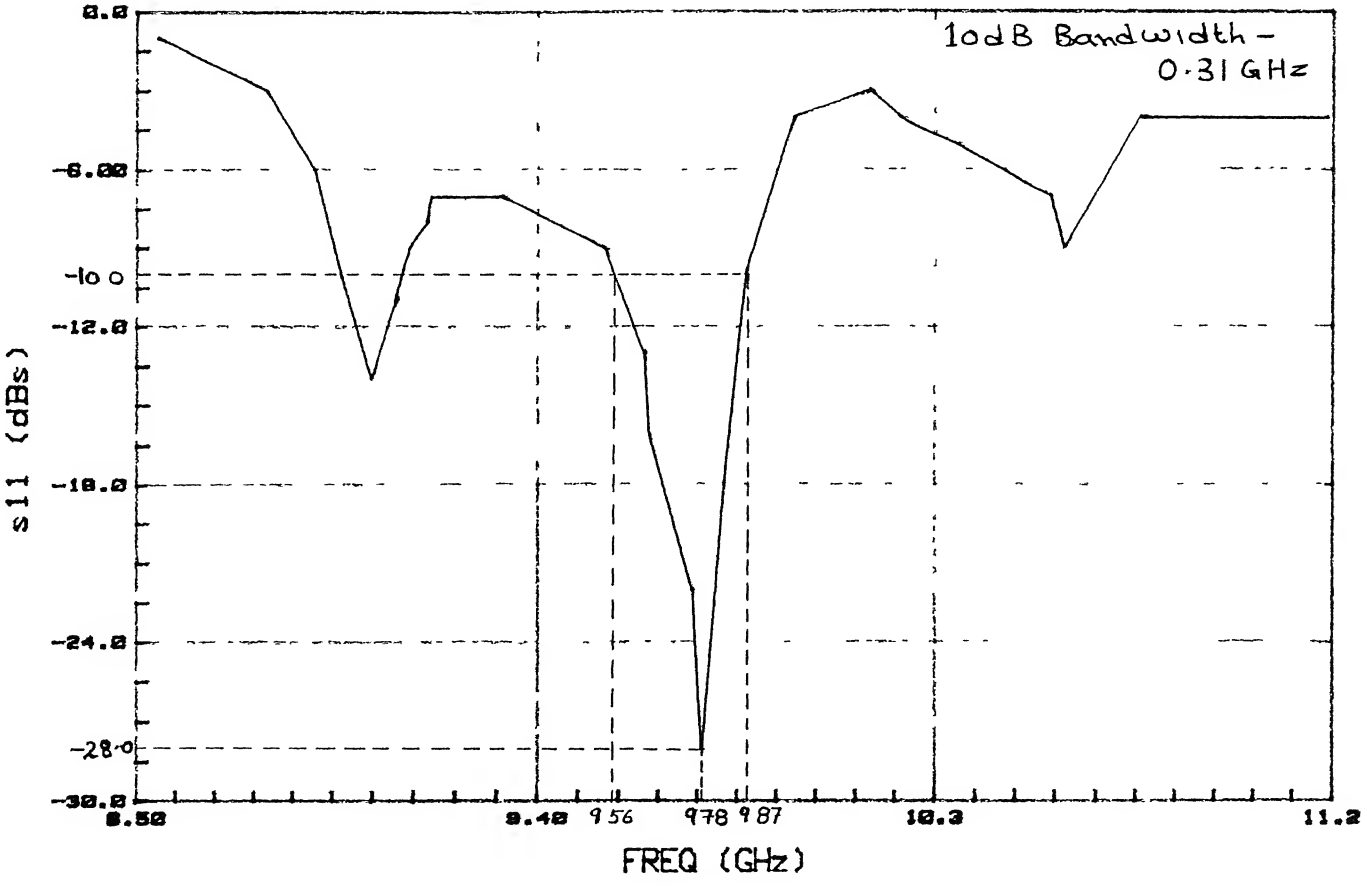

IMPEDANCE PLOT: TAPER 23/30

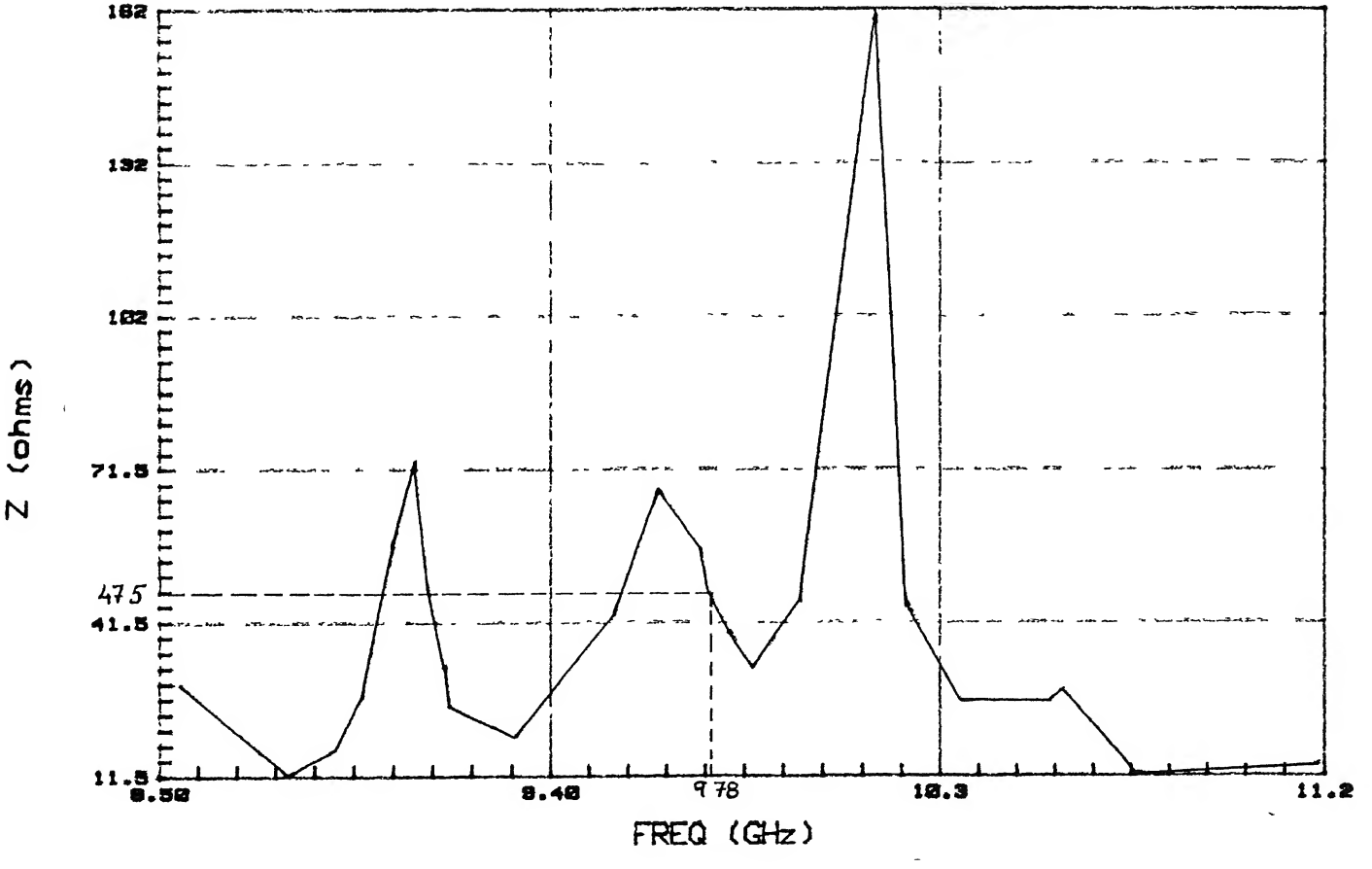

PHASE PLOT: TAPER 23/30

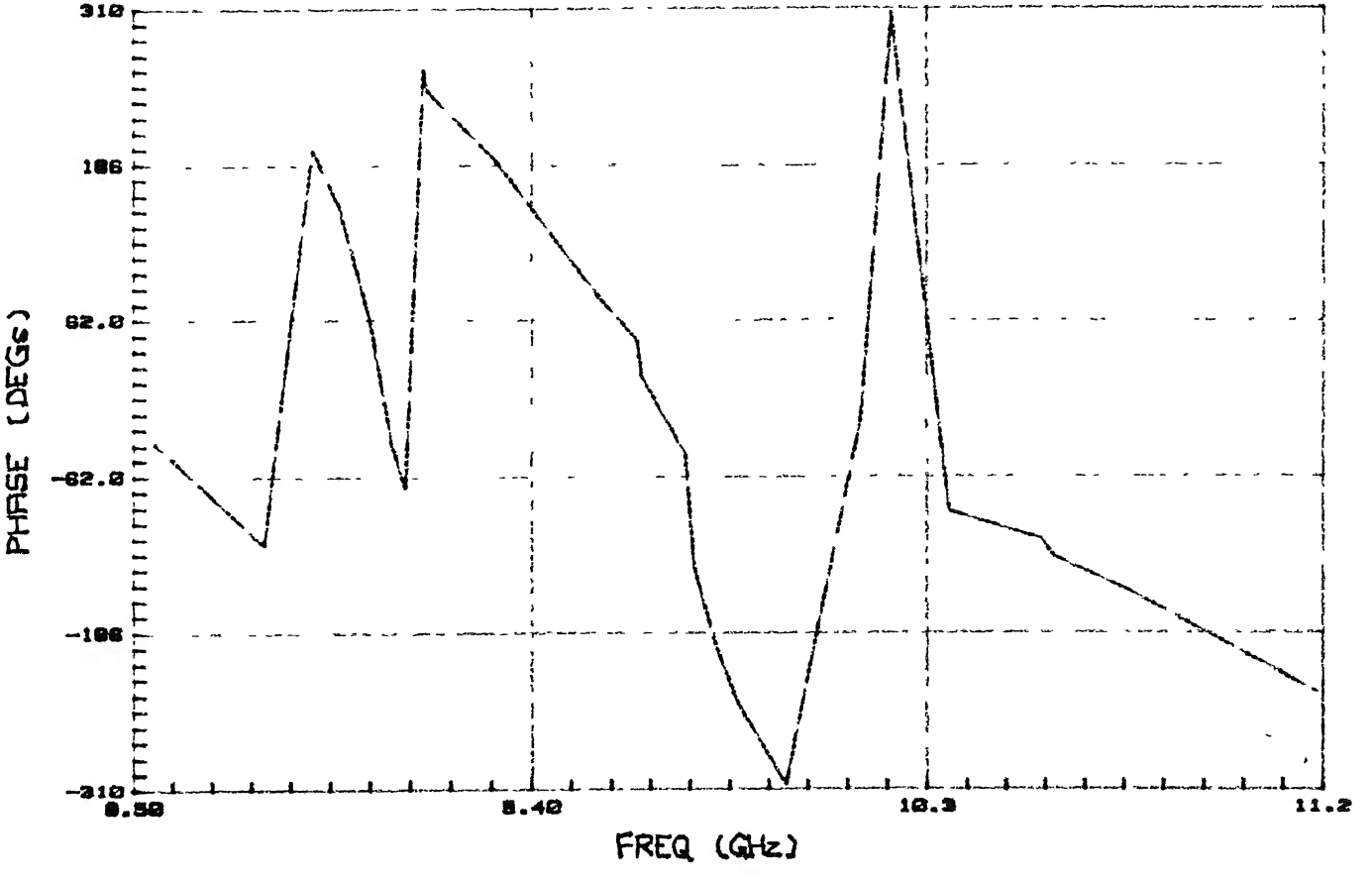

PLOTS: TAPER 23/30

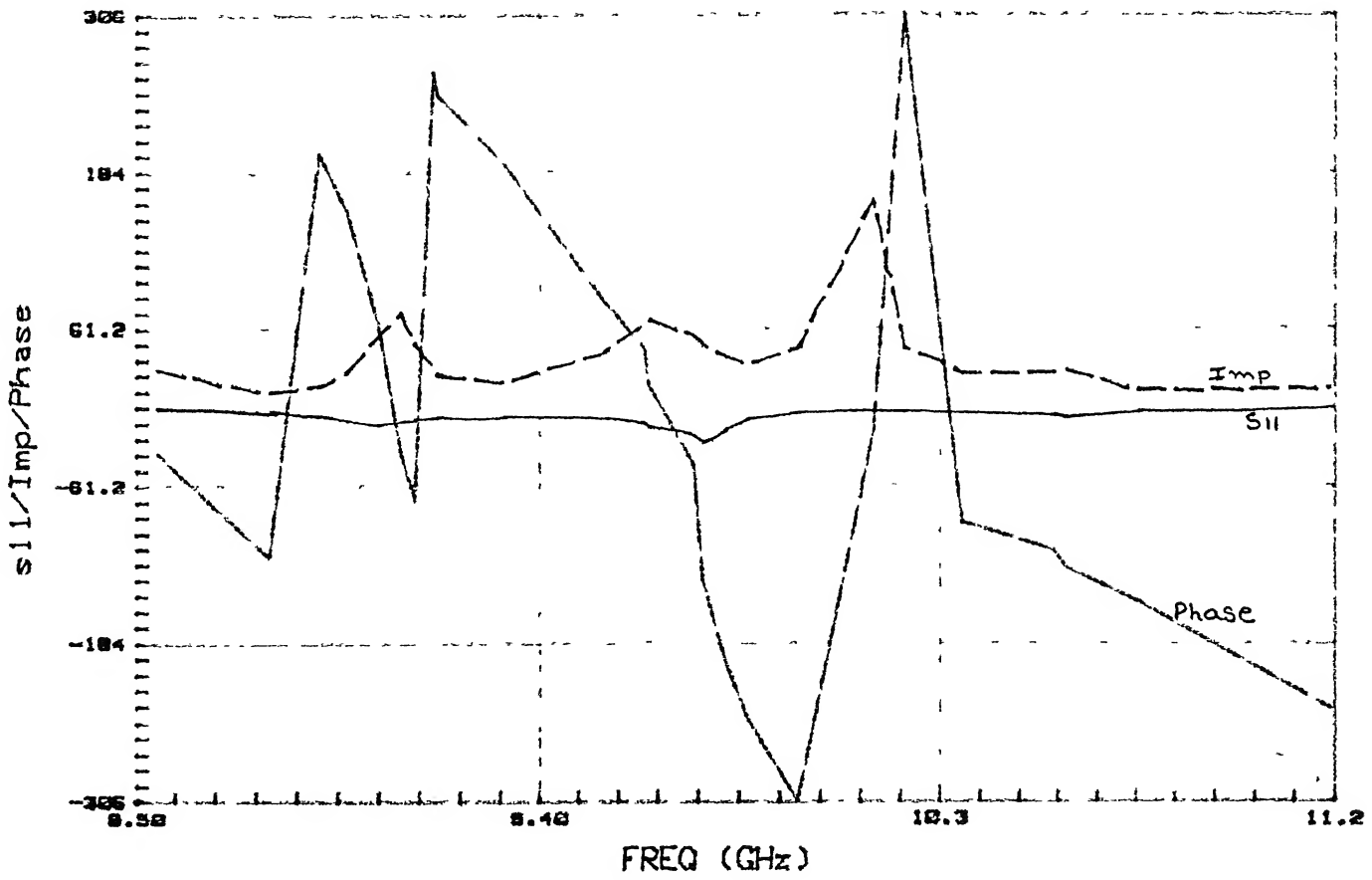

RADIATION PLOT: TAPERED/E-plane

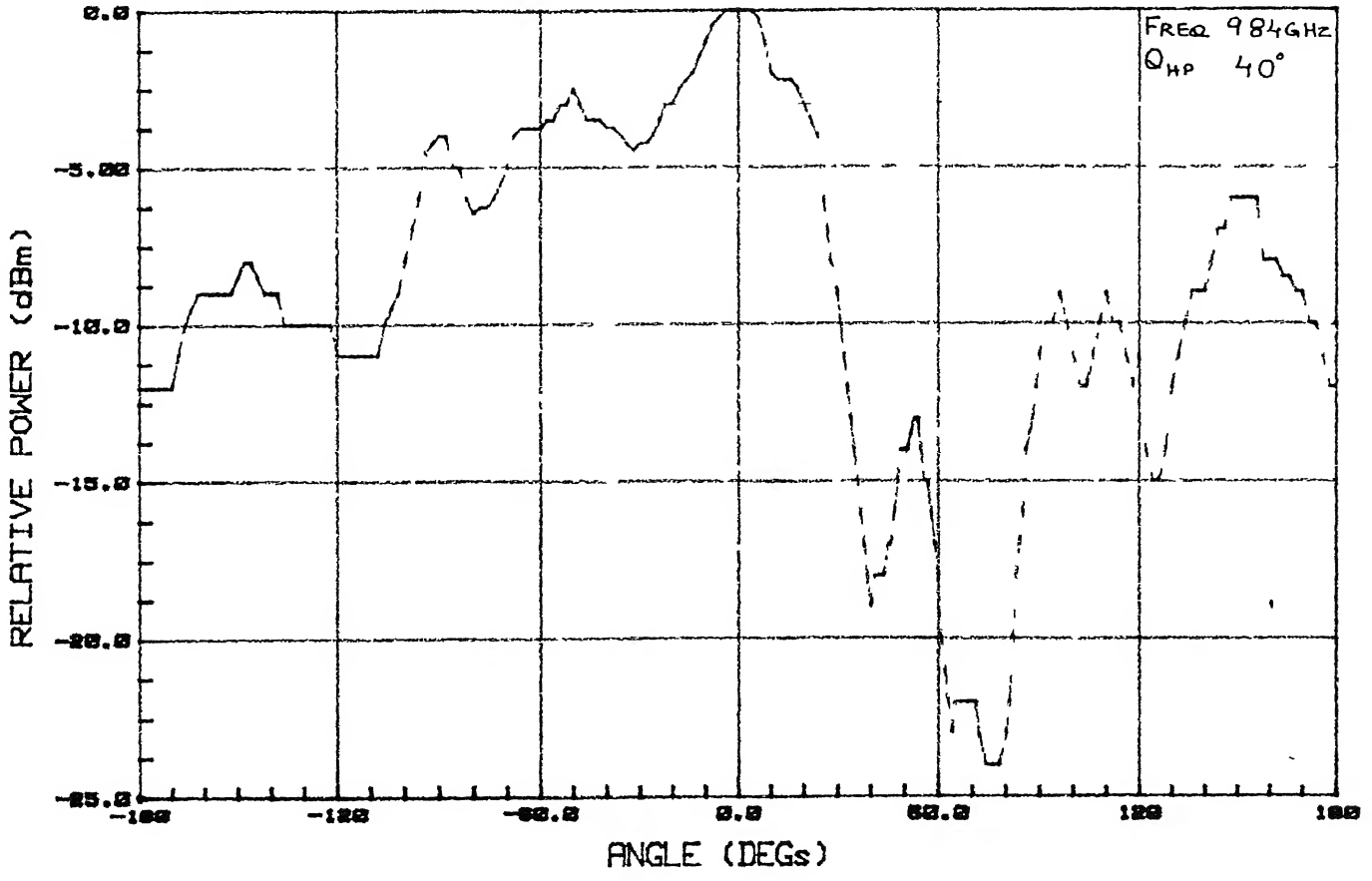

RADIATION PLOT: TAPERED/H-plane

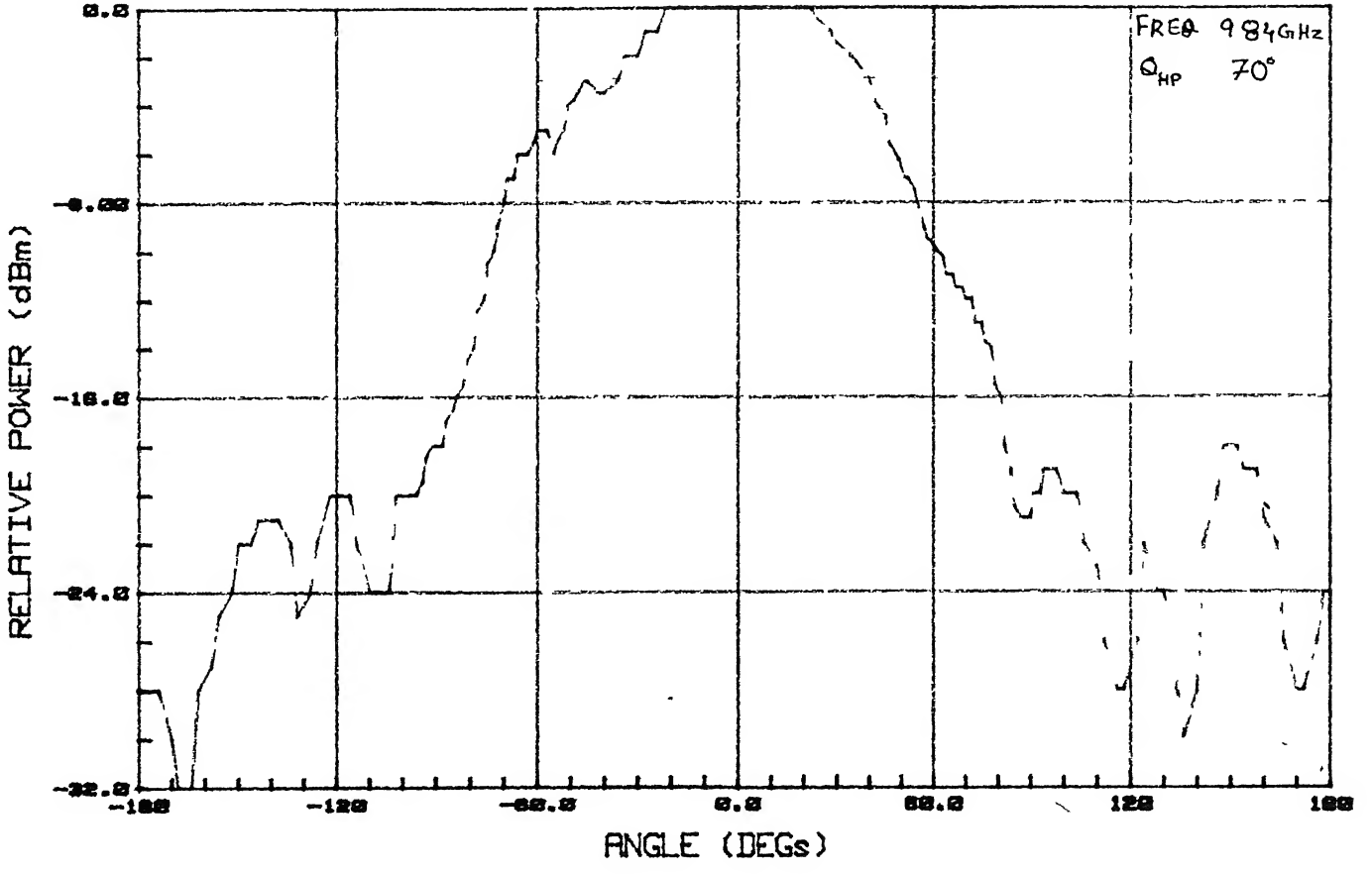

RADIATION PLOT: TAPERED/E, H

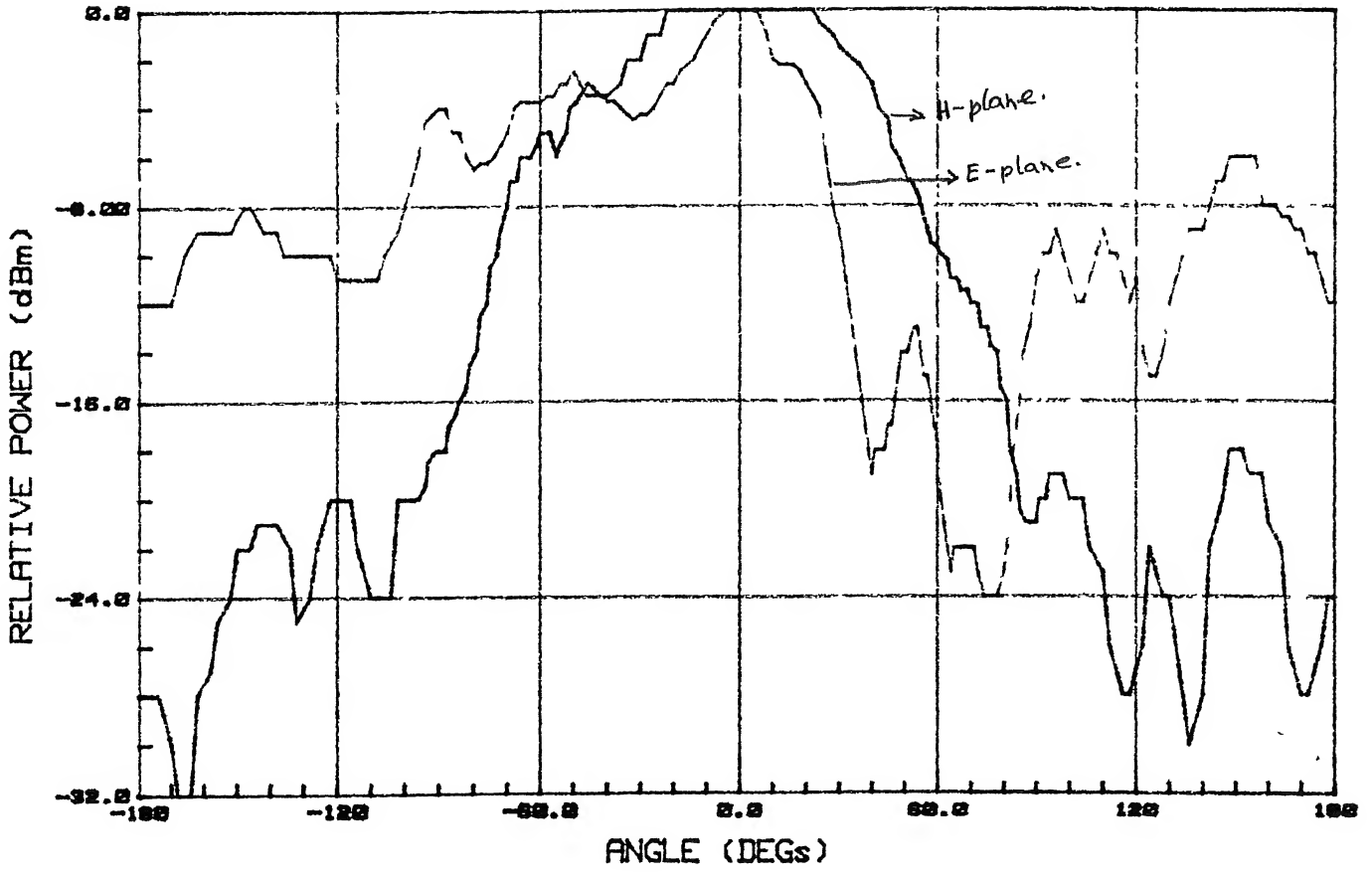

RADIATION PLOT: 20mm/E-plane

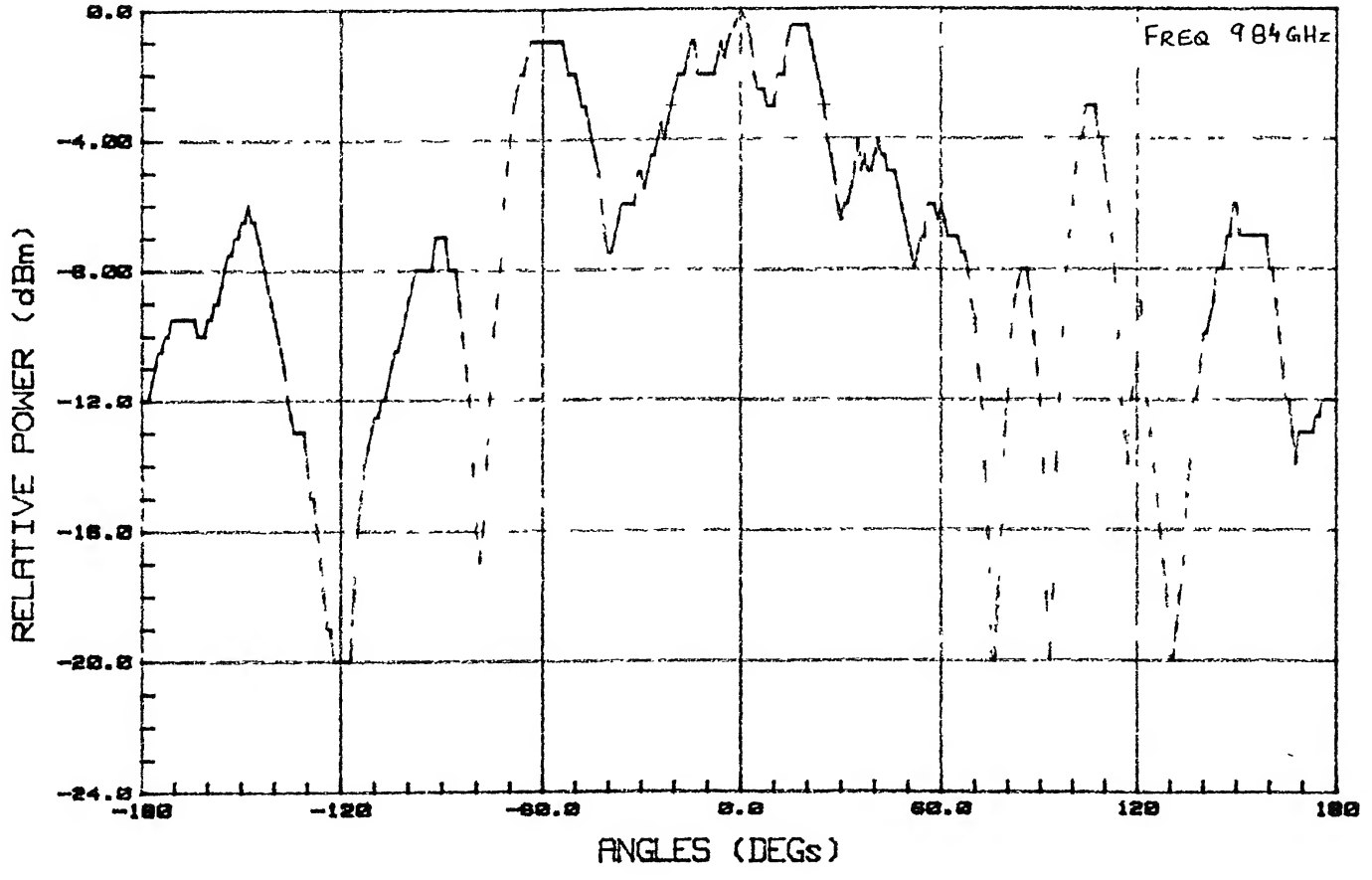

RADIATION PLOT:20mm/H-plane

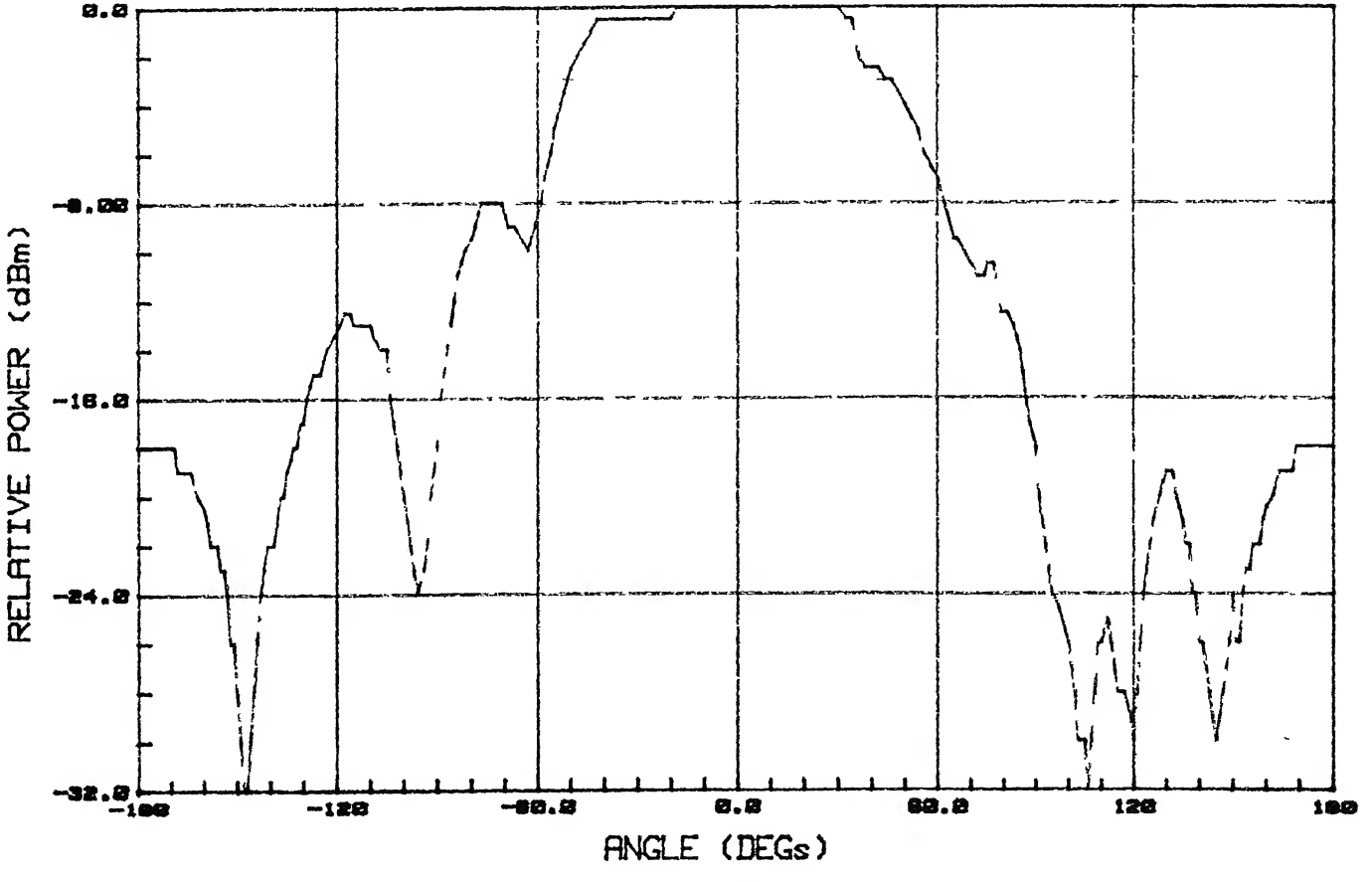

RADIATION PLOT: 20/E, H-plane

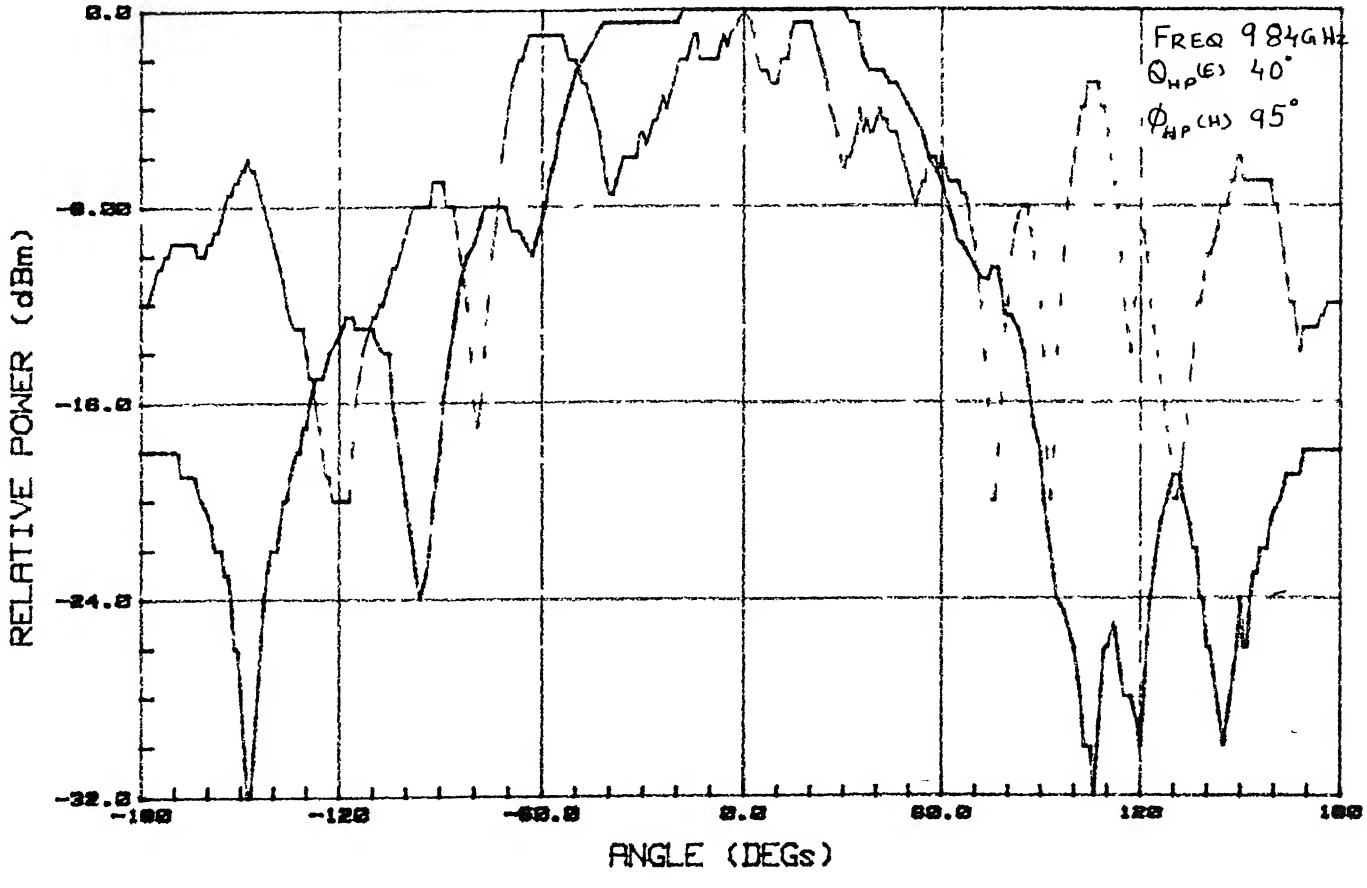

RADIATION PLOT: PLAIN ROD/E

20 mm

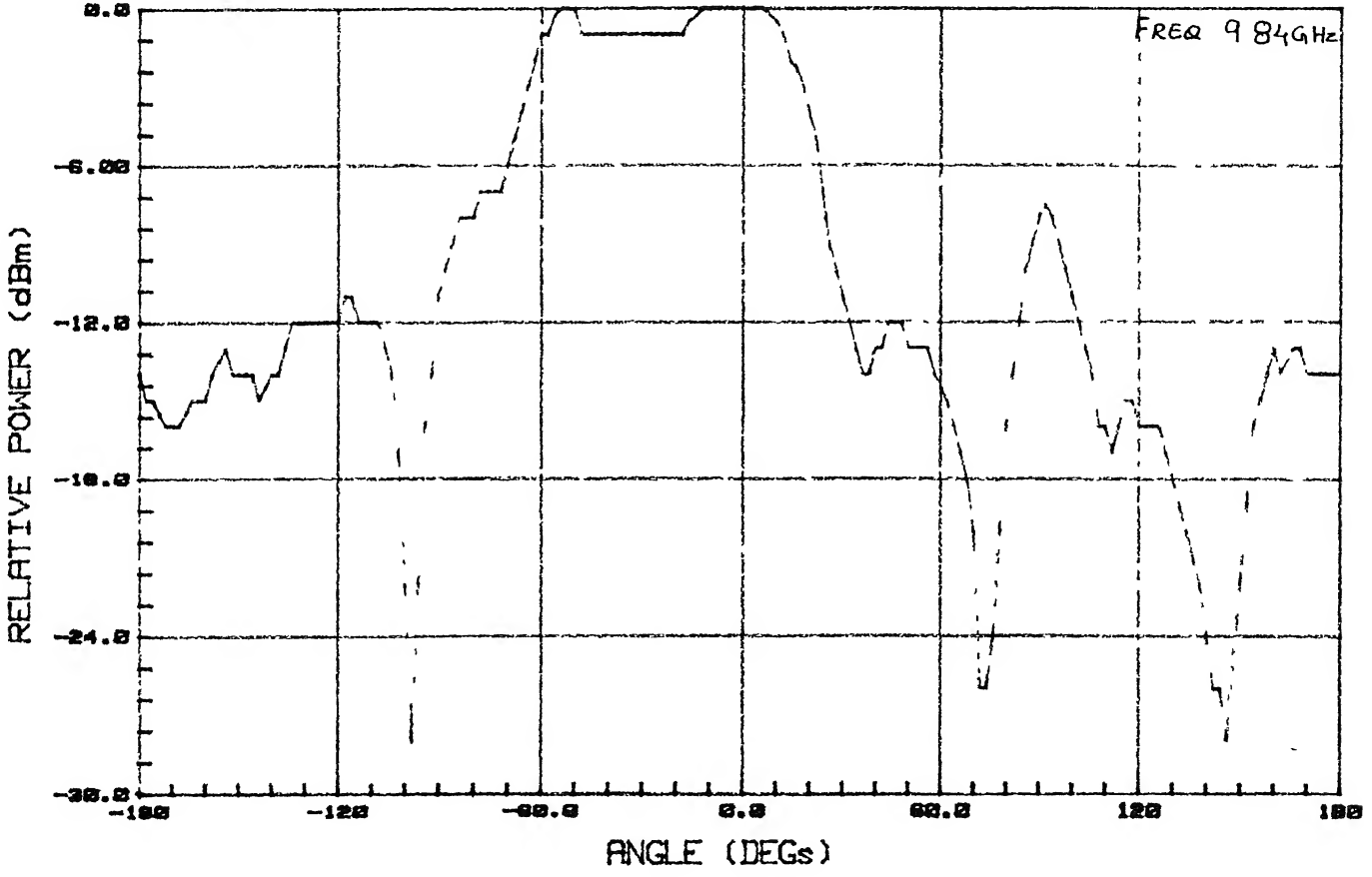

RADIATION PLOT :PLAIN TAPER/E

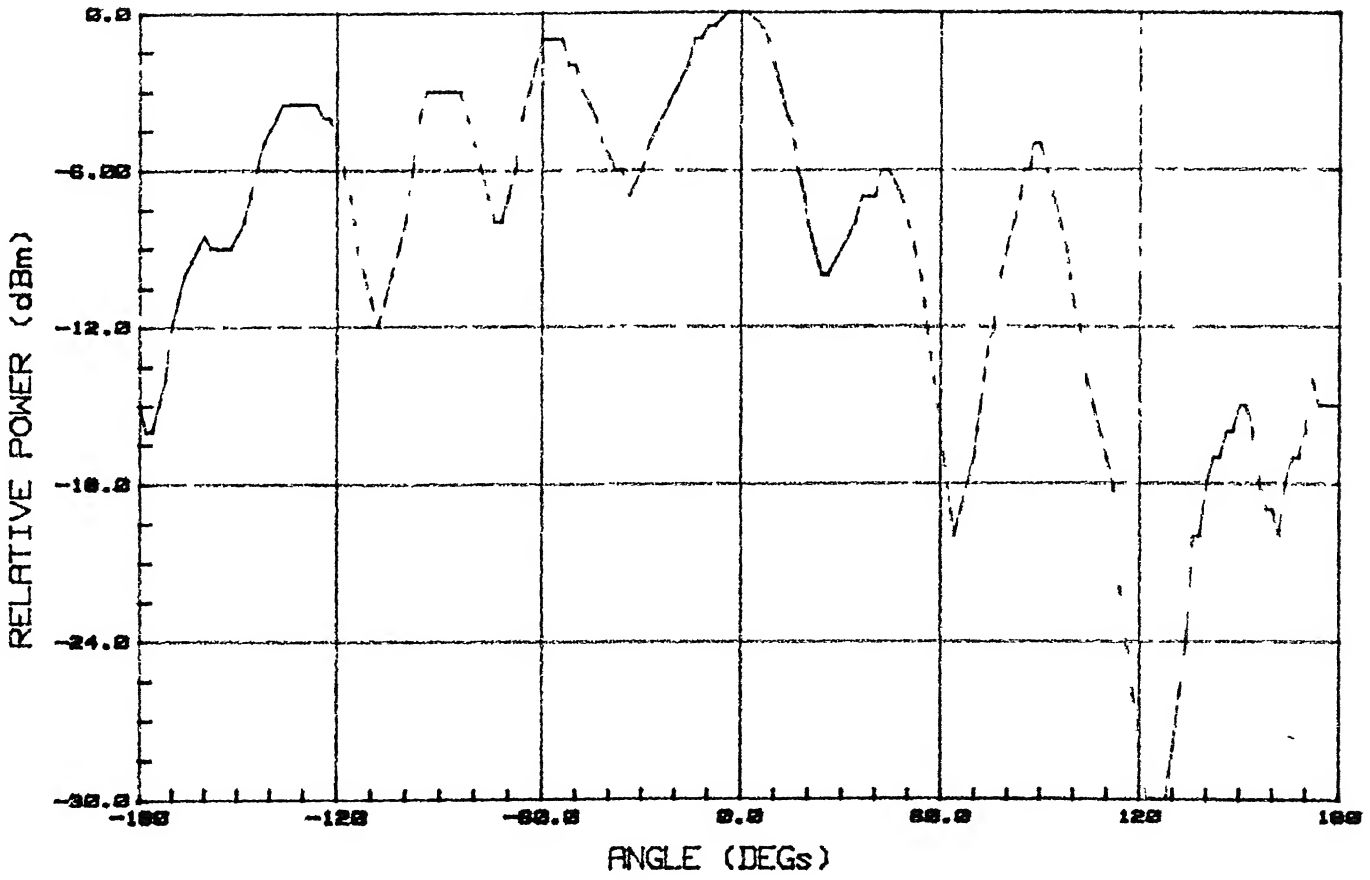

RADIATION PLOT: ROD/TAPER